Integration, evaluation and modeling of physiological signals to optimize emergency ventilation and cardiopulmonary resuscitation

Arnaud Lesimple

DOCTORAT BIOLOGIE BRETAGNE SANTE LOIRE

université angers

THESE DE DOCTORAT DE

L'UNIVERSITE D'ANGERS

ECOLE DOCTORALE N° 605
Biologie Santé
Spécialité : « *Physiologie, Physiopathologie, Biologie Systémique Médicale*»

Par
Arnaud LESIMPLE

Integration, evaluation and modeling of physiological signals to optimize emergency ventilation and cardiopulmonary resuscitation

Thèse présentée et soutenue à Annecy, le mercredi 26 avril 2023
Unité de recherche : Laboratoire Mitovasc UMR CNRS 6015 - INSERM U1083

Rapporteurs avant soutenance :

Pr Alain Cariou	CHU Cochin – Paris – université Paris Cité
Pr Aurora Magliocca	Ospedale Maggiore Policlinico - Milan

Composition du Jury :

Président :	Pr Laurie Morrison	Sunnybrook Health Science Centre - Toronto
Examinateurs :	Pr Laurent Brochard	St. Michael's Hospital - Toronto
	Pr Renaud Tissier	Ecole Vétérinaire de Maisons Alfort – Maisons Alfort
	Mr Thierry Boulanger	Air Liquide Healthcare
Dir. de thèse :	Pr Alain Mercat	CHU Angers - Université d'Angers
Co-dir. de thèse :	Pr Jean-Christophe Richard	CHU Angers - Air Liquide Medical Systems

Invité(s)

Pr Pierre Asfar	CHU Angers - Université d'Angers
Pr Dominique Savary	CHU Angers - Université d'Angers
Dr Sylvain Roy	Ecole Polytechnique Fédérale de Lausanne

REMERCIEMENTS

Au Professeur Jean-Christophe Richard,
Pour m'avoir transmis ta passion pour la recherche, pour la richesse de tes idées et pour m'avoir accompagné tout au long de la thèse.

Au Professeur Alain Mercat,
Pour tes conseils avisés, et pour m'avoir fait découvrir le service de réanimation d'Angers.

Au Professeur Laurent Brochard,
Pour ta bienveillance, la qualité de nos échanges et pour avoir suivi ma thèse.

Au Professeur Pierre Asfar,
Pour votre soutien et pour avoir suivi ma thèse.

Au professeur Dominique Savary,
Pour ton soutien, ton énergie et ton accompagnement.

Aux professeurs Alain Cariou et Aurora Magliocca pour avoir acceptés d'être rapporteurs de ma thèse.

Aux professeurs Laurie Morrison, Renaud Tissier, Thierry Boulanger et Sylvain Roy pour avoir accepté d'être jury de ma thèse.

A toute l'équipe du Med$_2$Lab, Alexandre Broc, Eloise De Beaufort, Mathilde Lefranc, Laura Polard, Marius Lebret, Nathan Prouvez, Bilal Badat, Manon Hannoucene pour votre soutien, votre bonne humeur et les bons moments passés ensemble.

A toute l'équipe du Vent'Lab, François Beloncle, Dominique Savary, François Morin, Nathan Prouvez, Alice Vuillermoz, Bertrand Pavlovsky, Christophe Desprez, Antonin Courtais, Dara Chean, Mathilde Taillantou-Candau et Elise Yvin pour l'énergie de groupe permettant la réalisation de beaux projets.

A toute l'équipe de CAVIAR, Stéphane Delisle, Emmanuel Charbonney, Paul Ouellet, Thomas Piraino, pour votre esprit d'équipe et votre bonne humeur.

A toute l'équipe de l'école vétérinaire de Maisons-Alfort, Renaud Tissier, Fanny Lidouren, Alice Hutin, pour m'avoir guidé et fait découvrir votre domaine.

A Lionel Genix, Lise Thomas, Charlotte Muller, Bérengère De Lestoille et Franck Galvaing pour m'avoir accompagné et fait confiance.

A ma famille, Michèle, Serge et Nicolas.

Summary

Introduction

Many patients in emergency situations present a respiratory failure. Mechanical ventilation is often required to maintain gas exchange by replacing or assisting respiratory muscles in patients exhibiting a life-threatening respiratory distress. A quick and efficient strategy must be put in place in the pre-hospital field and/or at emergency department admission. For this specific purpose, different devices can be used, ranging from the most simple bag valve masks to more sophisticated transport ventilators. Those devices are based on different working principles that may potentially impact the quality of ventilation delivered to the patient (1). Critically ill patients with the need for mechanical ventilation show complex interactions between respiratory and cardiovascular physiology. These interactions are important as they may guide the clinician's therapeutic decisions to optimize ventilator settings and possibly, affect patient outcome. Noticeably, the first reason to use a ventilator in United States in the pre-hospital field is respiratory distress; cardiac arrest being another important category (2, 3). Interestingly, bag valve mask ventilation is still the most common device used to ventilate cardiac arrest patients and present several limitations (4). Nevertheless, very few solutions have been specifically developed on ventilators for this specific setting until recently. Likewise, particular complications associated with ventilation after a cardiac arrest emerged from literature only recently (5, 6).

Cardiac arrest is estimated to be the third leading cause of death in the United States (7). When the heart stops functioning, there is cessation of blood flow to the rest of the body. Consequently, restoring circulation and possibly oxygen delivery to vital organs as quickly as possible is important for improving overall patient survival rates. Aside the absolute priority to consider defibrillation, cardiopulmonary resuscitation (CPR) that combines chest compressions with lung insufflation to restore perfusion and oxygenation to the body (8) should be started promptly following cardiac arrest. Despite the important role of oxygen delivery, we currently do not know the best way to ventilate the lungs during CPR nor do we know when and how much ventilation is necessary for successful resuscitation and good outcomes (7). In addition, the potential deleterious interaction of ventilation with circulation should be taken into account. The optimal ventilation strategy during cardiopulmonary resuscitation (CPR) remains to be determined.

International recommendations suggest end tidal CO2 (EtCO2) monitoring during CPR, but several studies highlighted the limits of this parameter in clinical practice (9, 10). A novel

interpretation of the capnogram (CO2 signal) identified specific CO2 patterns during chest compressions that may reflect non-optimal ventilation conditions during CPR (11, 12). Indeed, these authors suggest that CO2 patterns may reflect thoracic lung volume during CPR, which could be associated to ventilation and circulation efficacy. The different models available (bench, cadaver and animal) may be judiciously combined to properly assess the performances of ventilation devices and new CPR strategies, such as the one based on capnogram analysis.

This manuscript is organized as follows:

- Part 1:
    - The first section reviews the fundamentals of positive pressure ventilation and the different working principles of available transport ventilators.
    - Physiological determinants of cardiopulmonary resuscitation and the importance of CO2 signal and lung volume during cardiac arrest will be reminded.
- Part 2: Two already published studies which are part of my thesis project will be presented, detailed and discussed:
    - A study evaluating the performances of transport ventilators that have been used to extend intensive care units capacity in the context of the COVID crisis, and that are used to manage cardiac arrest patients in the pre-hospital field.
    - A study describing a novel capnogram analysis during cardiopulmonary resuscitation to guide ventilation, based on clinical and experimental observations.
    - The development of a new bench model specifically dedicated for cardiac arrest patients, allowing a physiological evaluation of medical devices and ventilation strategies.
- Finally, perspectives and further steps on evaluating CO2 as a tool to guide ventilation during cardiopulmonary resuscitation will be proposed.

Part 1: Emergency ventilation and the importance of CO2 during Cardio Pulmonary Resuscitation

1.1. Emergency ventilation in the prehospital field and constrained environment

Emergency medicine refers to the management of life-threatening situations to rescue one or several patients in a constrained environment, either inside the hospital or in the prehospital field. A quick and efficient strategy must be put in place to increase favorable outcomes. Patients treated in emergency situations present a wide range of conditions that may require mechanical ventilation, including cardiac arrest, pneumonia, asthma, chronic obstructive pulmonary disease (COPD), cardiogenic pulmonary edema, acute respiratory distress syndrome, stroke, trauma, drug overdose, severe sepsis, shock…

Mechanical ventilation, also called positive-pressure ventilation, is a form of respiratory therapy that should be adapted to the condition and characteristics of the patient. It interacts in a complex process with respiratory physiology and can be delivered through different types of devices, especially emergency ventilators. Ventilatory strategies vary according to the clinical scenario, and to provide optimal care, it is paramount to understand the fundamental concepts of mechanical ventilation, including modes of ventilation, and the different working principles of emergency ventilators.

1.1.1. Principles of positive pressure ventilation

Spontaneous breathing and gas exchange

Spontaneous breathing or physiological breathing refers to the movement of air into the lungs called inspiration and out of the lungs called expiration. Spontaneous breathing is delivered by respiratory muscles, especially the diaphragm and intercostal muscles. Upon inspiration, the diaphragm contracts and enlarges the chest cavity. This contraction creates a vacuum or negative pressure, which pulls air into the lungs. Upon expiration, relaxation of the diaphragm and the natural elasticity of lung tissue and the thoracic cage force air out of the lungs. Consequently, spontaneous breathing can be referred as negative pressure ventilation. The objective of spontaneous breathing is to provide gas exchange: bring oxygen (O2) to the blood during inspiration and remove CO2 during expiration. Oxygen is transported by the blood from

the lungs to the different tissues and organs for different reasons for cellular respiration. The main by-product of cellular respiration is CO2, that is transported by the blood from the different tissues and organs to the lungs to be eliminated during expiration.

Positive pressure ventilation

When patients are unable to properly breathe on their own, gas exchange are not maintained thus spontaneous breathing must be assisted partially or totally by a mechanical device called a ventilator that is based on positive pressure ventilation. Positive pressure ventilation is a form of respiratory therapy that involves the delivery of an air oxygen mixture by positive pressure into the lungs.

1.1.2. Respiratory mechanics and the equation of motion

Respiratory mechanics

One important determinant of patient physiology that may interfere with mechanical ventilation is the respiratory mechanics (also called respiratory impedance). The two main characteristics of respiratory mechanics are compliance and resistance. Compliance is a measure of the respiratory system expandability, and thus refers to its ability to stretch and expand. Respiratory system compliance (Crs) depends on the contribution of lung (Clung) and chest wall (Ccw) compliances ($\frac{1}{Crs} = \frac{1}{Ccw} + \frac{1}{Clung}$). Resistance refers to the degree of resistance to air flow through the respiratory tract during inspiration and expiration. The determination of the respiratory mechanics of the patient is very useful at the bedside to deliver a protective ventilation and personalize ventilation settings. The product of compliance and resistance is the time constant, which represents the time required for the respiratory system to inflate up to 63% of the final volume (volume at end of inspiration), or deflation by 63%. In other words, it is an indication of the time required for the lungs to fill during inspiration and to empty during expiration. The formula of tidal volume deflation during expiration based on time constant is as follows:

$$V(t) = Vt \times e^{-\tau \times t} = Vt \times e^{-R \times C \times t}$$

With Vt the tidal volume;

Of note, it takes three time constants for 95% of the volume change to be achieved ($V(t) = Vt \times 0.05$)

Respiratory system as a single-compartment model

The simplest strategy to model the mechanical properties of the respiratory system is the single-compartment model (13). In this model, the lung is represented as a balloon sealed over the end of a pipe (see figure 1). This model presents a clear analogy to a real lung: the pipe represents the conducting airways and is characterized by the resistance, while the balloon represents the elastic tissue of the alveoli and is characterized by the compliance. Inspiration and expiration can be reproduced by the inflation and deflation of the balloon, respectively.

Figure 1 : Hydraulic representation of respiratory system

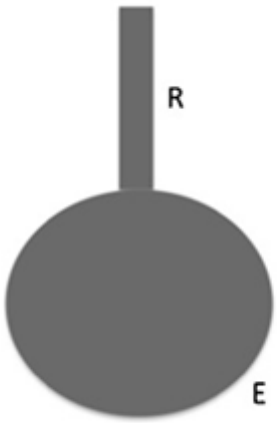

Figure 1: figure corresponding to figure 2a from Carvalho et al. (13). Representation of respiratory system considering the linear single-compartment model, represented by a balloon sealed over the end of a pipe.

The equation of motion

Respiratory system mechanics can be calculated from this graphical single-compartment model determined based on a mathematical correlate, called the equation of motion. It is essentially a force balance equation.

At any point in time during inspiration, the total pressure required to generate a certain level of ventilation is the sum of:

- The starting pressure: Total PEEP (PEEPtot) where PEEPtot is the pressure in the lungs at the end of expiration

- The resistive pressure (Pres) or resistive load: Pressure to overcome the inspiratory resistance. Pres is the product of inspiratory resistance and inspiratory flow.
- The elastic pressure (Pel) or elastic load: Pressure to overcome respiratory system compliance. Pel is the ratio of tidal volume to respiratory system compliance:

Note that the total pressure is a sum of the total pressure delivered by the ventilator (Pvent or Paw) and the pressure generated by the patient's respiratory muscles (Pmus). Importantly, in a paralyzed patient, Pmus is zero.

$$Ptot = PEEPtot + Pres + Pel$$

$$Paw + Pmus = PEEPtot + (flow \times Resistance) + \frac{Vt}{Compliance}$$

How to calculate compliance and resistance on a ventilator ?

Ventilation requirements

From the equation of motion, it is possible to calculate the respiratory mechanics of the patient if we consider a sedated and curarized patient with Pmus at zero. The easiest way to determine compliance and resistance of a patient is to use on the ventilator a mode of ventilation where flow is controlled and constant during inspiration (see figure 2). If we consider the equation of motion at the end of inspiration, we have:

$$Paw = PEEPtot + (flow \times Resistance) + \frac{Vt}{Compliance}$$

Where Vt is the tidal volume or volume insufflated to the lungs at the end of inspiration.

Measuring the total PEEP

Total positive end-expiratory pressure (PEEPtot) is the positive pressure that will remain in the airways at the end of the expiration that is greater than the atmospheric pressure. It is the sum of the extrinsic PEEP delivered by the ventilator and the potential intrinsic PEEP or autoPEEP. Intrinsic PEEP may be present if the lung does not completely deflate during expiration, leaving air trapped inside the lung at the end of expiration and generating a positive pressure that remains in the lungs.

$$PEEPtot = PEEP\ extrinsic + PEEP\ intrinsic$$

This PEEPtot can be measured on the ventilator using an expiratory occlusion manoeuver.

Measuring the plateau pressure and compliance

It is also possible to perform an occlusion maneuver on the ventilator at the end of inspiration, resulting in an inspiratory flow equal to zero. The pressure during this maneuver is called plateau pressure (Pplat). In addition, when flow is equal to zero, the resistive load becomes zero. Thus, the equation of motion becomes:

$$Pplat = PEEPtot + \frac{Vt}{Compliance}$$

Consequently,

$$Compliance = \frac{Vt}{Pplat\ - PEEP\ tot}$$

Interestingly, the elastic pressure at end of inspiration is

$$Pel = \frac{Vt}{Compliance} = Pplat - PEEPtot$$

Measuring the peak pressure and resistance

The pressure at the end of inspiration is measured by the ventilator as Ppeak.

Following the equation of motion,

$$Ppeak = PEEPtot + Pres + Pel$$

Thus,

$$Pres = Ppeak - PEEPtot - Pel = Ppeak - Pplat$$

We know that

$$Pres = flow * Resistance$$

Consequently,

$$Resistance = \frac{Pres}{flow} = \frac{Ppeak - Pplat}{flow}$$

As flow is set on the ventilator, it is possible to calculate the resistance.

To summarize, expiratory and inspiratory occlusion manoeuvers are necessary to measure PEEPtot and Pplat respectively, which can be used to calculate both compliance and resistance of the patient's respiratory system.

Figure 2: Schematic representation of airway pressure and flow signals with information necessary for respiratory mechanics calculation

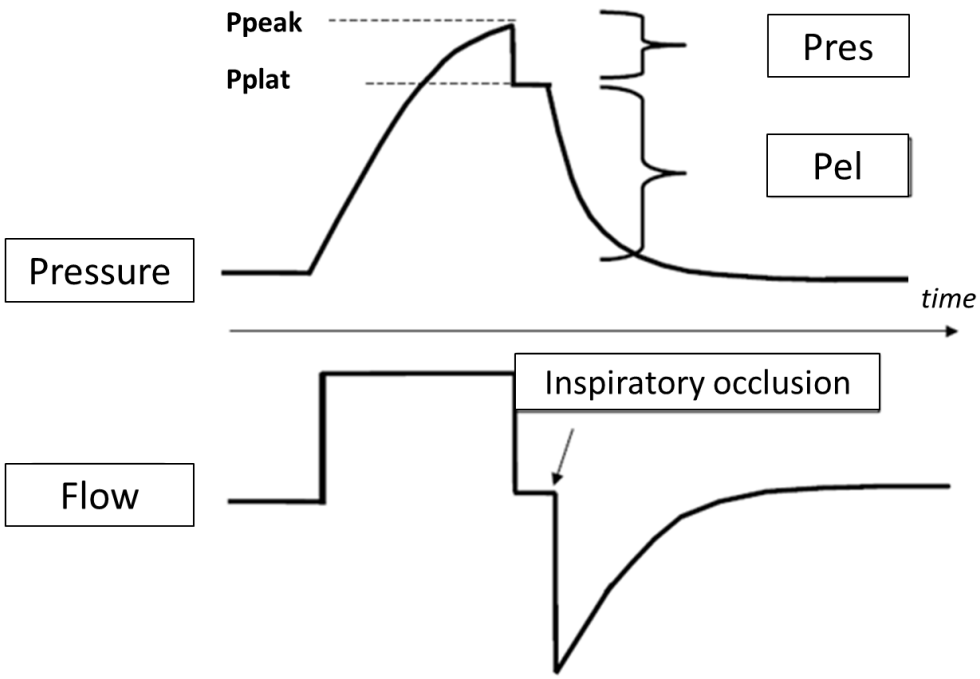

Figure 2: From top to bottom illustration of ventilator curves of airway pressure and airway flow according to time. One ventilator breath in flow (volume) mode of ventilation is shown. Both the resistive and elastic pressure are displayed on the schematic, as well as peak pressure and plateau pressure. Of note, plateau pressure is measured during an inspiratory occlusion at the end of inspiration, when airway flow is null.

1.1.3. Ventilation modalities and modes of ventilation mainly used in emergency ventilators

Bag-valve mask ventilation

Bag-valve-mask (BVM) ventilation (4) is an essential and simple airway management technique that allows for basic oxygenation and ventilation of patients. In an emergency situation, a bag-valve-mask may be the most simple and effective way to assist ventilation (14). It is also the most commonly used device to ventilate patients in cardiac arrest. It consists of a bag and a reservoir filled with oxygen at a flow rate of 15 liters per minute. When the rescuer squeezes the bag, oxygen is insufflated to the patient. Release of the bag allows expiration of the patient through the expiratory valve. Most BVMs are designed with a one way non rebreathing valve to manage flow in and out of the patient during insufflation and expiration respectively. Some PEEP valves may be implemented to add positive end expiratory pressure. Several risks are associated with BVM ventilation, especially gastric insufflation as airways are not secured, and excessive or insufficient ventilation.

Modes of ventilation: the initiation – controlled or assisted ventilation

The ventilator delivers ventilation cycles that includes inspiration while the expiration is passive. Those ventilator breaths are defined by three main characteristics: the initiation, the regulated variable and the cycling. The initiation refers to the beginning of inspiration. If the patient is sedated and curarized, patient's inspiratory muscles do not generate any inspiratory effort. In this case, cycle is initiated only by the ventilator: this is called controlled ventilation. On the opposite, when the patient generates inspiratory efforts, cycle can be initiated or triggered by the patient: this is called assisted ventilation. In this case, the ventilator detects patient's effort by a change in airway flow (increase) or pressure (decrease) or a combination of both. Then, it accompanies patient spontaneous effort and assist patient's inspiration by supplying supplemental flow and pressure. Assisted ventilation allows spontaneous breathing activity to restore more or less physiological displacement of the diaphragm.

Modes of ventilation: the regulated variable – volume or pressure

Once a cycle is initiated, the ventilator must replace or assist patient spontaneous breathing, depending if we are in controlled or assisted ventilation respectively. To deliver this inspiration, the ventilator can regulate either pressure or flow (sometimes volume). In fact, most ventilation

modes available on a ventilator result from pressure or flow regulation and sometimes a combination of both, as shown on figure 3.

- Flow (volume) modes of ventilation are defined by the control of the flow within a defined inspiration time that can be set on the ventilator. As volume corresponds to the integral of flow over time, the volume can be set and regulated. Consequently, airway pressure is not regulated and may vary depending on patient's condition and respiratory mechanics. This is the reason why pressure should be cautiously monitored with volume mode of ventilation.
- Pressure modes of ventilation are defined by the control of a constant pressure that can be set on the ventilator and regulated. Consequently, volume (or flow) is not regulated and may vary depending on patient's condition and respiratory mechanics. This is the reason why flow and volume should be cautiously monitored with pressure mode of ventilation.

Figure 3: Illustration of airway pressure and flow curves in flow (volume) and pressure modes of ventilation

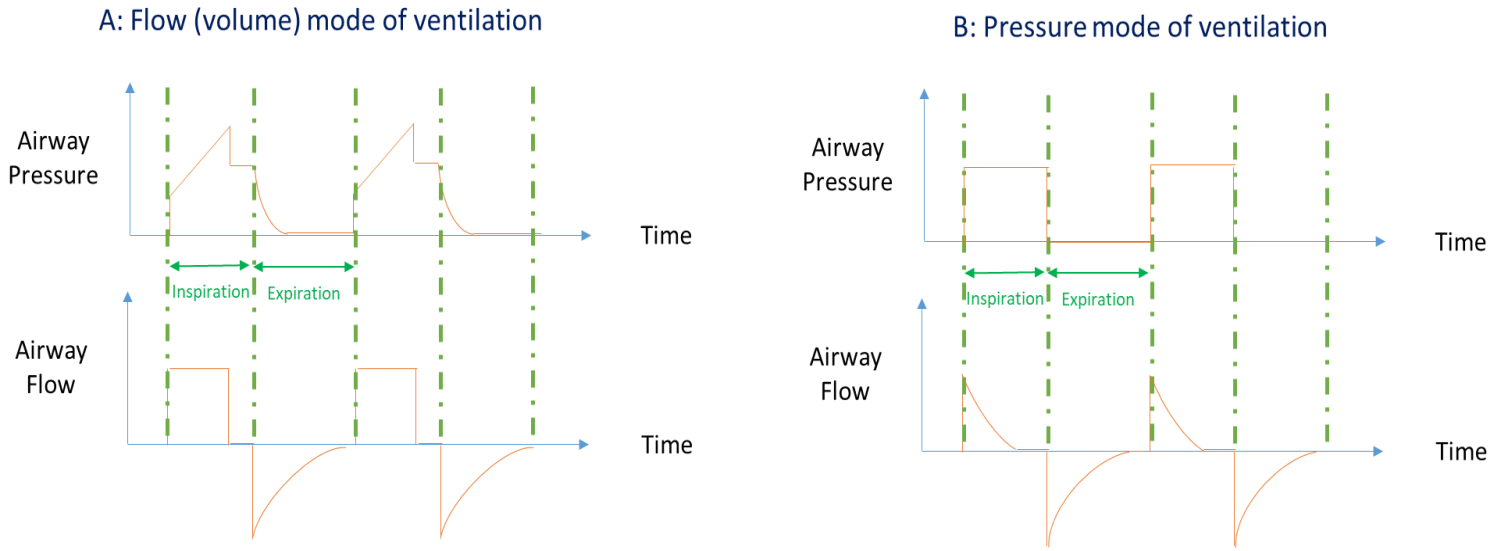

Figure 3: From top to bottom illustration of ventilator curves of airway pressure and airway flow according to time. **Panel A** illustrates a flow (volume) mode of ventilation and **panel B** illustrates a pressure mode of ventilation. Green dotted lines delimit inspiration from expiration. For each ventilator mode, two consecutive breaths are shown.

Modes of ventilation: the cycling

After the initiation and the delivery of the regulated variable during inspiration – either volume or pressure – the transition from inspiration to expiration is called cycling.

- The cycling can be time-triggered, meaning that inspiratory time is set on the ventilator (either with flow or pressure regulated modes). Once inspiratory time is reached, transition from inspiration to expiration ensues, allowing passive expiration. Pressure goes back to the positive end expiratory pressure (PEEP) set on the ventilator.
- The cycling can also be patient-triggered for pressure support ventilation, meaning that transition from inspiration to expiration is launched when patient flow decreases below a threshold value set on the ventilator corresponding to a percentage of the maximum inspiratory flow.
- Other cycling settings have been proposed in older (IPPB), hybrid or more sophisticated modes of ventilation (PAV - NAVA).

1.1.4. Main working principles of emergency ventilators

Pneumatic ventilators

A pneumatically powered ventilator uses compressed gas as its power source. Most conventional intensive care unit (ICU) ventilators are pneumatically powered and require two sources of pressurized gas for oxygen and air to generate ventilation. Ventilators powered by compressed gas usually have internal pressure-reducing valves so that the normal operating pressure is lower than the source pressure. Ventilators can operate without interruption from hospital-piped gas sources, which are usually regulated to 50 psi (pounds per square inch) but are subject to periodic fluctuations. Minimal pressure required to properly manage ventilation depends on patients respiratory mechanics and demand. This pressure is often called "working pressure". Importantly, most pneumatically powered ICU ventilators still require electrical power to support their control functions. The output control valve regulates the flow of gas to the patient. It may be a simple on/off exhalation valve, as in the Newport E100i transport ventilator (Newport NMI Ventilators; Newport Medical Instruments, Newport Beach, CA). Alternatively, the output control valve can shape the output waveform, as in most of modern conventional ICU ventilators with a proportional valve.

Venturi pneumatic ventilators

Several transport ventilators are based on the combination of pneumatic systems with Venturi mechanism for gas mixing. Thus, they require only one source of pressurized gas for oxygen. The "Venturi-distributor" technology works as a flow generator. It is based on the principle that a high-pressure oxygen is delivered through a small conduit at a very high speed. Due to Bernoulli's law, once the high-speed oxygen moves into a larger conduit, it generates a decrease of the lateral pressure, which becomes subatmospheric and entrains air from the external atmosphere (15). In this way, starting from a pure flow of oxygen, it is possible to achieve a much higher flow of a mixture of oxygen and air, allowing to vary inspired fraction of oxygen (FiO2). Those systems can be coupled with a proportional inspiratory valve like with the Oxylog 3000. Interestingly, Venturi pneumatic transport ventilators have been used for decades both for in- and out-of-hospital transport. The main limit of the Venturi system is that air entrainment is dependent on the impedance of the patient. For instance, high respiratory system resistance may result in a significant drop of inspiratory flow associated with a concomitant FiO2 increase. Nevertheless, their robustness and their relative technological simplicity could potentially facilitate massive industrial production.

Turbine ventilators

Others transport ventilators use an internal turbine for pressurization, as illustrated on figure 4. Indeed, room air is injected into the ventilator through a filter and the turbine powered by a battery generates flow. Nevertheless, those systems need a pressurized gas source of oxygen to reach high FiO2 values. Low-pressure oxygen source at around 15L/min may also be used with specific turbine ventilators, but the resulting FiO2 will be theoretically limited by the oxygen flow source. Interestingly, performances of turbine ventilators are often excellent and have been well described (1, 16). The most valuable advantage of turbine over the simple pneumatic systems lead in its ability to generate pressure even with leaks. As results, turbines are perfectly adapted to invasive or non-invasive ventilation. In flow (volume) control mode, an inspiratory proportional valve or a smart algorithm accelerating turbine speed during insufflation to maintain flow constant are required.

Figure 4: Photo of Monnal T60 turbine

Figure 4: photo of the turbine present in the Monnal T60 ventilator (Air Liquide Medical Systems, Antony, France)

Piston ventilators

Piston ventilators can be used as transport ventilators such as the Newport HT 50 and are also present in the operating room as an integral part of anesthesia workstations. They work with electricity as their driving force and do not require a driving gas. The piston ventilator design is uniquely suited to deliver tidal volume accurately under a large variety of clinical conditions, as shown in figure 5. Since the area of the piston is fixed, the volume delivered by the piston is directly related to the linear movement of the piston. When the user sets a volume to be

delivered to the patient in volume mode of ventilation, the piston moves the distance necessary to deliver the required volume into the breathing circuit. In pressure mode of ventilation, the rigid coupling between the piston and its drive mechanism allows for fine control over the movement of the piston and continuous adjustment of inspiratory flow to maintain the desired inspiratory pressure.

Figure 5: Working principle of a piston ventilator

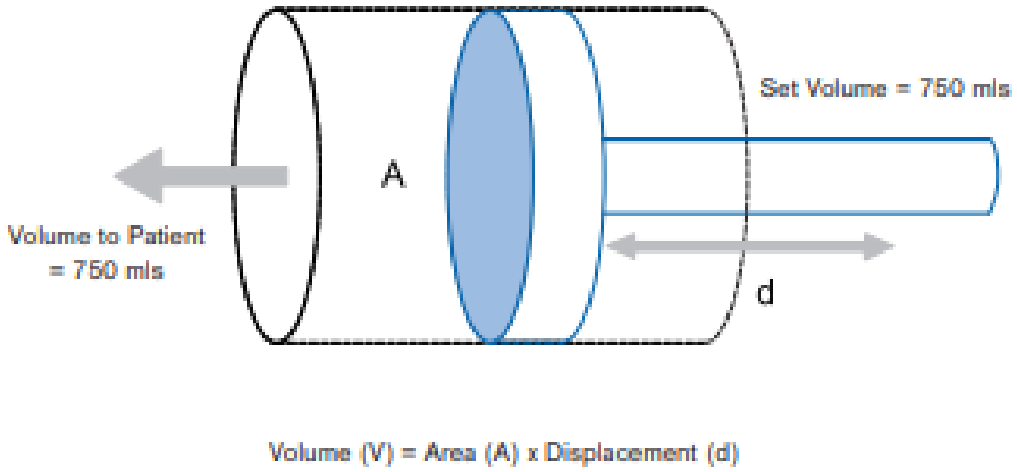

Figure 5: Illustration of the working principle of a piston ventilator (shematic obtained from Draeger website). The volume delivered by the piston is determined by the distance the piston moves. When a volume is set to be delivered (e.g. 750 ml), the piston is moved the distance required to deliver the set volume to the patient.

(https://www.draeger.com/library/content/9049447_the_anesthesia_ventilator_8seitig_en_101209_fin.pdf)

1.1.5. Bench models to test and compare ventilators

Several bench models exist to evaluate the performances of ventilation devices, especially ventilators.

- The landmark setup (also the simplest one) is the TTL Michigan test lung (Michigan Instruments, Kentwood, MI, USA) that consists of a portable analog dual lung system which accuratley simulates human pulmonary function for training or testing ventilators under simulated load conditions. It is possible to tailor resistance and compliance of the test lung to simulate different types of patients and provide accurate representations of adult pulmonary mechanics. It is possible to measure volumes, pressures and flow rates of medical equipment. In addition, it is also possible to simulate spontaneous breathing on this model. One chamber of the test lung is defined as the driving lung while the other chamber is connected to the ventilator being tested. A lung-coupling clip allows a connection between the two chambers, so that a positive pressure created in the driving lung (by the driving ventilator) induces a negative pressure in the experimental lung, leading to trigger the ventilator tested.
- A more complex bench model is the ASL 5000 test lung (Ingmar, Pittsburgh, PA, USA), a sophisticated breathing simulator capable of simulating a full range of patients – neonatal to adult. The ASL 5000 is able to breathe spontaneously even while being ventilated. It is possible to tailor resistance and compliance, but also the characteristics (shape, amplitude…) of the muscle pressure generating spontaneous breathing.

Figure 6: Photos of Michigan TTL tests lung and ASL 5000 simulator

Panel A ***Panel B***

Figure 6*: This figure shows the Michigan test lung on panel A and the ASL 5000 lung simulator on panel B*

1.2. Circulation and ventilation during cardiopulmonary resuscitation

Cardiac arrest is one of the most significant cause of mortality with an incidence of nearly 55 cases per 100‘000 person-years worldwide. The red thread of cardiac arrest management lies in the chain of events called “chain of survival” that combines the recognition of cardiac arrest, the alert of emergency services, and the rapid initiation of Cardiopulmonary resuscitation (CPR). CPR refers to the management of cardiac arrest patients. It consists mainly of chest compressions (CC) allowing to generate circulation and defibrillation to restore when needed a shockable rhythm into a stable perfusing heart rhythm, called return of spontaneous circulation (ROSC) (8). Ventilation is not necessary at the initial phase but becomes rapidly essential to properly manage gas exchange.

1.2.1. Circulation during CPR

As a reminder, heart anatomy is described in figure 7.

Figure 7: Heart anatomy

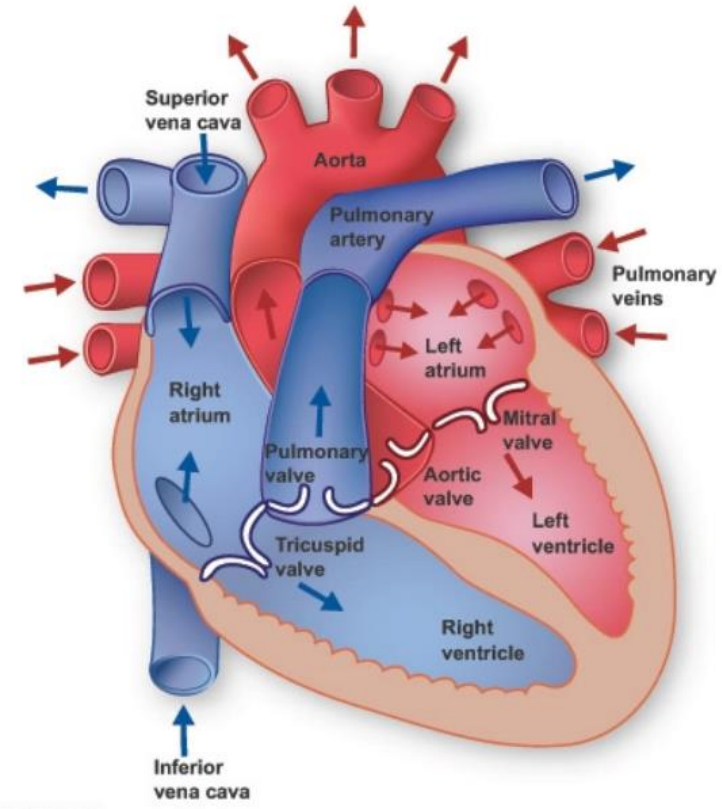

Figure 7: Illustration of heart anatomy (figure obtained from *https://www.texasheart.org/heart-health/heart-information-center/topics/heart-anatomy/* website). The heart has 4 chambers. The upper chambers are the left and right atria, and the lower chambers are the left and right ventricles. Four valves regulate blood flow: the tricuspid valve (between the right atrium and right ventricle), the pulmonary valve (between the right ventricle and the pulmonary arteries), the mitral valve (between the left atrium and the left ventricle) and the aortic valve (between the left ventricle and the aorta).

1.2.1.1. The three phases of cardiac arrest

Weisfeldt and Becker (17) proposed a time-sensitive model for the treatment of cardiac arrest, with three phases: electrical, circulatory, and metabolic. According to this model of cardiopulmonary resuscitation (CPR), the optimal treatment for cardiac arrest is phase specific and depends on ischaemic time (i.e. time from collapse to return of spontaneous circulation).

1. **Phase I**: During the first "**electrical**" phase, optimal resuscitation occurs with purely correction of an electrical problem by defibrillation (in case of ventricular fibrillation). At this point, there is no need for artificial circulation (chest compressions) and a very limited metabolic or cardiac embarrassment.
2. **Phase II**: The "**circulatory**" phase is defined by a lack of oxygenation resulting in a drop of myocardial ATP to critical levels; thus limiting the efficiency of defibrillation. There is a need to provide a brief period (90 s to 3 minutes) of effective chest compressions in order to boost myocardial ATP stores and increase the likelihood that a perfusing rhythm will result after a defibrillation shock (18). In addition, circulation must be maintained by minimizing interruptions to obtain optimal results. Defibrillation after providing circulatory support is required for ventricular fibrillation (19).
3. **Phase III**: In the "**metabolic**" phase, there is an increasing evidence of metabolic embarrassment, limiting the effect of artificial circulation and proper electrical treatment (defibrillation). In this case, extracorporeal cardiopulmonary resuscitation (commonly known as ECPR) may be considered.

Recent findings suggest that the transition from the electrical to circulatory phase may occur at approximately 5 minutes, and the circulatory phase may extend to approximately 15 minutes (20, 21). Ideally, this time-sensitive approach may work but the priority of intervention based on this model has not been definitively demonstrated (22, 23).

1.2.1.2. Mechanisms of blood flow

The mechanisms by which chest compressions produce and maintain blood flow during cardiopulmonary resuscitation are still debated. Two main competing theories exist.

Cardiac pump theory

Kouwenhoven et al. (24) were the first to investigate the mechanisms of blood flow and proposed the cardiac pump theory. This theory postulates that blood flow is driven by direct compression of the heart. The hypothesis is that during compression, the heart is directly squeezed between the spine and the sternum, generating blood flow. During compression, both ventricles are squeezed resulting in a rise in intraventricular pressure (active "systolic" contraction mechanism). Ventricular direct compression results in the closure of the atrioventricular valves generating forward flow from the ventricles to the arteries. This ejection of blood reduces ventricular volume. During decompression, a passive "diastolic" suction mechanism is generated by the reduction in the intraventricular pressure allowing the atrioventricular valves to open and ventricular filling. This sequence of events resembles the normal cardiac cycle.

Different studies exploring the mechanisms of blood flow during cardiac arrest supported this "cardiac pump" theory, in dog models and also clinical data using echocardiography (see table 1 obtained from Cipani et al. study (25)).

Thoracic pump theory

In the early 1980s, some studies proposed a different explanation for the mechanism leading to blood flow during CPR. According to this alternative theory, blood flow does not occur by direct cardiac compression, but rather by a thoracic pump mechanism. During compression, forward blood flow is generated by a uniform increase of intrathoracic pressure within the whole intrathoracic compartment that exceeds extrathoracic vascular pressure. In other words, the blood is forced to flow from the thoracic to the systemic vessels, with the heart acting as a passive conduit rather than a pump. Retrograde venous flow is inhibited by the collapse of veins. Importantly and unlike the cardiac pump theory, the mitral valve (separating left atrium from left ventricle) remains open throughout the whole cardiac cycle, and ventricular sizes should not change significantly. Chest decompression is essential during CPR because the generation of negative intrathoracic pressure increases venous return, improving hemodynamics by providing cardiac preload prior to the next chest compression phase (26). As

for the cardiac pump theory, several studies and observations provided support to this theory (see table 1 obtained from Cipani et al. (25)).

Which theory?

Based on the current evidence, a single theory is probably not sufficient to explain how chest compressions produce blood flow. Observations suggest that simultaneous mechanisms might be involved. It is possible that the relative importance of these mechanisms depends on several factors, including delay from collapse to starting of resuscitation, compression depth and rate. Noticeably for both theories, effective circulation requires to limit CC interruption.

Interestingly, Porter et al. (27) reported on a cohort of 17 adult patients two distinct groups during closed-chest CPR, one matching the cardiac pump theory and the other matching the thoracic pump theory with evidence of mitral valve opening during chest compression. Patients whose mitral valves were open ("thoracic pump") showed worse clinical outcomes compared to the patients supporting the "cardiac pump" theory.

Newer hypotheses including the "atrial pump", the "lung pump", and the "respiratory pump" theories were also proposed but their clinical relevance remains to be demonstrated (28, 29).

The literature review from Cipani et al. (25) concluded that the cardiac pump theory or a combination of the cardiac pump and thoracic pump theory might best represent the most realistic mechanism of forward flow into the aorta during CPR in humans. The cardiac pump theory is likely to be the main mechanism during the initial phases of CPR while the importance of the thoracic pump mechanism may increase during resuscitation, becoming more relevant in prolonged CPR. It is important to have in mind that results obtained in animal models concerning the main mechanisms of blood flow during CPR are not directly translatable to human cardiac arrest, as thorax anatomy may differ between the different models.

Table 1: Main studies exploring the mechanisms of blood flow during cardiopulmonary resuscitation (table obtained from Cipani et al. study (25))

First author	Technique	Supported theory
Kouwenhoven (1960)[8]	Clinical	Cardiac pump
Rudikoff (1980)[61]	Esophageal balloon catheter	Thoracic pump
Rosborough (1981)[15]	Clinical	Thoracic pump
Werner (1981)[62]	TTE	Thoracic pump
Maier (1984)[9]	TTE and TOE dog model	Cardiac pump
Higano (1990)[11]	TOE	Cardiac pump
Redberg (1993)[12]	TOE	Cardiac pump
Pell (1994)[13]	TOE	Cardiac pump
Ma (1995)[5]	TOE	Left atrial pump
Shaw (1997)[4]	Clinical	Lung pump
Kim (2008)[14]	Contrast echocardiography	Cardiac pump
Convertino (2011)[7]	Impedance threshold device	Pulmonary pump

TOE: transesophageal echocardiography; TTE: transthoracic echocardiography.

1.2.1.3. How to assess circulation during CPR?

1.2.1.3.1. Circulation during CPR

Following a cardiac arrest, the blood supplying the heart muscle through the coronary arteries, also called myocardial blood flow or coronary blood flow, is reduced and completely dissipated after 5 min (30). The blood that flows through the pulmonary circulation and that is necessary for gas exchange in the lungs also decreases after cardiac arrest and disappear over time. Importantly, the heart stops pumping blood to vital organs and especially the brain. With a decrease in blood flow to the brain, the victim falls unconscious. The brain can suffer damage in as few as three minutes without proper blood flow. Without blood flow to the brain, there can be irreversible damage (31).

Theoretically, CPR should properly manage the different circulations (heart, pulmonary, systemic, cerebral) to be optimal. If we focus on the short-term prognosis, it is important to consider the acute and immediate effect of cardiac arrest (heart stops functioning), and the necessity to resume and enhance coronary blood flow (heart circulation) to favor the occurrence of return of spontaneous circulation. Pulmonary circulation is also necessary for adequate gas exchange and oxygenation of the blood to increase the chances of resumption of cardiac activity. In parallel, it is definitely crucial to support cerebral circulation to protect the brain as much as possible considering the dramatic long-term consequences induced by brain hypoxia. (32).

Distinct mechanisms are at stake to drive the different circulations (coronary, pulmonary or cerebral). CPR solutions may favor either one or several of these circulations depending on the chosen approach, and their physiologic determinants should be recognized in order to optimize the way CPR is performed. This is the reason why consistent and relevant circulation monitoring parameters are necessary in research to evaluate CPR strategies and their impact on the respective circulations. The hemodynamic parameters usually considered to assess circulation physiology during cardiopulmonary resuscitation are described below.

1.2.1.3.2. Cardiac output

Why measuring this parameter ?

Cardiac output (CO) is defined as the volume of blood ejected by the ventricle per minute; and thus enables an estimation of circulation efficacy. This volume of blood is called the stroke volume. During CPR, cardiac output is significantly reduced and varies depending on chest compression quality. Interestingly, observations in pigs confirmed that the increase in venous partial pressure of CO2 ($Pvco_2$) in the blood and the concurrent decrease in end tidal CO2 ($EtCO_2$) in the lungs reflect a critical reduction in cardiac output during CPR. Indeed, alveolar blood flow reduction limits carbon dioxide clearance by the lung that fails to keep pace with systemic CO2 production (33). Aufderheide et al. (34) have shown that both high-quality chest compression (adequate depth, force, and duration) and complete chest wall decompression are needed to maximize stroke volume and improve venous filling. Preventing the chest to recoil completely during decompression decreases cardiac output (35) and thus venous return.

How to measure this parameter ?

Cardiac output is the product of heart rate (HR) and stroke volume (SV) and is measured in liters per minute. The stroke volume is the volume of blood ejected per each beat or systole.

$$cardiac\ output = frequency \times stroke\ volume$$

Different approaches can be used to measure blood flow such as the thermodilution technique or the Fick method.

- Thermodilution is the most popular method used for measuring cardiac output (CO) in the clinical setting during CPR. The transpulmonary thermodilution technique (see figure 8) measures distally via an arterial line catheter equipped with a thermistor the temperature change (decrease) of a fixed volume of cold saline injected into the right atrium via a central venous catheter (36). The cardiac output can be estimated based on the decrease in blood temperature along time (see figure 8).

Figure 8: illustration of thermodilution technique to measure cardiac output

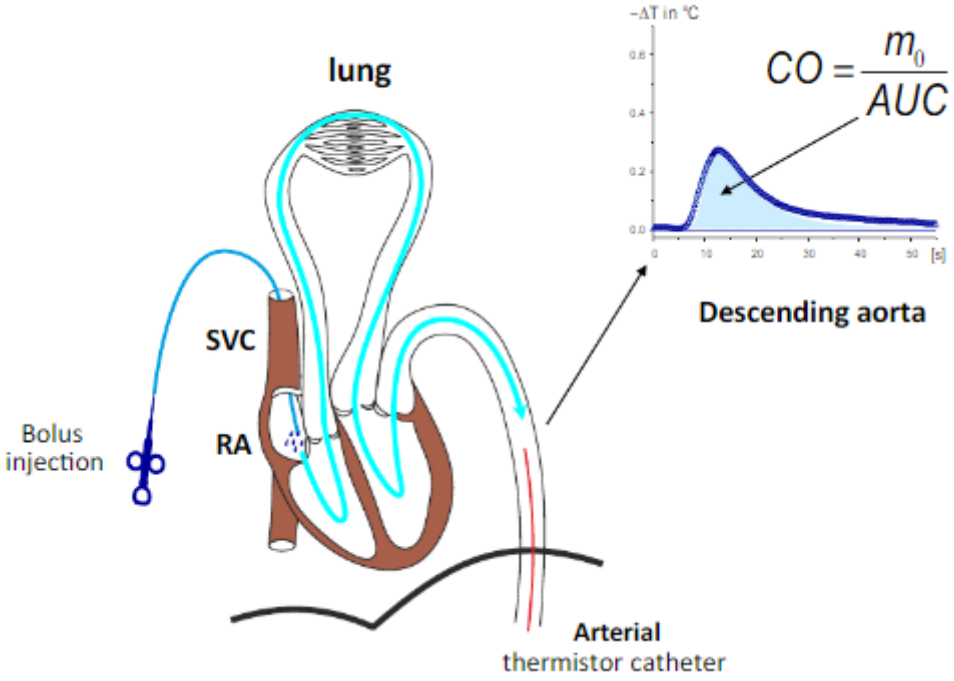

Figure 8: Illustration of the working principle of the thermodilution method to measure cardiac output (figure obtained from Teboul et al. study (37)). After injecting a cold indicator (usually saline) into the right atrium (RA) via a central venous catheter, the resultant thermodilution curve (upper right of the figure) can be derived in the descending aorta. Here, this is an example of transpulmonary thermodilution, as temperature change is measured within the pulmonary circulation. The cardiac output (CO) is calculated based on the amount m_0 of injected cold saline solution and the area under thermodilution curve (AUC) related to the decrease in blood temperature along time.

- SVC = superior vena cava
- RA = right atrium

- The Fick principle relies on the assumption that the total uptake of oxygen by the peripheral tissues is equal to the product of the blood flow (cardiac output) and the arterial-venous oxygen concentration difference (38). Cardiac output is therefore calculated using the following formula:

$$Cardiac\ output = \frac{oxygen\ consumption}{Arteriovenous\ oxygen\ gradient}$$

Implications and limits

Studies in dogs and pigs suggested that during optimal CPR, cardiac output is between 25 and 40% of pre-arrest values (33). It has also been shown that optimal cardiac output occurred at a

compression rate of 120 compressions/min (39). This value should be monitored to assess the efficacy of a CPR strategy on circulation.

1.2.1.3.3. Coronary blood flow

Why measuring this parameter ?

The coronary arteries are blood vessels responsible for supplying the heart with oxygen. By monitoring the transit of blood through the coronary arteries, it measures how well the blood flows within the heart. Coronary blood flow is retrograde during the compression phase and antegrade (moving forward) during the decompression phase (40). Due to its difficulty to measure in clinical settings, there is a very limited amount of clinical data with coronary blood flow measurements.

How to measure this parameter ?

Coronary blood flow can be measured by different techniques, including electromagnetic cuff flow probes and the radiomicrosphere technique (41). We will focus on electromagnetic cuff flow meter, whose working principle is based on Faraday's law resulting in electromotive force. The cuff flow probes produce a magnetic field, and as the blood flows within this magnetic field, a voltage is induced, whose magnitude is proportional to the velocity and volume of the blood flow (42). This voltage is retrieved by the blood flow transducer probes, and the coronary blood flow is calculated. The magnetic flow probe is usually inserted and fitted around the circumflex artery for coronary blood flow estimation (41). Nevertheless, coronary blood flow measurement remains very challenging, especially in the clinical setting.

Implications and limits

As its measurement is challenging, coronary blood flow is rarely reported in the literature. Other circulation parameters have been investigated to estimate coronary circulation. Coronary perfusion pressure has been shown as the primary determinant of coronary blood flow, and appears easier to measure during CPR. The coronary perfusion pressure will be investigated more in details in the next section.

1.2.1.3.4. Coronary perfusion pressure

Why measuring this parameter ?

Coronary perfusion pressure (CoPP) during cardiac arrest is a key component allowing to assess the efficacy of resuscitation. CoPP has been correlated with both coronary blood flow generated by chest compressions (43) and ultimately with resuscitation outcome (44). Studies have demonstrated a positive correlation between coronary perfusion pressure and return of spontaneous circulation. In fact, the probability of ROSC is low when the coronary perfusion gradient is low, as shown in humans (45) and in animal models (46, 47).

How to measure this parameter ?

CoPP (measures in mmHg) corresponds to the aortic-to-right atrial pressure gradient during the diastolic or decompression portion of chest compression-decompression, as shown on figure 9. Pressure transducer catheters can be introduced through the left femoral artery and vein for continuous measurement of aortic pressure and right atrial pressure respectively.

$$CoPP = aortic\ pressure - right\ atrial\ pressure$$

Figure 9 : Tracings of Aortic blood pressure and right atrial pressure obtained on a pig model during CPR

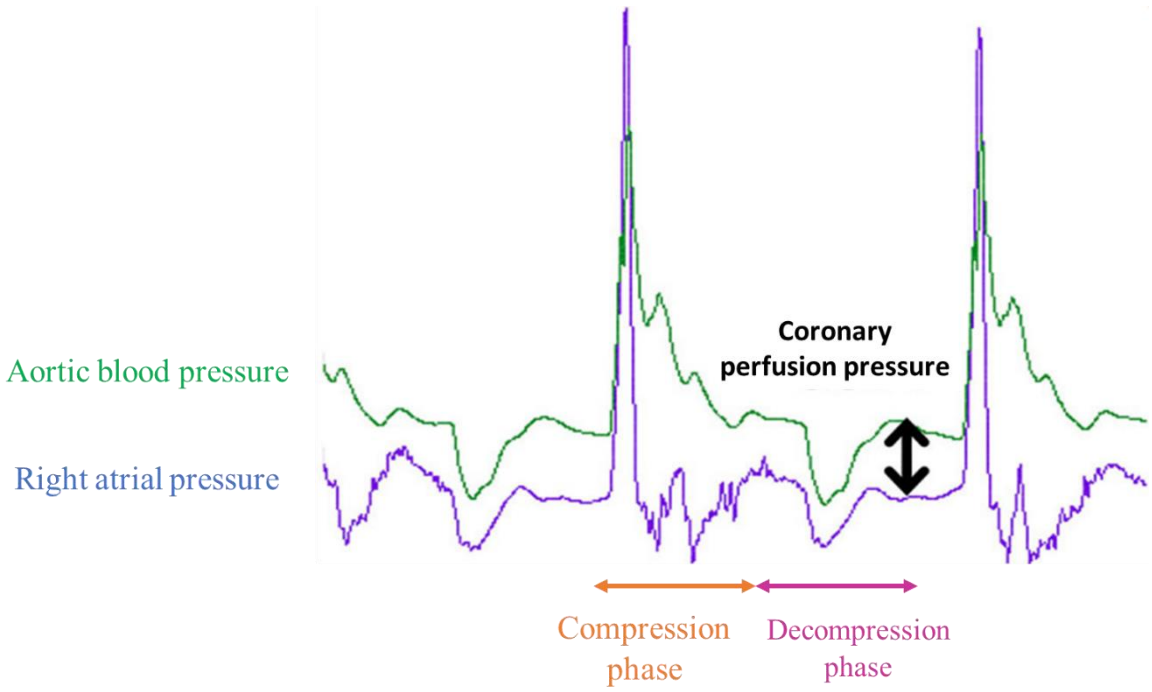

Figure 9: This figure was derived from Fletcher et al. study (48). It depicts tracings of Aortic blood pressure and right atrial pressure obtained in an experimental swine ventricular fibrillation model during CPR. Those signals are used to calculate coronary perfusion pressure (CoPP). The green tracing is aortic blood pressure and the blue tracing is right atrial pressure. The orange horizontal arrow (including the peak) corresponds to the compression phase of CPR, while the purple horizontal arrow represents the decompression (or relaxation) phase. Coronary blood flow and oxygen delivery occur during the relaxation phase of chest compressions and is correlated to coronary perfusion pressure (CoPP), which corresponds to the difference between aortic pressure and right atrial pressure at the end of the relaxation phase, as denoted by the double arrowed vertical line. The tracing was obtained during mechanical chest compressions (100/min) delivered by the LUCAS device to an anesthetized pig with ventricular fibrillation arrest.

Implications and limits

CoPP remains the mostly used parameter to evaluate coronary circulation (43, 46). Of note, it does not provide a perfect surrogate for coronary blood flow as this measurement is also likely to be impacted by pressure on coronary microvessels (44). Despite its difficulty to acquire in clinical settings, especially because of the time needed to insert the pressure-measuring catheters close to the atrium, CoPP has been measured in patients undergoing CPR. Alternative non-invasive measures of coronary perfusion could be of high added value. Expired end-tidal carbon dioxide has been one suggested possibility (44).

1.2.1.3.5. Carotid blood flow or cerebral blood flow (CeBF)

Why measuring this parameter ?

Cerebral blood flow is a major neuro-prognostic factor during CPR. It is defined as the blood volume that flows per minute in the brain tissue. The carotid arteries are a pair of blood vessels located on both sides of the neck that deliver blood to the brain. Carotid blood flow takes over a minute to reach optimal plateau levels following the initiation of chest compressions. Even brief interruptions of compressions result in a dramatic reduction in carotid blood flow (49).

How to measure this parameter ?

Ultrasound measurement of carotid blood flow during CPR is also feasible. This technique indirectly evaluates cerebral perfusion but cannot provide a direct measure of the blood that has been delivered to a brain region (50).

Direct methods for measuring Cerebral blood flow exist and include for example single-photon emission computed tomography (SPECT), positron emission tomography (PET) or magnetic resonance imaging (MRI) with contrast agents (51). All these methods are based on the measurement of the amount of a tracer delivered to the human brain tissue by blood flow (50).

Implications and limits

Much of the morbidity associated with cardiac arrest survivors can be attributed to global brain hypoxic ischemic injury (52). It has also been shown that adequate cerebral perfusion is critical for preservation of brain function (53, 54). An animal study reported that if CPR is started immediately and coronary perfusion pressures are held above 25 mmHg, cerebral blood flow was maintained at approximately 60% of pre-cardiac arrest values. But when CPR was delayed for 12 min, even a high level of coronary perfusion pressure failed to restore cerebral blood flow, demonstrating the potential devastating effects of delaying CPR initiation (49, 55). Cerebral perfusion pressure is the primary determinant of cerebral blood flow and easier to measure during CPR.

1.2.1.3.6. Cerebral perfusion pressure

Why measuring this parameter ?

Cerebral perfusion pressure (CePP) is the net pressure gradient that drives blood to cerebral tissue (26). A high cerebral perfusion during CPR may favor better neurological outcomes. The force of chest compressions is transmitted in the brain and increase intracranial pressure during the compression phase. It means that the positive pressure generated during CC may in turn affect cerebral perfusion. Additionally, cerebral perfusion pressure may decrease markedly when delivering positive pressure ventilation. Ventilation may generate high intrathoracic pressures that can be conducted through the spinal cord veins and cerebrospinal fluid, which in turn may increase dramatically intracranial pressure, aggravating cerebral perfusion pressure and post-resuscitation brain injury (49, 56).

How to measure this parameter ?

CePP is the difference between the mean arterial pressure (MAP) and the intracranial pressure (ICP), measured in millimeters of mercury (mm Hg).

$$CePP = MAP - ICP$$

The mean arterial pressure measurement will be detailed in the next section. Considering ICP, two main measurement methods exist.

- An intraparenchymal microsensor can be utilized. Microtransducer-tipped and fibreoptic monitoring systems can be inserted into the brain parenchyma through a cranial access device or into the subdural space via a craniotomy. The rate of complications is relatively low, but the resulting ICP value may not represent global pressure, especially in the injured brain (57).
- An intraventricular catheter (more invasive) can also be used to estimate global ICP while offering in vivo calibration and therapeutic drainage of cerebrospinal fluid. To insert an intraventricular catheter, a hole is drilled through the skull. The catheter is inserted through the brain into the lateral ventricle. This area of the brain contains the cerebrospinal fluid, a liquid that protects the brain and spinal cord. Nevertheless, catheter placement remains challenging and at risk of catheter-associated ventriculitis (57).

Implications and limits

Cerebral blood flow during cardiopulmonary resuscitation (CPR) is a major determinant of neurological patient's outcome although not clinically feasible for routine assessment and monitoring. In this context, a surrogate marker for cerebral perfusion during CPR is highly desirable, and CePP is the most promising one (58). Indeed, an optimal cerebral perfusion pressure is associated with better neurological outcomes (55).

1.2.1.3.7. Cerebral oximetry

Why measuring this parameter ?

Although the weight of the brain only accounts for approximately 2% of the total body weight, cerebral blood flow (CBF) volume accounts for 15–20% of the cardiac output and roughly 20% of the whole-body oxygen consumption (59). Tissue oximetry monitors cerebral oxygenation, as it measures the amount of oxygen entering the brain. Even when CPR is performed according to guidelines, it can only deliver approximately 20% of normal blood flow to the brain (60). Without sufficient blood flow and oxygen, the brain stops working and the cells may undergo changes that lead to damage and potentially cell death. Interestingly, patients with good resuscitation outcomes have significantly higher cerebral oxygenation saturations during resuscitation than their counterparts (61).

How to measure this parameter ?

The Near infrared spectroscopy (NIRS) is the main non-invasive technique dedicated to measure cerebral blood oxygen saturation (ScO2). This technology has been used during cardiac arrest because of its ability to give measures in low-blood-flow situations. The spectrometer emits near-infrared rays into the patient's forehead and is based on the different spectral absorption features of oxyhemoglobin (HbO2) and reduced hemoglobin (HbR) within the near-infrared optical window (700–950 nm) to detect changes in oxygen saturation in the brain (62).

Implications and limits

Higher cerebral oxygenation during CPR is associated with a higher rate of return of spontaneous circulation (ROSC) and neurologically favorable survival to hospital discharge (61). Thus, achieving better brain oxygenation during resuscitation may optimize the chances of cardiac arrest favorable outcomes.

1.2.1.3.8. Arterial blood pressure

Why measuring this parameter ?

During CPR, arterial blood pressure reflects the functioning of the left ventricle induced by the pumping action of the chest compressions. During each compression (termed systole), blood pressure increases allowing the ejection of the blood through the aorta. The highest systemic pressure generated within the arteries is termed the "systolic pressure". During chest decompression, the ejection of the blood through the aorta stops and the left ventricle relaxes and refills: this phase is called diastole. During diastole, the arterial pressure drops as the arterial blood rapidly flows out of the arterial compartment into the capillaries. The lowest arterial pressure during this rest phase of the left ventricle is termed the "diastolic pressure". It is also possible to calculate an average arterial blood pressure throughout one chest compression cycle comprising systole and diastole. It is called the mean arterial blood pressure (MAP). Thus, as for the intracranial pressure, the pressure generated by the chest compressions on the thorax is transmitted to the arterial pressure, creating chest-compressions induces arterial pressure oscillations.

How to measure this parameter ?

A cuff manometer can be used to estimate the systolic arterial pressure during CPR by palpating the brachial artery or listening over it for flow with a peripheral Doppler device. More accurate

invasive measurements of systolic and diastolic pressure can be obtained by inserting an arterial line into the radial, brachial, or femoral artery.

Implications and limits

Interestingly, maintenance of both systolic and diastolic arterial pressures is essential during CPR. Because flow to most vital organs (except the heart) occurs during systole, a minimal systolic arterial pressure of 50 to 60 mm Hg is usually required to resist arteriolar collapse (35). Diastolic pressure is also important because it is a critical determinant of the coronary perfusion pressure.

1.2.1.3.9. Circulation variation during ventilation

Recordings of circulation parameters obtained in an animal model of CPR are displayed on figure 10. Continuous chest compressions were applied while positive pressure mechanical ventilation was delivered with a transport ventilator in volume controlled mode. Interestingly, circulation parameters are oscillating in concert with ventilation. Insufflation time is associated with a global increase of aortic blood pressure, right atrial pressure, intracranial pressure, coronary perfusion pressure and cerebral perfusion pressure waveforms, that gradually return to baseline during expiration time. Those ventilation-induced waveforms on circulation parameters emphasize the potential impact of ventilation on circulation, and the importance to properly manage ventilation. In fact, ventilation interactions with circulation is a complex process that can render ventilation either harmful or beneficial for circulation. Too much ventilation may jeopardize circulation by mainly affecting venous return and also generating respiratory alkalosis. Interestingly, high intrathoracic pressure associated with ventilation may enhance heart ejection during chest compression (63) but unfortunately, may jeopardize cerebral perfusion by increasing intracranial pressure. Interestingly, a method for newborn cardiac arrest patients consists in providing continuous chest compression superimposed with a high distending pressure or sustained inflation (64). Even if current available data is mostly limited to animal experiments, this technique significantly improved time to return of spontaneous circulation (ROSC) and survival (65). Different studies demonstrated an increased carotid flow associated with sustained inflation, and improved brain perfusion by enhancing cerebral perfusion pressure (66), showing the potential beneficial effect of ventilation on circulation.

Figure 10: Illustration of the main circulation parameters recorded on a pig test animal

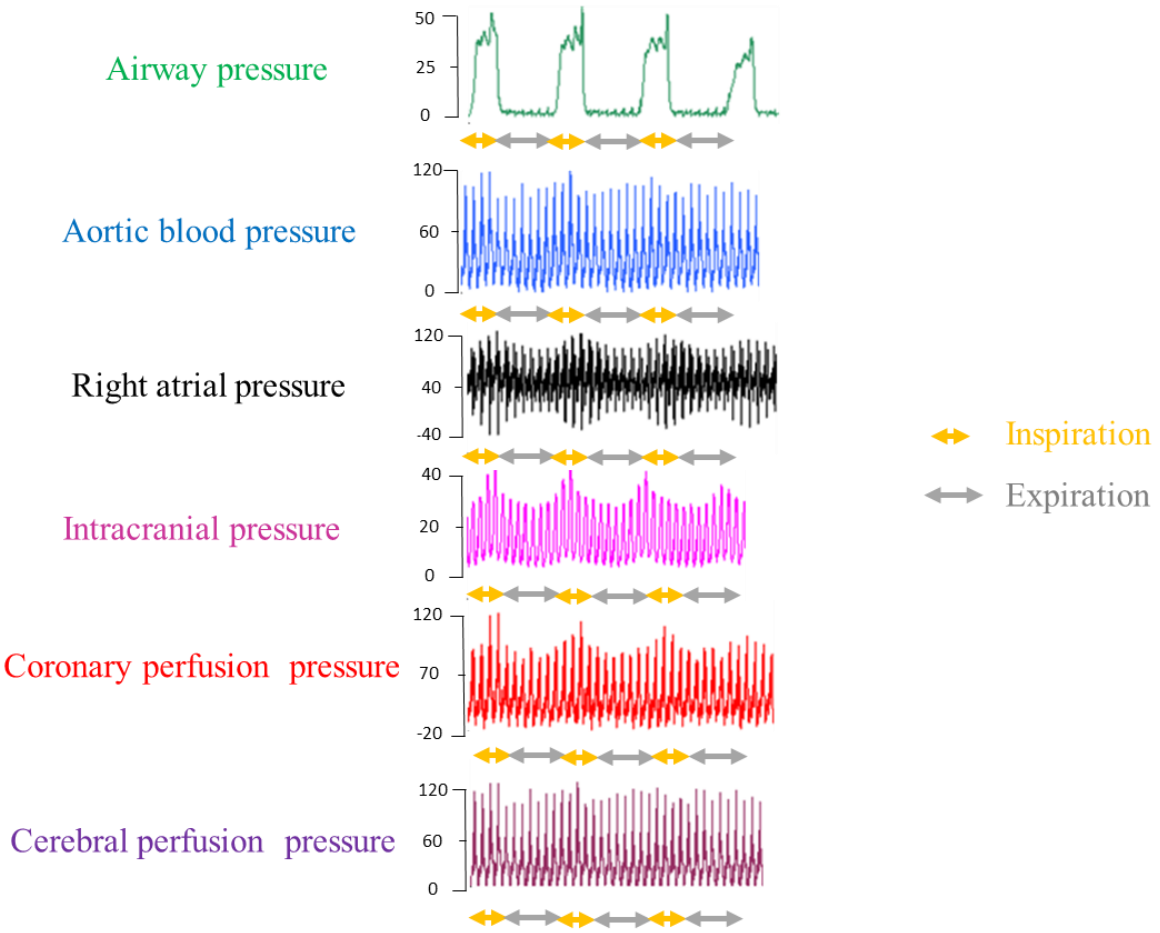

Figure 10: Recording tracings of airway pressure, aortic blood pressure, right atrial pressure, intracranial pressure, coronary perfusion pressure (aortic blood pressure minus right atrial pressure), cerebral perfusion pressure (mean arterial pressure minus intracranial pressure) during CPR in volume controlled mode of ventilation. Vt was set at 15 ml/kg and automatic chest compressions were applied with the LUCAS system. Three complete ventilatory cycles are displayed. Inspiration is shown with the orange arrow and expiration with the grey arrow.

1.2.1.4. Evolution of circulation guidelines

High quality cardiopulmonary resuscitation (CPR) is recognized as one of the main determinants of survival. International CPR guidelines allow to guide rescuers in the management of cardiac arrest patients by suggesting the best practices and solutions available to improve outcome, based on a deep investigation of CPR literature. Those guidelines are written by a group of experts and cover the entire process of CPR, from basic life support to advanced life support. Guidelines on high quality CPR are intended to optimize circulation. Nevertheless, ventilation has been neglected for years and its adverse effects on circulation are now clearly recognized (7).

Main circulation recommendations for adults are as follows:

• Start chest compressions as soon as possible.

• Hand position: deliver compressions on the lower half of the sternum (‘in the center of the chest’).

• Depth: compress the chest to a depth of at least 5 cm but not more than 6 cm

• Frequency: Compress the chest at a rate between 100 and 120 per minute.

• Decompression: Allow the chest to recoil completely after each compression; do not lean on the chest.

• CPR fraction: CPR fraction is the percentage of time during which chest compressions are performed over the entire duration of the CPR. A CPR fraction above 60% is recommended (67, 68).

1.2.2. Ventilation during CPR

The objective of ventilation during CPR is to properly manage gas exchange - bring oxygen (O2) to the blood during insufflation and remove CO2 during expiration - while preserving circulation efficacy, which remains definitively the primary objective. Several solutions have been described to manage ventilation during CPR, from simple oxygen administration to recent solutions put on specific devices or ventilators.

1.2.2.1. Specificities of ventilation during CPR: lung volume below FRC

Lung volume during conventional ventilation

Conventional positive pressure ventilation aims to deliver tidal volumes to the patient to properly manage gas exchange. Lung volume during mechanical ventilation is maintained above the resting lung volume (considered at the end of passive expiration) called the functional residual capacity (FRC). FRC is also the point at which two forces are at equilibrium; the inner recoil forces of the lung, and the chest wall which wants to expand outwards (69). Even if the FRC may change depending on disease evolution and ventilation settings, the lung volume will not go below this resting volume (see figure 11).

Figure 11: Illustration of the different components of lung volume

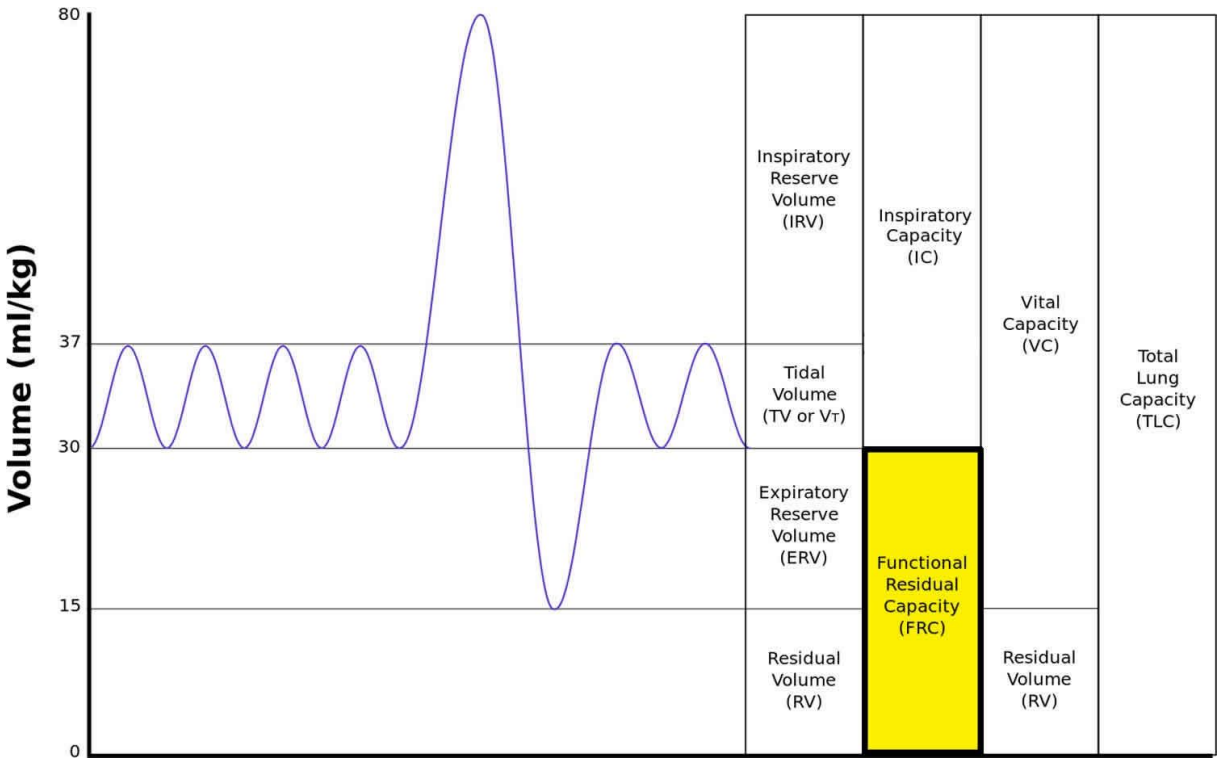

Figure 11: Schematic (obtained from the following website: *https://healthjade.net/functional-residual-capacity/* representing lung volumes). Functional Residual Capacity (FRC) is the volume of air present in the lungs at the end of passive natural exhalation. It corresponds to the sum of Expiratory Reserve Volume (ERV) and Residual Volume (RV) and measures approximately 2400 mL in an average sized person with no lung pathology. The total lung capacity comprises the FRC and the inspiratory capacity (IC).

Lung volume during CPR

CPR is a unique situation during which lung volume may be reduced below FRC, as chest compressions squeeze the thorax and thus decrease lung volume. During CPR, chest compressions compress the chest and as a result tend to reduce lung volume below the FRC depending on the way the patient is ventilated. Overall, increasing chest compressions depth and frequency will enhance lung volume reduction. On the opposite, increasing ventilation (either tidal volume or respiratory rate) or positive end expiratory pressure (PEEP) will limit this effect. Interestingly, guidelines evolution associated with outcome improvement tend to reduce lung volume. Cordioli et al. (12) evaluated the impact of CPR on lung volume using the POUTAC bench model that permits generation of chest compressions starting from FRC. A non-breathing patient under cardiac arrest was simulated, reproducing the elastic recoil properties of the thorax. Dynamic thoracic volume change was calculated as the difference between the FRC and the lung position at the end of decompression. In this study, despite different levels of continuous positive pressure, lung volume was continuously below FRC. Noticeably, recordings in patients reported in the same study confirmed a major loss of lung volume below FRC during CPR, even with ventilation (almost 400 ml). During compression, the blood is ejected from the heart into the systemic and pulmonary circulation while during decompression, thoracic recoil generates negative pressure and allows venous return. Importantly, lung volume certainly plays a major role in the generation of circulation during chest compressions by majoring or limiting thoracic recoil and negative pressure. Recent findings suggest that this negative pressure is no longer effective when lung volume is above FRC at the end of decompression (70).

1.2.2.2. Passive ventilation

Two types of ventilation exist during cardiopulmonary resuscitation: passive ventilation generated by the chest compressions and active ventilation that delivers supplementary volume

into the lungs during insufflation with the help of a ventilation device such as a bag valve mask or a ventilator.

Passive ventilation and gas exchange

Chest compressions can be divided into two phases:

- The compression phase squeezes the thorax and allows some air containing CO2 to be exhaled from the lungs.
- During decompression, recoil forces generate negative intrathoracic pressure responsible for the entry of fresh gas containing oxygen into the thorax. Fresh gas may generate CO2 wash-out.

This ventilation resulting from the succession of compressions and decompressions during CPR is called passive ventilation. Peter Safar et al. (71) showed that manual chest compressions produced an average tidal volume of 156 ml in 30 curarized intubated subjects. The tidal volumes were larger than the estimated dead-space volume in 17 and smaller in 13 patients. Dead space represents the volume of ventilated air that does not participate in gas exchange. On the opposite, no tidal exchange was measured in 12 cardiac arrest patients. This major loss of passive ventilation for cardiac arrest patients compared to healthy subjects may be explained by different reasons. They hypothesized that the decrease of lung compliance due to pulmonary edema or atelectasis, the closure of bronchioles and alveoli due to lung volume reduction and the increase in the surface tension of pulmonary fluid might explain, at least in part, those results (71). Another study evaluated the amount of passive ventilation during CPR (72). Mechanical chest compressions on cardiac arrest patients generated small Vt with a median of 41.5 ml (33.0-62.1 ml) per compression, which was considerably less than measured dead space. Consequently, passive ventilation has a low contribution in gas exchange.

Passive ventilation and intrathoracic airway closure

Intrathoracic airway closure is a phenomenon that has been first suggested in Acute Respiratory Distress Syndrome (ARDS). In these patients, lung inflation starts when airway pressure reaches a critical level of opening pressure called the airway opening pressure (AOP) (73). This complex phenomenon that was unrecognized until recently, may be due to the partial or complete collapse of airways at end-expiration (74). The exact mechanism and the actual location of this collapse is unknown, but it could occur in terminal bronchioles as suggested by animal models (75) and histological examination of ARDS lungs. Complete airway closure can

be measured by the inflection point on the initial portion of a low-flow inflation pressure–volume or pressure–time curve, as shown on figure 12.

Figure 12: low flow inflation pressure-volume curve to detect airway closure and airway opening pressure

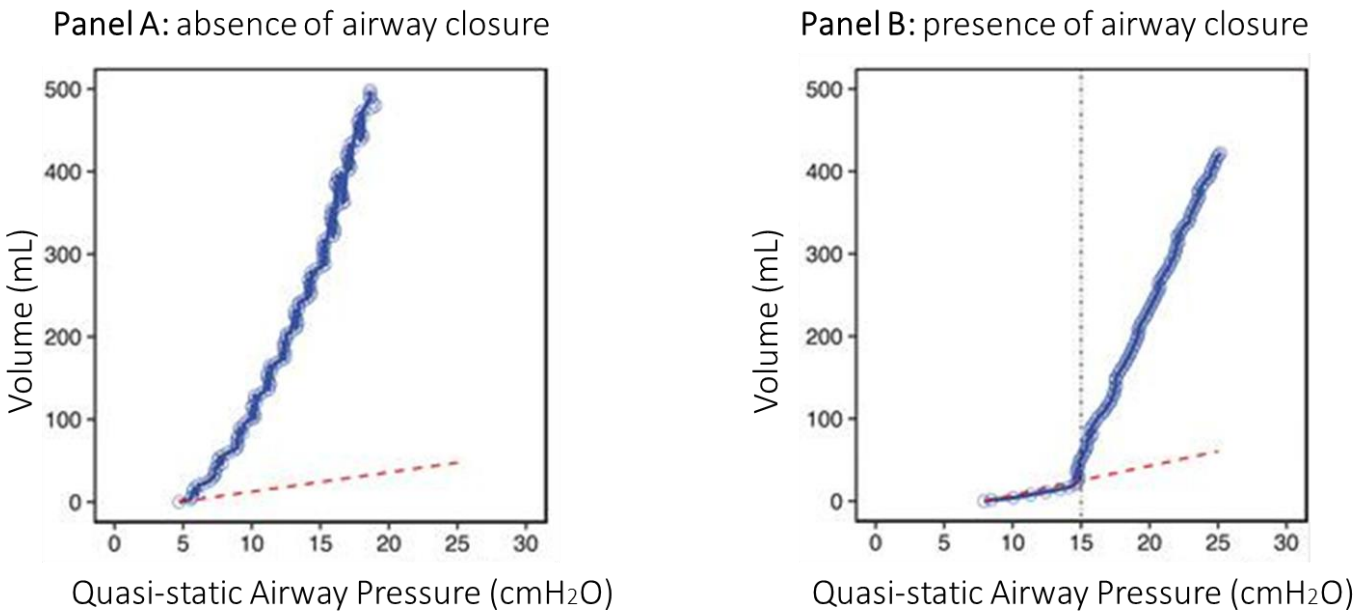

Figure 12: this figure was derived from Coudroy et al. study (74). It depicts low flow inflation pressure-volume curves from representative patients without (panel A) and with (panel B) complete airway closure. Red dashed line represents pressure-volume curve of an occluded circuit (compliance 2.4 ml/cm H2O). Black dash-dotted line represents the airway opening pressure (AOP). In panel A, pressure-volume curve of the patient and the occluded circuit separate immediately. In panel B, the initial part of the pressure-volume curve of the patient is very flat, and superimposed to that of the occluded circuit, suggesting that gas is compressed in the circuit and airways are closed. Above a pressure level named airway opening pressure (15 cm H_2O in this example), the two curves separate as the slope of the patient's pressure-volume curve increases, suggesting lungs are open.

Airway closure has been suspected and identified in cardiac arrest patients, with some similarities with airway closure in ARDS (76). The first description of intrathoracic airway closure in out of hospital cardiac arrest patients has been done by Cordioli et al. (12) based on the continuous recording of flow and airway pressure curves during chest compressions. As shown on figure 13, in some patients, a significant flow limitation was observed during chest

decompression, limiting passive ventilation when PEEP was reduced. Authors hypothesized that airway closure may explain this phenomenon that was associated with a significant reduction of lung volumes below the FRC. Indeed, the relative low contribution of passive ventilation in gas exchange during CPR, first described several years ago by Safar et al. (71), may be explained at least in part, by this recently described phenomenon of intrathoracic airway closure. In fact, the continuous application of chest compressions may gradually reduce lung volume below the FRC and may generate "intrathoracic airway closure" (11). In this situation, the pressure applied on the thorax by the chest compressions is not transmitted to the airways or significantly reduced, limiting passive ventilation. Grieco et al. (11) showed on a Thiel cadaver model and on the POUTAC bench model that minute ventilation was significantly reduced in case of airway closure. Interestingly, Beloncle et al. showed that patients admitted in the ICU after cardiac arrest had a lower end expiratory lung volume with airway closure (77). This phenomenon occurring during CPR is also defined by a threshold pressure below which airways are closed and above which airways are open. This airway opening pressure (AOP) has specific values for each individual depending of patients' characteristics and maybe CPR metrics.

We hypothesized that, as thoracic airway closure is likely to appear after prolonged resuscitation, passive ventilation is more likely to participate to gas exchange at the beginning of CPR. Interestingly, passive ventilation is considered sufficient during the first minutes of resuscitation, and supplementary ventilation (or active ventilation) is not recommended in the guidelines at first.

Figure 13: Clinical recording of flow and airway pressure signals at two levels of PEEP during CPR

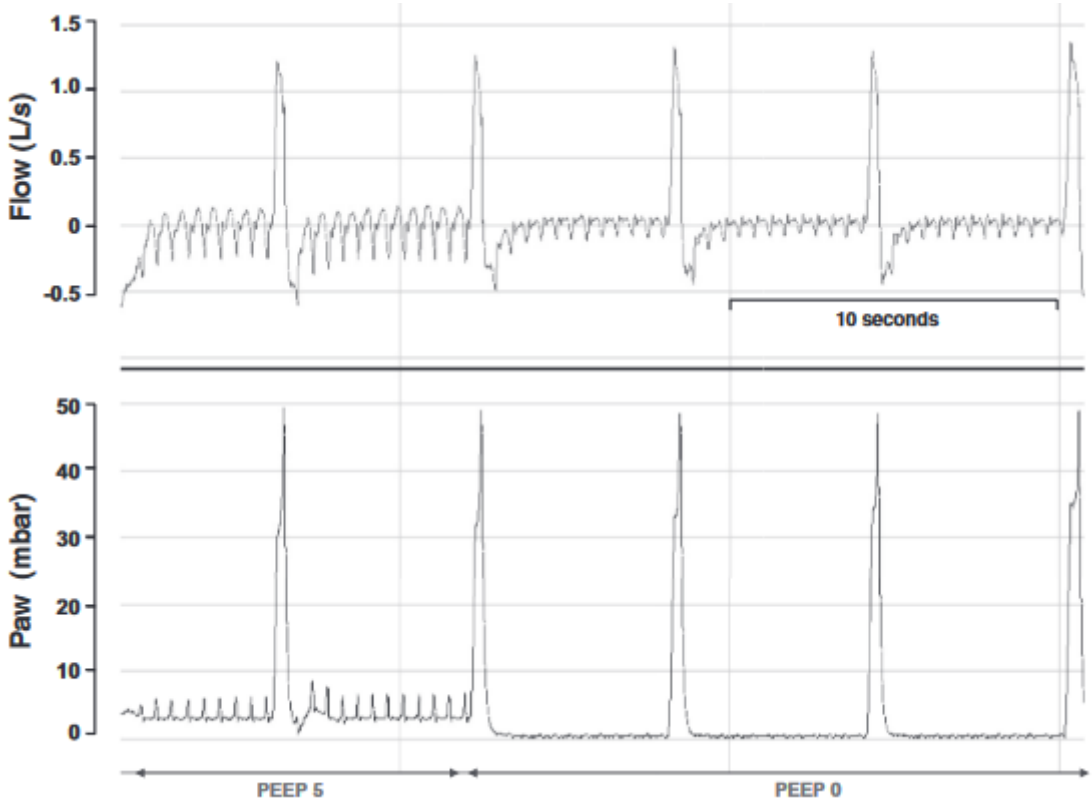

Figure 13: Figure obtained from Cordioli et al. study (12). Recordings of flow (upper panel) and airway pressure (Paw – lower panel) in a patient during CPR using a positive end-expiratory pressure (PEEP) of 5 cm H2O (left) and no PEEP (right) using Monnal T60 ventilator (Air Liquide Medical Systems, Antony, France). A significant limitation of inspiratory flow is visible during decompression when PEEP is removed (right). In addition, chest compressions-induced oscillations of airway pressure during expiration disappear when PEEP is removed (right), despite the application of chest compressions. Authors hypothesized that airway closure was present without PEEP (right) and may explain those observations.

Ventilation devices to enhance passive ventilation

Contribution of passive ventilation to gas exchange during CPR may be relatively low and often insufficient. This is the reason why it has been proposed to develop ventilation devices to specifically enhance passive ventilation. The main technology developed by Georges Boussignac for this purpose is based on continuous flow insufflation (CFI). It provides positive pressure to a level that generates an air entrainment mechanism while allowing uninterrupted

chest compressions. This positive pressure may also open airways and increase lung volume. The hypothesis is that enhanced passive ventilation with continuous flow insufflation may be sufficient to participate to gas exchange without necessitating additional ventilation. Initially, the system was developed on a specific endotracheal tube to be used during initial intubation. Later on, Boussignac developed the B-card (Vygon, Ecouen, France - see figure 14) which permitted to generate CFI via a facial mask before intubation. Bench studies previously reported that CFI limits the loss in lung volume, enhances CC-induced positive intrathoracic pressure during compression, maintains negative intrathoracic pressure during decompression, and generates more alveolar ventilation (12). Several clinical studies evaluated the impacts of CFI using the Boussignac Cardiac arrest device called B-card (Vygon, Ecouen, France - see figure 14) compared to traditional mechanical ventilation. There were no significant differences in outcome, especially regarding return of spontaneous circulation (ROSC). However, favorable effects regarding oxygenation (78, 79), hemodynamics (80) and fewer complications in terms of rib fractures (78) were associated with CFI. Animal studies were also performed and globally confirmed that similar rates of sustained ROSC or survival to hospital discharge were obtained with CFI compared to other ventilation techniques (81). To summarize, despite recent studies published on this technology, its impact on patient-centered outcomes remains uncertain (82).

Figure 14: Photo of B-card system

Figure 14: Photo of the Boussignac Cardiac arrest device called B-card (Vygon, Ecouen, France), which represents the most used continuous flow insufflation (CFI) device in clinical practice.

1.2.2.3. Active ventilation

Active ventilation and gas exchange

As passive ventilation may become insufficient after the first minutes of CPR, an additional ventilation can be delivered to the patient: this is called active ventilation. The objective is to complete passive ventilation (often insufficient) by insufflating at a preset frequency (around 10/min) a volume of air oxygen mixture to the lungs. Consequently, active ventilation could be considered most of the time as the main determinant of gas exchange during resuscitation. Conceptually, passive ventilation could be enough at the early stage of resuscitation based on the notion that early after cardiac arrest, CO2 removal with active ventilation is not essential. However, the international liaison committee on resuscitation (ILCOR) and the European Resuscitation Council suggest that bystanders who are trained, able, and willing to give immediately rescue breaths (active ventilation) and chest compressions do so for all adult patients in cardiac arrest (83, 84). Passive ventilation during CPR has been recently reviewed and the 2022 ILCOR recommendations suggest (weak recommendation) against the routine use of only passive ventilation techniques during conventional CPR, with very low certainty evidence (83).

How to deliver active ventilation?

Different devices exist to deliver active ventilation. The first-line ventilation method used during CPR is bag-valve-mask ventilation. It consists of a bag filled with oxygen that is compressed by the healthcare practitioner to insufflate oxygen to the patient, and released to allow expiration. More sophisticated systems can be used such as ventilators, with either volume controlled or pressure controlled modes.

1.2.2.4. Evolution of ventilation guidelines

As passive ventilation induced by chest compressions is considered sufficient for gas exchange at the beginning of CPR, it is not recommended to perform active ventilation during the first minutes following cardiac arrest. Then, active ventilation becomes necessary (8). The optimal ventilation strategy during CPR remains to be determined but current adult recommendations, based on several studies reporting harmful effects associated with excessive ventilation (8, 85), are as follows:

• Use bag-mask ventilation or an advanced airway strategy in any setting.
• Deliver the highest feasible inspired fraction of oxygen (FiO2) during CPR.
• Once a tracheal tube or a supraglottic airway (SGA) has been inserted, ventilate the lungs at a rate of 10 min^{-1} and continue chest compressions without pausing during ventilations.
• Deliver each breath over approximately 1s, giving a volume that corresponds to normal chest movement (protective ventilation).

How to deliver active ventilation in association with chest compressions ?

Interrupted 30:2 CC strategy corresponds to the delivery of two consecutives insufflations (ventilation) every 30 CC, with an interruption of CC during the insufflations. Continuous CC strategy refers to the continuous application of CC, with a delivery of one insufflation every 6 seconds. It is recommended to perform either interrupted chest compressions strategy or continuous chest compressions strategy when ventilation is performed with a mask (noninvasive), while continuous chest compressions are preferred once the patient is intubated (invasive). Historically, the interrupted chest compressions strategy was recommended essentially to reduce the risk of gastric insufflation compared to continuous chest compressions strategy, but the rationale supporting this recommendation is weak (86). Nevertheless, the potential negative impact on circulation associated with interrupted chest compressions has not been confirmed in a large randomized controlled trial that did not find significant difference between continuous and interrupted chest compressions strategies (87).

1.2.3. Interactions between ventilation and circulation

1.2.3.1. Harmful effects of ventilation and U-curve theory

Ventilation may exert detrimental hemodynamic effects that must be balanced with its expected benefits. However, ventilation is mandatory for adequate gas exchange as soon as CPR is prolonged. The optimal ventilation strategy during Cardio-Pulmonary Resuscitation (CPR) remains challenging, but it has been shown that both excessive and insufficient ventilation can jeopardize circulation or negatively impact gas exchange and as result affect the success of CPR. Consequently, the risks associated with ventilation may be seen as a U-curve, where risks increase with too much or insufficient ventilation as shown in figure 15.

Figure 15: illustration of potential harmful effects of ventilation during CPR as a U-curve theory

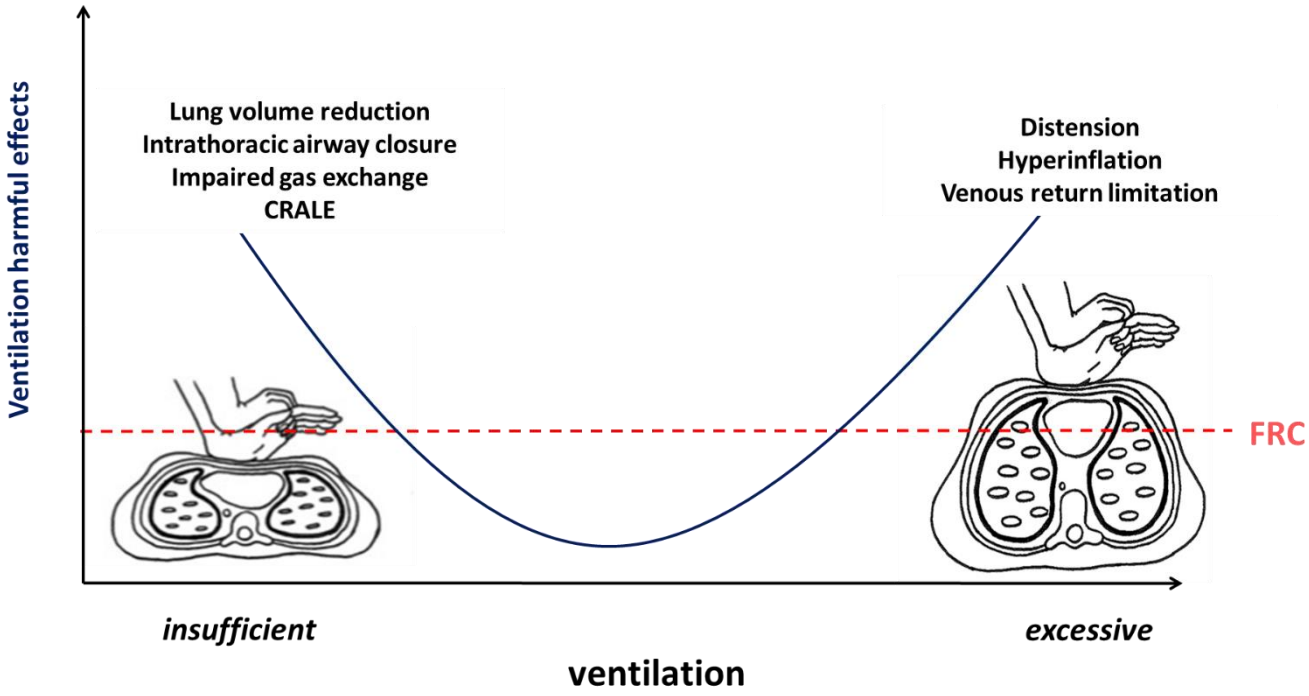

Figure 15: illustration of the potential harmful effects of ventilation during CPR, represented as a U curve. Y-axis represents the ventilation harmful effects, with a higher value associated with higher risk of inadequate ventilation. X-axis represents the amount of ventilation, being insufficient on the left and excessive on the right. The red dotted line symbolizes the functional residual capacity (FRC), while lung volumes are also illustrated. Both insufficient (left part) and excessive (right part) ventilation are associated with increased ventilation harmful effects. If ventilation is insufficient, lung volume may be

significantly reduced below the FRC and generate intrathoracic airway closure. Gas exchange could be impaired, resulting in hypercapnia and hypoxia. In addition, Cardiopulmonary Resuscitation-associated Lung Edema (CRALE) may appear. On the other hand, if ventilation is excessive, lung volume may increase above the FRC and potentially generate distension and hyperinflation. In addition, excessive ventilation may limit venous return. Consequently, ventilation harmful effects could be considered as a U-shape curve, with an optimal ventilation (not insufficient and not excessive) associated with the best outcomes.

1.2.3.2. Not enough ventilation ?

As discussed above, the application of chest compressions may significantly reduce lung volume below the Functional Residual Capacity and generate intrathoracic airway closure (11). As a result, passive ventilation may be significantly reduced, thus affecting gas exchange resulting in hypercapnia and hypoxia. Noticeably, active ventilation tends to limit this reduction of lung volume. In addition, insufficient ventilation may favor Cardiopulmonary Resuscitation-associated Lung Edema (CRALE) that was recently described by Magliocca et al. and that will be further detailed in the next section (5).

1.2.3.3. Too much ventilation ?

An extreme illustration of the negative impact of too much volume during resuscitation is the Lazarus phenomenon, which is described as delayed return of spontaneous circulation (ROSC) after cessation of CPR. It is mainly the result of impaired venous return due to excessive ventilation (85). This may be seen as an overdistension of the lungs. During active ventilation and continuous chest compressions, insufflation generates positive pressure during both compression and decompression. It is likely that the application of positive pressure during decompression may limit the negative pressure generated by the recoil of the chest allowing venous return (88). Berg et al. reported that ventilation during CPR was associated with substantially lower “integrated coronary perfusion pressure” and left ventricular blood flow than compression-only CPR (89).

Even if excessive ventilation is deleterious for venous return, some data suggest that positive pressure may enhance systolic ejection during compression. The animal study by Rudikoff et al. (63) showed that increasing intrathoracic pressure by mean of an end inspiratory occlusion

resulted in a transient but dramatic increase in aortic blood pressure and carotid blood flow, thus evidencing the thoracic pump theory, which was the main purpose of this study. Interestingly, it is the occlusion (that results in a complete transmission of chest compressions induced pressure inside the thorax) rather than the insufflated Vt per se, that is responsible for the circulation benefit observed. This method gave birth to a CPR strategy for newborn cardiac arrest patients called sustained inflation: it consists in providing continuous chest compression superimposed with a high distending pressure (64). Different studies demonstrated an increased carotid flow associated with sustained inflation, and improved brain perfusion by enhancing cerebral perfusion pressure (65, 66). Those results also emphasize the benefit of increasing thoracic pressure to enhance chest compression effect, provided that one can preserve as much as possible the effect of chest recoil (decompression) for venous return.

1.2.3.4. Devices dedicated to manage ventilation for circulation

Different solutions have been developed with the will to manage ventilation taking into account circulation. We can arbitrarily separate solutions that mainly focus on ventilation optimization in order to limit its harmful effects from solutions focusing on improving circulation by managing airway pressure.

Solutions to improve circulation

As previously discussed airway pressure directly interfere with circulation during both chest compression and decompression. The idea behind these solutions is to optimize airway pressure to improve circulation efficiency while maintaining optimal oxygenation. Ventilation per se and CO2 elimination are not the primary objectives.

- ***The impedance threshold Device (ITD)***

  The technology was developed by Zoll and is called ResQPOD. It is a simple, non-invasive device that delivers intrathoracic pressure regulation (IPR) therapy during CPR. The ResQPOD ITD lowers intrathoracic pressure during the recoil phase of CPR by selectively restricting unnecessary airflow into the chest. This might in turn enhance venous return and cardiac output. Use of the ITD increased vital organ blood flow (left ventricular and myocardial blood flow) on a porcine model of CPR (90, 91) but did not significantly improve survival among patients with out-of-hospital cardiac arrest

receiving standard CPR (92). Based on our observations, the working principle of the ITD may favor the decrease of lung volume below the FRC over the course of CPR that may generate intrathoracic airway closure and thus limit passive ventilation. To compensate, The ITD can be added between the ventilator or the bag valve mask and the patient.

- ***Chest compressions synchronized ventilation (CCSV)***

  Chest compressions synchronized ventilation (CCSV) is a novel type of pressure-controlled ventilation developed by Weinmann and available on Medumat ventilator, that provides short insufflations synchronized with chest compressions, which are interrupted before decompression begins (93). The idea is to favor systolic ejection during the chest compression by a "cough effect" generated by extremely high positive pressure while preserving venous return during chest decompression. Interestingly, on a pig model of cardiac arrest, CCSV led to higher arterial pressure of oxygen (PaO2) and avoided an arterial blood pressure drop during resuscitation compared to the gold standard volume control mode of ventilation (94). Nevertheless, the safety and especially the impact of intrathoracic airway closure on the synchronization of insufflations with CCSV should be assessed. In fact, the synchronization between ventilator insufflations and chest compressions is permitted (trigger) by the constant detection of airway pressure variations induced by chest compressions. In case of intrathoracic airway closure, those oscillations may be significantly reduced or disappear as shown on figure 13; which could prevent the ventilator to trigger insufflations. To limit this risk, the system has a volume controlled back-up mode. In addition, any phase shift from the ventilator may authorize to continue insufflation during the decompression phase, which could dangerously jeopardize venous return and as a result circulation.

Solutions to optimize mainly ventilation

On conventional ventilators, the ventilator settings must be adapted for cardiac arrest: respiratory rate, tidal volume, inspired fraction of oxygen (FiO2), Positive End Expiratory Pressure (PEEP), time of insufflation, maximum peak pressure. This specific settings' adjustment for cardiac arrest patients represents a potential risk if not applied rigorously. Moreover, most of those settings are not easily controlled when using bag valve mask

ventilation during CPR. For these reasons, industrials recently developed specific modes of ventilation adapted to the specific constraints of CPR. The idea is to facilitate and optimize ventilation and in addition, to limit its circulation harmful effects.

- ***Cardio Pumonary Ventilation (CPV)***

  CPV is a mode of ventilation dedicated to cardiac arrest patients, with a specific monitoring on CPR quality and CO2. It was developed by Air Liquide Medical Systems, and is available on the Monnal T60 ventilator. It is a pressure-controlled ventilation without inspiratory triggers allowing to combine chest compressions with insufflation (95). Default settings associates respiratory rate, tidal volume, inspired fraction of oxygen (FiO2), Positive End Expiratory Pressure (PEEP), time of insufflation and maximum peak pressure alarm according to international recommendations, thus permitting to start directly ventilation without the need to adapt settings for cardiac arrest ventilation. In addition, the internal algorithm was specifically designed to reduce the airway pressure during decompression while slightly increasing it during the compression, with the objective to protect circulation. All settings can be modified by the physician.

- ***CPV like modes*** are today available in several transport or ICU ventilators. The main purpose is quite similar with a priority regarding ventilation management simplification, safety and protective approach for circulation.

1.2.4. Available models to simulate CPR

It is essential to develop research with the objective to advance our understanding of the physiological phenomena occurring during CPR and better apprehend the optimal strategy that may optimize both circulation and ventilation. To do that, different models are available, with their strengths and limitations.

1.2.4.1. Animal models

Animal models can be used for research in CPR. Swine models are very interesting because they share similarities with human physiology, especially in terms of circulation. Invasive monitoring is feasible, thus both ventilation and circulation can be assessed during CPR through different parameters (e.g. blood pressure, coronary or cerebral perfusion pressure for circulation). As cardiac arrest is induced, it is possible to resuscitate pigs with defibrillation, and study what happens after a return of spontaneous circulation (ROSC). Finally, lung damage can be evaluated through autopsy. Different strategies can be evaluated, such as extracorporeal cardiopulmonary resuscitation (96)

Swine model presents also limitations in the interpretation of results. The lung physiology shows some differences with human lungs. The thorax anatomy is also shaped differently compared to a human thorax. This difference may significantly change the behavior of ventilation and as a result of circulation during CPR. Neither the chest compressions mechanical devices nor the ventilation are easily transposed to human anatomy. In addition, the pig thorax anatomy that present lateral small conduct airway connections in the bronchial tree close from the alveoli may limit the occurrence of intrathoracic airway closure we observe in humans during resuscitation (97). This explains why translation from animal studies to clinical studies may be challenging and may generate conflicting results. Moreover, animal models are often costly and time-consuming and according to the principle of Replacement of the 3R (Replacement, Reduction and Refinement), alternative approaches which directly replace or avoid the use of animals in experiments are needed. Importantly, Ethics Committee are responsible for reviewing and overseeing the conduct of studies on animal welfare and ethics.

1.2.4.2. Bench: the POUTAC

Bench models can also be used to study CPR and evaluate different circulation or ventilation strategies (98, 99). They have the advantage to control the different tested variables and allow

the evaluation of many configurations in a reliable fashion. A thoracic lung model called POUTAC (prototype reported in the Cordioli et al.'s study (12)) was specifically designed to study ventilation during CPR. It can reproduce the mechanical properties of the respiratory system during CPR (76). A bellow on which chest compressions can be applied mimics the lung with an adjustable equilibrium volume representing the Functional Residual Capacity (FRC). Most importantly, this model is designed to allow ventilation either above (as allowed by all lung models) or below FRC (a unique situation specific to CPR). A wide range of respiratory mechanics (resistance and compliance) can be tailored. By providing CO2 to the base of the bellow, this model simulates the production of CO2, which allows capnograms to be recorded (76).

Bench models such as the POUTAC (see figure 16) are powerfool tools allowing to evaluate and compare different CPR strategies, and thus better understand interactions between ventilation and circulation during CPR. Nevertheless, such systems also show important limitations, as CPR bench lack the complexity of physiological models. The interpretation of data should be done carefully as results obtained on the bench may not be directly translatable to clinical settings.

Figure 16: POUTAC bench model

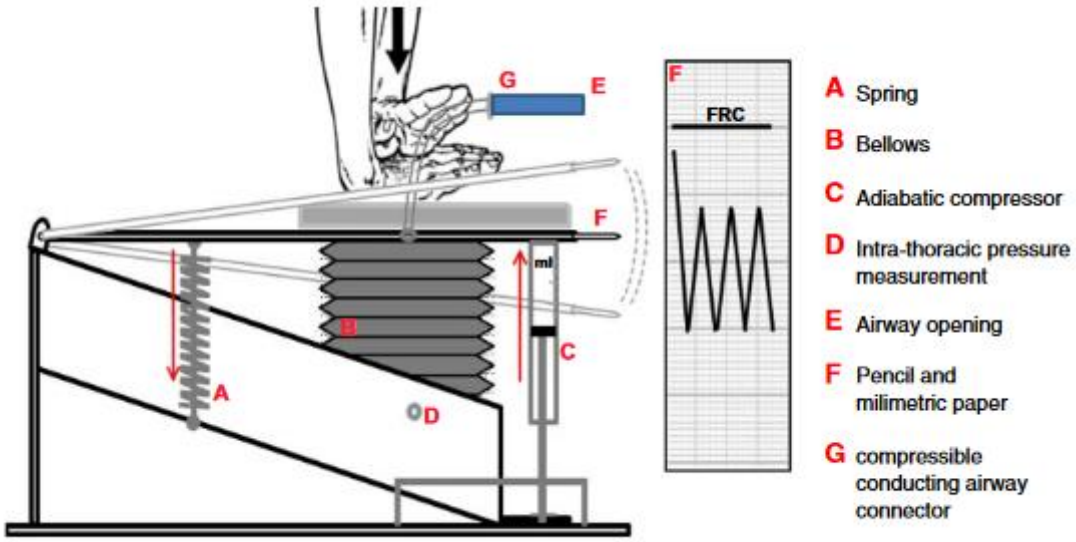

Figure 16: Figure from Cordioli et al. study (12). Schema of the mechanical lung model called POUTAC, designed to reproduce the physical proprieties of thoracic compartment and to perform chest compression. FRC, functional residual capacity.

1.2.4.3. Cadavers

Human cadaver is an interesting and promising model to study CPR. Recently, fresh and treated cadavers have been proposed as a model in cardiac arrest research. Among these, Thiel embalmed human cadavers were validated as a robust model to study ventilation during CPR (76), as they were reported to reliably reproduce human respiratory mechanics during cardiac arrest, thereby allowing realistic measurements. Those cadavers present soft texture and color very close to that of living organism. One important advantage of the human cadaver model, besides its capacity to reflect human respiratory physiology, is the possibility to perform physiological measurements (i.e. the intrathoracic pressure). Moreover, it has been proposed to simulate CO2 production on this model and record in real time capnograms. CO2 is constantly delivered via a catheter placed in the bronchial tree, which permits to reproduce constant CO2 lung fraction that can be used as a surrogate of real CO2 production during CPR. Interestingly, Thiel cadavers may present intrathoracic airway closure, as in cardiac arrest patients. Orlob et al. showed that this cadaver model could be used to evaluate mechanical ventilation during continuous chest compressions, comparing different transport ventilators in this study (100).
Despite its great potential to push CPR research forward, this model also exhibits some limitations. Even if the latter permits an increased understanding of the variety of physiological phenomena that occur during CPR, the lack of circulation remains a major limit of cadaver models (101).

1.3. *Significance of CO2 signal during cardiopulmonary resuscitation and place of CO2 monitoring*

1.3.1. CO2 production, transport and elimination during CPR

CO2 production

In the human body, carbon dioxide is formed as a byproduct of metabolism. Carbon dioxide production occurs in cells, mainly during glycolysis and the citric acid cycle in the cytoplasm and mitochondria, respectively (102). Glycolysis, also named cellular respiration, converts ingested nutrients in the form of glucose (C6H12O6) and oxygen to energy in the form of adenosine triphosphate (ATP). CO2 is produced as a byproduct of this reaction that, ultimately, needs to be removed.

CO2 transport and elimination

CO2 is transported in the bloodstream to the lungs where it is ultimately removed from the body through expiration into the surrounding environment. There are three means by which carbon dioxide is transported in the bloodstream from peripheral tissues to the lungs: (1) bicarbonate, (2) dissolved gas, and (3) carbaminohemoglobin bound to hemoglobin (and other proteins).

1. Bicarbonate is the primary means by which carbon dioxide is transported throughout the bloodstream. Carbon dioxide combines with water via a chemical reaction forming carbonic acid. Carbonic acid almost immediately dissociates into a bicarbonate anion (HCO3-) and a proton (H+) according to the equation CO2 + H2O --> H2CO3 --> H+ + HCO3-. The proton formed by this reaction is buffered by hemoglobin, while the bicarbonate anion diffuses out of the red blood cell and into the serum. Then, in the lungs, those chemical processes are reversed, generating carbon dioxide. The carbon dioxide diffuses out of the red blood cells, through the capillary walls, and into the alveolar spaces. Thus carbon dioxide becomes especially crucial in regulating the pH of the blood, as production of protons decrease pH. Should the partial pressure of carbon dioxide increase or decrease, the body's pH will decrease or increase, respectively.
2. As carbon dioxide diffuses into the bloodstream from peripheral tissues, approximately 10% of it remains dissolved either in plasma or the blood's extracellular fluid matrix, to a partial pressure of about 45 mmHg.
3. The remaining 10% of the carbon dioxide that diffuses into the bloodstream and, subsequently, into the red blood cells, binds to the amino terminus of proteins,

predominantly hemoglobin, to form carbaminohemoglobin. Of note, this site is different from the one to which oxygen binds.

This complex process of carbon dioxide production, transport, and elimination plays various roles in the human body including regulation of blood pH, respiratory drive, and affinity of hemoglobin for oxygen (O2). Fluctuations in CO2 levels are highly regulated and can cause disturbances in the human body if normal levels are not maintained.

1.3.2. CO2 as a reflect of circulation during CPR

Efficient circulation during CPR and CO2

CO2 levels in the blood depend of CO2 production, transport and elimination. During CPR, as the heart in not capable of producing effective blood flow, chest compressions aim to replace the heart and generate circulation and blood flow. High quality chest compressions are associated with improved outcomes. In fact, high quality of chest compressions should increase circulation efficiency, thus blood flow is increased as well as transport of CO2, that will favor the elimination of CO2 in the lungs and ultimately increase expired CO2 (103).

Altered circulation during CPR and CO2

On the opposite, if blood flow is not maintained due to the absence or low quality of chest compressions, transport of the blood containing CO2 to the lungs is impaired and CO2 elimination is thus reduced, resulting in a decrease of the expired CO2. Consequently, the concentration of CO2 will increase in the blood generating acidosis.

The expired CO2 as a reflect of circulation during CPR

The expired CO2 is monitored during CPR as the end-tidal CO2 (EtCO2). It represents the partial pressure of CO2 at the end of expiration. As explained above, expired CO2 may be a good indicator reflecting circulation. As shown by Sandroni et al. (104), EtCO2 provides a competent and technically simple, noninvasive monitor that highly correlates with cardiac output under conditions of constant ventilation during experimental CPR. Consequently expired CO2 may serve as a simple measurement of the blood flow generated by chest compressions during cardiopulmonary resuscitation (CPR).

1.3.3. Current ventilation guidelines on CO2 signal

CO2 monitoring is recommended in clinical practice by International guidelines (8). More specifically, it is the end-tidal CO2 (EtCO2) that is monitored and corresponds to the partial pressure of CO2 at the end of expiration. EtCO2 can be used for different reasons:

- To check proper placement of the tracheal tube
- To monitor respiratory rate to avoid hyperventilation
- To assess quality of chest compressions
- To detect return of spontaneous circulation (ROSC) without interrupting chest compressions

However, the application of chest compressions during CPR influences CO2 waveform and complicates its interpretation (9, 10). Oscillations in the capnogram have been reported by several authors and affect the majority of patients receiving chest compressions, resulting in high variability and chest compression-induced artefacts that could possibly hamper an accurate interpretation of EtCO2.

1.3.4. Recent advances: Intrathoracic airway closure, CO2 and lung volume

A significant proportion of patients with cardiac arrest exhibit “intrathoracic airway closure”. Based on the few studies investigating this phenomenon, the incidence is between 20% and 50% (7, 9). Airway closure is associated with lung volume reduction and impedes ventilation generated by chest compressions, which overall limits the total delivered ventilation. This phenomenon can be reversed by the application of small levels of positive end-expiratory pressure. Interestingly, a novel interpretation of the capnogram (expired CO2 signal recorded during chest compressions) permits to identify intrathoracic airway closure and can rate the magnitude of this phenomenon (11). In case of airway closure, the pressure applied on the thorax during chest compressions is no longer (or only partially) transmitted to the airways, resulting in a non or poorly oscillating capnogram during expiration. A specific index evaluating the magnitude of those chest compressions-induced oscillations was developed to assess the degree of intrathoracic airway closure: it is called the airway opening index and can vary between 0% and 100%. An airway opening index close to 100% indicates fully oscillating capnograms while an airway opening index close to 0% indicates non oscillating capnograms, as shown on figure 17. An AOI lower than 30% is considered as intrathoracic airway closure.

The threshold of 30% was defined based on the results of the Grieco et al.'s study showing that below an AOI of 30%, the impact on ventilation and as result on CO2 washout was substantial.

$$AOI = \frac{\sum_{i=1}^{n} \frac{\Delta CO2(i)}{CO2\max(i)}}{n}$$

Figure 17: illustration of Airway Opening Index on clinical capnograms

Panel A: Oscillating capnogram

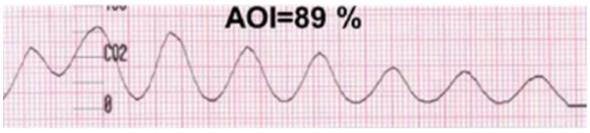

Panel B: Oscillating capnogram

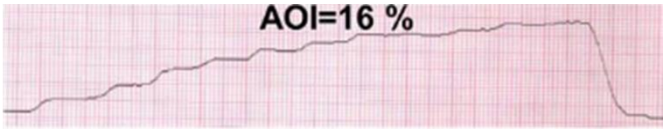

Figure 17: Clinical capnograms obtained from Grieco et al. (11) study during continuous chest compressions. Panel A displays an oscillating capnogram associated with an AOI of 89%, while panel B represents a non-oscillating capnogram associated with an AOI of 16%. The AOI being lower than 30%, capnogram in panel B would be considered as intrathoracic airway closure.

Grieco et al. (11) showed that the entire expired CO2 waveform (rather than EtCO2) could contribute to clarify the physiological meaning of exhaled CO2 and may help to assess the real amount of delivered ventilation during CPR.

1.3.5. Recent advances: Cardiopulmonary Resuscitation Associated Lung Edema

Grieco et al. (11) hypothesized that a dramatic reduction of lung volume below the functional residual capacity generated by the application of chest compressions may be responsible for the occurrence of intrathoracic airway closure during CPR. A recent study by Magliocca et al. (5) suggested that chest compressions may promote lung injury and as result the so called Cardiopulmonary Resuscitation Associated Lung Edema (CRALE). CRALE is defined by lung alterations associated with a derangement in mechanical properties and gas exchange that seem related with the intensity of intrathoracic pressure swings generated by chest compressions and potentially magnified by lung volume reduction. The loss in lung volume during CPR could possibly cause alveolar derecruitment, atelectrauma, and consequently a loss of aeration and

compliance. Interestingly, Beloncle et al. (77) recently showed on a cohort of 43 patients admitted in the ICU after out of hospital cardiac arrest, that 60% of patients were considered to have a CRALE. Among them, 33% were identified with intrathoracic airway closure, associated with a lower end expiratory lung volume compared to patients without airway closure. Those findings support the study of Magliocca et al. suggesting that intrathoracic airway closure during CPR may be generated by a dramatic reduction of lung volumes below the FRC (5). To what extend a strategy limiting lung volume reduction by slightly increasing PEEP may limit this life-threatening complication without affecting chances of CPR success is definitely an unresolved question that deserves to be addressed.

1.4. Unresolved issues and concerns regarding interaction between ventilation and circulation during cardiopulmonary resuscitation

Several aspects of the interaction between positive pressure ventilation and circulation remain unclear when we consider the physiological determinants of organs circulations, gas exchange and ventilation during CPR.

From one side, the harmful impact of too much positive pressure ventilation on venous return is well demonstrated in animal models and even in clinical studies. The Lazarus phenomenon (85, 88) is probably the most representative illustration of how excessive ventilation may prevent any chance of return of spontaneous circulation. This phenomenon is mainly the result of thoracic distension above FRC that prevents thoracic recoil and as a result limits durably venous return.
On the opposite, too much negative pressure during decompression has been incriminated in a paradoxical reduction of venous return, possibly due to the collapse of veins at the entrance of the thorax, which could be associated with a dramatic reduction of lung volumes.
In between, even with moderate positive pressure ventilation, continuous chest compressions tend to reduce lung volume below the FRC, which allows to generate a negative pressure during decompression due to the recoil forces of the thorax, thus protecting venous return.

Consequently, we can hypothesize that lung volume at which CPR operates (related to FRC) is possibly more informative than dynamic change in airway pressure per se to assess ventilation beneficial and harmful effects

Even if expired CO2 remains difficult to interpret since its depends on both circulation quality (cellular metabolism) and ventilation, the information carried by capnogram during chest compressions may be informative regarding lung volume changes related to FRC and as result may be an interesting surrogate of the global quality of CPR.

In the second part of the thesis, we will discuss different aspects of positive pressure ventilation, CO2 elimination and the potential significance of lung volume during CPR.

Part 2: the importance of physiological signals to guide ventilation in emergency situations

The main purpose of this thesis lies in the evaluation and modeling of physiological signals to guide ventilation in constrained environments to optimize emergency ventilation and cardiopulmonary resuscitation. More specifically, the objectives of this work can be summarized as follows:

1. In special surge situations such as during the covid crisis, we may wonder if is it possible to safely ventilate severe patients using available transport ventilators to extend intensive care units capacity. More precisely, it is important to define the potential limits of transport ventilators and evaluate to which extent the working principles of those devices impact their performances.

2. The optimal ventilation strategy during CPR remains to be determined. Recent studies suggest that analysis of CO2 signal may potentially be a reflect of lung volume during CPR and thus give important information on ventilation and circulation during CPR. The objective of this work is to evaluate if the recognition of specific CO2 patterns during chest compressions is feasible and could potentially guide ventilation.

3. Based on the two previous studies, it appears essential to be able to test different ventilation strategies or to evaluate ventilation devices performances in emergency situations such as constrained environments or during CPR. Those tests should be performed on dedicated models that permit the monitoring and analysis of physiological signals such as lung volume and CO2. In this context, a new bench model was developed and its performances investigated.

Those three axes of research were realized with different groups of research, mainly in the Vent'Lab (Intensive Care department of the university hospital of Angers) supervised by professors Alain Mercat and François Beloncle and in the MedLab from Air Liquide Medical Systems in Antony supervised by the professor Jean-Chritophe Richard.

2.1. Performances of transport ventilators in constrained simulated environment

2.1.1. Context

During the pandemics, Intensive Care Units (ICU) had to manage a massive influx of COVID-19 patients with acute hypoxemic respiratory failure (AHRF), and have often been overwhelmed. In this context, extending ICU capacity was required, often in an environment constrained by the healthcare personal resources and the limited possibilities to connect ICU ventilators on oxygen/air pressure sources. Additionally, the transfer of patients by train or by plane has been massively experienced. Rapidly, transport ventilators requiring only one O2 source have been considered for this purpose. The objective of the study (that was performed during the COVID-19 crisis) was to evaluate the performances of four transport ventilators compared to one ICU ventilator in simulated severe respiratory failure conditions to validate their possible use to extend possibilities to manage severe ventilated patients outside the walls of the ICU.

2.1.2. Methods

This study was conducted in the Vent'Lab in Angers University Hospital. My role was to design the bench test protocol based on clinical observations of COVID-19 patients and to conduct its feasibility. I also performed the data acquisition using Acqknowledge Biopac systems, and the data analysis using python programming software.

Four transport ventilators were evaluated and compared with a pneumatic ICU ventilator (Engström Carestation—GE Healthcare), considered as a gold standard. Transport ventilators were composed of two Venturi pneumatic ventilators, (Oxylog 3000, Draeger; Osiris 3, Air Liquide Medical Systems) and two turbine transport ventilators (Elisee 350, ResMed; Monnal T60, Air Liquide Medical Systems). All devices were tested on a Michigan test lung.

Volume performances and PEEP reliability

- The ability for the ventilator to deliver accurately the volume and the PEEP set by the clinician was evaluated. A passive patient was simulated with respiratory mechanics representing severe COVID-19 patients (compliances of 20 or 50 ml/cmH2O and a

resistance of 15 cmH2O/l/s). Three set volumes (350 ml, 450 ml and 550 ml) and two PEEP (10 and 15 cmH2O) were tested.

- The performances of Venturi pneumatic ventilators in terms of volume delivery could be impacted by set inspiratory flow values, as Venturi systems are characterized by loss of air entrainment at lower gas flows (15). In this context, the impact of the inspiratory flow on volume error was assessed on the Osiris 3 ventilator.

Triggering performances

- The ability for the ventilator to assist spontaneous respiratory effort from a simulated patient was evaluated. More specifically, the triggering performances were assessed and correspond to the delay between the beginning of the patient effort and the initiation of the respiratory cycle by the ventilator. The lower the triggering delay, the better the performances. The ventilatory settings were chosen to achieve a moderate or a strong effort consistent with efforts described in COVID patients. To simulate spontaneous breathing, tested ventilators were connected to the double chamber Michigan test lung (see Fig. 1 from the study). One chamber of the test lung was defined as the driving lung, while the other chamber was connected to the ventilator being tested. A lung-coupling clip allowed a connection between the two chambers, so that a positive pressure created in the driving lung induced a negative pressure in the experimental lung, leading to simulated patient effort and thus triggering of the ventilator tested.

2.1.3. Main results

Volume performances and PEEP reliability

- When all conditions and set volumes were included, the Engström Carestation was the most accurate ventilator, and the Oxylog 3000 was comparable. The performance was considered as acceptable (delta Vt ± 0.5 ml/kg PBW) except for one turbine ventilator (Elisee 350). Differences between measured PEEP and set PEEP were less than 2 cmH2O.

- For the most basic Venturi pneumatic ventilator (Osiris 3), the lowest values of inspiratory flow were associated with a volume error higher than 8% (delta Vt ± 0.5 ml/kg PBW). Performances were acceptable when inspiratory flow was strictly above 30 L/min.

Triggering performances

- All simulated efforts triggered a ventilatory cycle. The Triggering Delay corresponding to a moderate effort was 42 ± 4 ms, 65 ± 5 ms, 151 ± 14 ms, 51 ± 6 ms and 64 ± 5 ms for Engström Carestation, Osiris 3, Oxylog 3000, Monnal T60 and Elisee 350, respectively. Ventilator performances were considered acceptable (TD < 100 ms) except for one pneumatic ventilator (Oxylog 3000).

2.1.4. Discussion

For most of the severe respiratory mechanics conditions tested, the volume and PEEP errors were considered as acceptable. Turbine ventilators' performances were very close to those of the ICU ventilator tested including volume delivery and reliability of PEEP. Inspiratory trigger reactivity was considered acceptable in the bench conditions tested except for one pneumatic transport ventilator.

Pneumatic transport ventilators were limited in terms of FiO2 settings, but provided acceptable volume accuracy in severe simulated conditions when the flow was properly set. In fact, volume error delivered by the simplest pneumatic ventilator with a FiO_2 set at 50-60% significantly increased when inspiratory flow was less than 30 L/min indicating a technological limit of the Venturi system. In fact, Coppadoro et al. (15) showed that there is a loss of air entrainment with the Venturi at lower gas speeds, potentially impacting volume accuracy at lower inspiratory flows. This technological limit of the most basic pneumatic transport ventilators illustrates the importance to be aware of the working principles of ventilators to consider their use in different clinical settings.

One other limit of the Venturi system is that air entrainment is dependent on the impedance of the patient. For instance, high respiratory system resistance may result in a significant drop of inspiratory flow associated with a concomitant FiO2 increase as previously demonstrated by

Coppadoro et al. (15). The clinical relevance of these findings outside the context of the pandemic could be the ventilation during CPR. In fact, repeated compressions of the thorax during insufflation could be considered as a massive increase in the impedance that may significantly affect the Venturi effect of the most basic ventilators. Nevertheless, this technological limit disappears when FiO2 is set at 100% (no Venturi). Volume error would be thus reduced at the 100% FiO_2 usually recommended and set during CPR.

Interestingly, turbine ventilators behaved very close from the ICU ventilators whatever the conditions tested. These observations confirmed that turbines available in recent ventilators are able to generate constant flow and guarantee volume delivery even when impedance increases. This indirectly suggests that the turbine working principle is perfectly adapted to a wide range of specific clinical settings such as CPR. Noticeably, turbine ventilators may properly ventilate even with the use of low pressure oxygen source, thus significantly enlarging the possibilities of clinical use in constrained environment.

Consequently, in the context of the COVID-19 worldwide crisis, associated in specific geographies with ventilators shortage, simple and easy to set transport ventilators can be considered outside the walls of the ICU as they only require one oxygen pressure source to function and they are able to reliably deliver lung protective ventilation. Nevertheless, the simple pneumatic ventilators should be reserved as rescue practice since they are limited in ventilation modalities and definitively not adapted to non-invasive ventilation. Turbine transport ventilators should be favored to adequately complete ICU ventilators when needed. This strategy has been successfully experienced during the crisis as nicely illustrated by Ferré et al. (105). Importantly, the results obtained in this study on a bench model necessitate some caution to be translated to the clinical practice. In addition, a monitoring of physiological signals, especially expired Vt, greatly facilitates adequate settings and is essential to guide ventilation.

2.1.5. The study

RESEARCH Open Access

Reliability and limits of transport-ventilators to safely ventilate severe patients in special surge situations

Dominique Savary[1,2*], Arnaud Lesimple[3,4], François Beloncle[5], François Morin[1], François Templier[1], Alexandre Broc[6], Laurent Brochard[7,8], Jean-Christophe Richard[5,9] and Alain Mercat[5]

Abstract

Background: Intensive Care Units (ICU) have sometimes been overwhelmed by the surge of COVID-19 patients. Extending ICU capacity can be limited by the lack of air and oxygen pressure sources available. Transport ventilators requiring only one O_2 source may be used in such places.

Objective: To evaluate the performances of four transport ventilators and an ICU ventilator in simulated severe respiratory conditions.

Materials and methods: Two pneumatic transport ventilators, (Oxylog 3000, Draeger; Osiris 3, Air Liquide Medical Systems), two turbine transport ventilators (Elisee 350, ResMed; Monnal T60, Air Liquide Medical Systems) and an ICU ventilator (Engström Carestation—GE Healthcare) were evaluated on a Michigan test lung. We tested each ventilator with different set volumes (Vt_{set} = 350, 450, 550 ml) and compliances (20 or 50 ml/cmH_2O) and a resistance of 15 cmH_2O/l/s based on values described in COVID-19 Acute Respiratory Distress Syndrome. Volume error (percentage of Vt_{set}) with $P_{0.1}$ of 4 cmH_2O and trigger delay during assist-control ventilation simulating spontaneous breathing activity with $P_{0.1}$ of 4 cmH_2O and 8 cmH_2O were measured.

Results: Grouping all conditions, the volume error was 2.9 ± 2.2% for Engström Carestation; 3.6 ± 3.9% for Osiris 3; 2.5 ± 2.1% for Oxylog 3000; 5.4 ± 2.7% for Monnal T60 and 8.8 ± 4.8% for Elisee 350. Grouping all conditions ($P_{0.1}$ of 4 cmH_2O and 8 cmH_2O), trigger delay was 50 ± 11 ms, 71 ± 8 ms, 132 ± 22 ms, 60 ± 12 and 67 ± 6 ms for Engström Carestation, Osiris 3, Oxylog 3000, Monnal T60 and Elisee 350, respectively.

Conclusions: In surge situations such as COVID-19 pandemic, transport ventilators may be used to accurately control delivered volumes in locations, where only oxygen pressure supply is available. Performances regarding triggering function are acceptable for three out of the four transport ventilators tested.

Keywords: COVID-19, Acute Respiratory Distress Syndrome, Respiratory failure, Mechanical ventilation, Respiratory mechanics

Introduction

During the COVID 19 pandemic, several hospitals experienced the greatest shortage of ventilators ever seen since the heroic times of the polio epidemic in the 1950s. In this context, alternative solutions including ventilator sharing, use of anesthesia ventilators and use of homecare ventilators have been considered to manage intubated patients with severe lung failure outside the walls of the ICU [1–3]. To be able to replace ICU ventilators in the early phase, ventilators must be relatively easy for the users, able to accurately control the delivered volume and provide assist control ventilation

*Correspondence: dominique.savary@chu-angers.fr
[1] Emergency Department, University Hospital of Angers, 4, Rue Larrey, 49933 Angers Cedex 9, France
Full list of author information is available at the end of the article

Reliability and limits of transport-ventilators to safely ventilate severe patients in special surge situations.

Dominique Savary [1,2], Arnaud Lesimple [3,4], François Beloncle [5], François Morin [1], François Templier [1], Alexandre Broc [6], Laurent Brochard [7,8], Jean-Christophe Richard [5,9] and Alain Mercat [5]

[1] Emergency department, University Hospital of Angers, Angers, France

[2] Inserm, EHESP, University of Rennes, IRSET (Institut de recherche en santé, environnement et travail) - UMR_S 1085, F-49000, Angers, France

[3] CNRS, INSERM 1083, MITOVASC, Université d'Angers, Angers, France.

[4] Med2Lab, ALMS, Antony, France

[5] Critical Care department, Angers University Hospital, Angers, France

[6] Telecom-Physic-Strasbourg, Strasbourg University France

[7] Keenan Research Centre for Biomedical Science, Li Ka Shing Knowledge Institute, St. Michael's Hospital, Toronto, Canada

[8] Interdepartmental Division of Critical Care Medicine, University of Toronto, Toronto, Canada

[9] INSERM UMR 955 Eq13

Corresponding author:

Dominique Savary, Emergency Department, University Hospital of Angers, 4, rue Larrey 49933 ANGERS cedex 9, phone number (+33) 672140468, dominique.savary@chu-angers.fr

Keywords

Covid-19, Acute Respiratory Distress Syndrome, respiratory failure, mechanical ventilation, respiratory mechanics.

Abstract

Background: Intensive Care Units (ICU) have sometimes been overwhelmed by the surge of COVID-19 patients. Extending ICU capacity can be limited by the lack of air and oxygen pressure sources available. Transport ventilators requiring only one O_2 source may be used in such places.

Objective: To evaluate the performances of four transport ventilators and an ICU ventilator in simulated severe respiratory conditions.

Materials and methods: Two pneumatic transport ventilators, (Oxylog 3000, Draeger; Osiris 3, Air Liquide Medical Systems), two turbine transport ventilators (Elisee 350, ResMed; Monnal T60, Air Liquide Medical Systems) and an ICU ventilator (Engström Carestation – GE Healthcare) were evaluated on a Michigan test lung. We tested each ventilator with different set volumes (Vt_{set} = 350, 450, 550 ml) and compliances (20 or 50 ml/cmH_2O) and a resistance of 15 cmH_2O/L/sec based on values described in COVID-19 Acute Respiratory Distress Syndrome. Volume error (percentage of Vt_{set}) and trigger delay during assist-control ventilation simulating spontaneous breathing activity with $P_{0.1}$ of 4 cmH_2O and 8 cmH_2O were measured.

Results: Grouping all conditions, the volume error was 2.9 ± 2.2 % for Engström Carestation; 3.6 ± 3.9 % for Osiris 3; 2.5 ± 2.1 % for Oxylog 3000; 5.4 ± 2.7 % for Monnal T60 and 8.8 ± 4.8 % for Elisee 350. Grouping all conditions ($P_{0.1}$ of 4 cmH_2O and 8 cmH_2O), trigger delay was 50 ± 11 ms, 71 ± 8 ms, 132 ± 22 ms, 60 ± 12 and 67 ± 6 ms for Engström Carestation, Osiris 3, Oxylog 3000, Monnal T60 and Elisee 350, respectively.

Conclusions: In surge situations such as COVID-19 pandemic, transport ventilators may be used to accurately control delivered volumes in locations where only oxygen pressure supply is available. Performances regarding triggering function are acceptable for three out of the four transport ventilators tested.

Introduction

During the COVID 19 pandemic, several hospitals experienced the greatest shortage of ventilators ever seen since the heroic times of the polio epidemic in the 1950s. In this context, alternative solutions including ventilator sharing, use of anesthesia ventilators and use of homecare ventilators have been considered to manage intubated patients with severe lung failure outside the walls of the ICU [1-3]. To be able to replace ICU ventilators in the early phase, ventilators must be relatively easy for the users, able to accurately control the delivered volume and provide assist control ventilation (ACV) in difficult mechanical conditions. Importantly, they must allow to vary FiO_2 without requiring two pressurized sources of gas, (i.e. wall air and oxygen at 50 psi). Of note, this is one of the main limits of the homecare ventilators that makes them incompatible for very hypoxemic patients. Several transport ventilators are based on pneumatic systems and Venturi systems for gas mixing. Others use an internal turbine for pressurization; but need a pressurized gas source of oxygen to reach high FiO_2 values. Pneumatic transport ventilators have been used for decades both for in- and out-of-hospital transport. Their robustness and their relative technological simplicity could potentially facilitate massive industrial production. They represent interesting solutions in this context and could fulfill the mentioned requirements. The general view on these ventilators is, however, that their limitations make them acceptable only for a short period like transport but make them incompatible with the safe delivery of difficult ventilation for very sick patients over prolonged periods. Undoubtedly, they have limited capacities regarding ventilation modes and monitoring, but knowing whether their reliability is sufficient for delivering lung protective ventilation in patients with ARDS merited to be tested with these objectives in mind. Indeed, discarding their use in a context of surge could limit the extension of beds outside the walls of the ICU for mechanically ventilated patients. Performances of turbine ventilators are often excellent and have been well described [4,5]. By contrast, limits of pneumatic ventilators have not been specifically tested with the appropriate settings in realistic conditions simulating the respiratory mechanics of patients with COVID-19 induced ARDS [6-9].

The aim of the present study was to evaluate the reliability and the limitations of ventilation provided by these different technologies mimicking patients with COVID-19 induced ARDS in simulated bench conditions of passive and partially assisted situation.

Materials and Methods

Performances during volume-controlled (VC) and ACV were evaluated with different conditions of simulated respiratory mechanics reproducing patients with COVID-19 induced ARDS. All experiments have been performed in the Ventilatory Laboratory of the Angers University Hospital, medical ICU.

1. Ventilators

Brands

Four transport ventilators necessitating only one O_2 pressurized gas source were included in the study. Two pneumatic transport ventilators using Venturi systems to mix air to oxygen were tested: the Oxylog 3000 (Draeger, Lubeck, Germany) and the Osiris 3 (Air Liquide Medical Systems, Antony, France). Two turbine transport ventilators, necessitating additional oxygen only to increase FiO_2 were also tested: the Elisee 350 (ResMed, Sydney, Australia) and the Monnal T60 (Air Liquide Medical Systems, Antony France). Performances of these ventilators were compared to a standard ICU ventilator: Engström Carestation (GE healthcare, Madison, USA). The characteristics of the five ventilators are given in Table 1.

Working principle and settings

In the two pneumatic transport ventilators tested (Oxylog 3000 and Osiris 3), the working pressure that generates ventilation comes from the high-pressure oxygen supply. These ventilators based on a "Venturi-distributor" technology work as flow generator.

With the Oxylog 3000, the air-O_2 mixing is regulated from 40% to 100% via a Venturi system coupled with a proportional inspiratory valve that also permits to directly set the volume (Vt_{set}). The inspiratory flow depends on both the respiratory rate (RR) and the Inspiratory:Expiratory (I:E) ratio. In other words, for a given set volume, changing RR and/or I:E ratio keep the set Vt but modifies inspiratory flow. The monitoring of the expired Vt is available via a specific flow sensor inserted between the endotracheal tube and the patient circuit.

With the Osiris 3, only two positions are available for FiO_2: 100% or 70%. A Venturi effect is used to obtain a FiO2 of 70% by mixing ambient air and O2 source. Inspiratory flow is delivered through a distributor. For a given combination of I:E ratio and respiratory rate, the Vt is set by

directly adjusting a Vt knob that also regulates the inspiratory flow. The monitoring of the expired Vt is available via a specific flow sensor inserted between the endotracheal tube and the patient circuit.

The Elisee 350 and T60 are two turbine-based ventilators which need oxygen only to adjust FiO_2. On those ventilators, the Vt and the inspiratory flow are directly set on the screen. Changing the respiratory rate does not affect neither Vt nor inspiratory flow. The monitoring of the expired Vt is available via a flow sensor close to the expiratory valve.

The Engström Carestation is a classical high-quality ICU ventilator requiring two sources of pressurized gas for oxygen and air (usually wall pressure at 50-55 psi). The monitoring of the expired Vt is available via a flow sensor located close to the expiratory valve.

2. Volume delivered and PEEP with different respiratory mechanics

We assessed the volume effectively delivered ($Vte_{measured}$) by the ventilators in different conditions of respiratory mechanics simulated on a Michigan test lung (Michigan Instruments, Kentwood, MI, USA). A linear pneumotachograph (PNT 3700 series, Shawnee, USA) and a pressure transducer (SD160 series: Biopac systems, Goleta, CA, USA) were used to measure flow and airway pressure between the test lung and the patient circuit. Signals were converted with an analog digital converter (MP150; Biopac systems, Goleta, CA, USA) at a sample rate of 200Hz, and stored in a laptop using a dedicated software (Acknowledge, Biopac Systems). $Vte_{measured}$ was obtained from numerical integration of the flow signal. All the tests were done in ATPD conditions and not corrected for BTPS conditions.

Three set volumes (Vt_{set}) were tested: 350 ml, 450 ml and 550 ml, which approximately cover 6 ml/kg of Predicted Body Weight (PBW) for 161 to 199 cm height in male adult patients and 166 to 203 cm height in female adult patients. We also tested 300 mL on the Osiris 3. The different respiratory mechanics conditions tested were compliance of 50 ml/cmH_2O and 20 ml/cmH_2O, both combined with a resistance of 15 cmH_2O/L/s. The combinations of compliance and resistance tested were based on recently described COVID-19 respiratory mechanics [6-9].

Assist Control Ventilation (ACV) mode was selected and similar ventilator settings were applied for each ventilator (respiratory rate 30 cycles/min).

The pneumatic transport ventilators were set with an Inspiratory:Expiratory ratio of 1:3 (I:E) whereas a flow of 60L/min was adjusted on the Engström Carestation, Elisee 350 and Monnal T60. For every condition tested, inspiratory flow was measured.

The three set volumes were tested with FiO_2 100% and 70% as follows: FiO_2 was selected, Vt_{set} was adjusted on the ventilator and $Vte_{measured}$ was recorded and averaged over 5 cycles after stabilization. As Osiris 3 does not have an oxygen sensor to monitor oxygen content, FiO_2 was measured on this ventilator when air-O_2 mix was selected with a PF300 gas analyzer (IMT Medical, Buchs, Switzerland) in different conditions (Vt = 350 - 450 - 550 ml and Compliance = 20 - 50 mL/cmH_2O).

The performances of Venturi-based ventilation in terms of volume delivery could be altered by set inspiratory flow values [10]. To assess in the Osiris 3 the impact of the inspiratory flow on Vte_{error}, we tested a Vt_{set} of 450 ml obtained with different inspiratory flows achieved by changing respiratory rate (RR). ACV mode with air-O_2 mix was selected, a resistance of 15 cmH_2O/L/s and a compliance of 20ml/cmH_2O were applied and we set a I:E ratio of 1:3. The lowest RR (6 cycles/min) was chosen and was progressively increased by 4 cycles/min until reaching the maximum RR of 40 cycles/min. Vt_{set} had to be adjusted in consequence at each RR increment to keep its value at 450 ml. Vte_{error} was estimated at each step.

Two levels of PEEP were applied (10 cmH_2O and 15 cmH_2O) and the accuracy of the effective PEEP ($PEEP_{measured}$) was assessed.

Volume error and PEEP end-points:

The relative volume error (Vte_{error}), which is the difference between the effective expired volume ($Vte_{measured}$) and the set volume (Vt_{set}) was calculated and averaged as previously described over the four different conditions [4,11] :

- Resistance = 15 cmH_2O/L/s, Compliance = 20 or 50 ml/cmH_2O, PEEP = 10 or 15 cmH_2O

The relative volume error was expressed in percentage and defined as follows:

$$Vte_{error} = \frac{|Vte_{measured} - Vte_{set}|}{Vte_{set}} \times 100$$

End-point for Vt_{error}: The three tidal volumes tested were chosen to cover theoretical "6 ml/kg PBW" in adult male or female patients (350, 450 and 550 ml correspond to 6ml/kg PBW for respectively 58, 75 and 92 kg PBW). Ventilation was considered safe and acceptable when $Vte_{measured}$ was within ± 0.5 ml/kg PBW, which covers a volume between 5.5 and 6.5 ml/kg PBW. This corresponds to an 8% difference between set and measured Vt.

End-point for PEEP: a difference between measured PEEP and set PEEP was acceptable when less than 2 cmH_2O.

3. Trigger performances

Assist control ventilation (ACV) with the inspiratory trigger function "on" was tested by connecting ventilators to the double chamber Michigan test lung to simulate spontaneous breathing (see figure 1). One chamber of the test lung was defined as the driving lung while the other chamber was connected to the ventilator being tested. A lung-coupling clip allowed a connection between the two chambers, so that a positive pressure created in the driving lung induced a negative pressure in the experimental lung, leading to trigger the ventilator tested.

The driving lung was connected to an Evita XL ventilator (Draeger, Lubeck, Germany), which was set in volume-controlled mode with constant flow. The respiratory rate was set at 25 breaths/ min. The ventilatory settings were chosen to achieve a moderate effort, with a decrease in airway pressure 100 ms after occlusion ($P_{0.1}$) of 4 cmH_2O (consistent with $P_{0.1}$ value recently described in COVID patients [12]) measured at the airway opening of the lung model [13,14]. A level of PEEP was applied to the driving lung to obtain a perfect contact of the lung-coupling clip between the two chambers at the end of expiration.

For each ventilator tested, volume assist-control ventilation (ACV) mode was selected, with a tidal volume of 450 ml, a respiratory rate of 20 cycles/min and a PEEP of 10 cmH_2O. I:E ratio was set at 1:3 for Osiris 3 and Oxylog 3000, while a flow of 60L/min was set on Elisee 350, Monnal T60 and the Engström Carestation ICU ventilator. Inspiratory triggers were set at their most responsive position while avoiding auto-triggering. The trigger of the Osiris 3 was set at -0.5 cmH_2O. Flow-triggered ventilators were set at 1 L/min for Engström Carestation and Oxylog 3000 and 2 L/min for Monnal T60 and Elisee 350. Two respiratory mechanics were tested: C=20 ml/cmH2O and 50 ml/cmH2O with R=15 cmH2O/L/sec.

For each configuration, trigger performance was assessed by measuring the airway pressure changes using the flow trace to determine the start of inspiration [11,15]. Negative pressure drop (ΔP, cmH_2O), Triggering Delay (TD, ms) and Pressurization Delay (PD, ms) as defined on figure 2 were measured. The overall Inspiratory Delay (ID) corresponds to the addition of TD and PD.

We repeated the tests for all the ventilators at a strong effort corresponding to a $P_{0.1}$ of 8 cmH_2O; we tested the effect of set volume (Vt_{set} = 350 - 450 - 550 ml), compliance (C = 20 - 50 ml/cmH_2O) and Positive End Expiratory Pressure (PEEP = 5 - 10 - 15 cmH_2O) on triggering delay performances (See additional file 1).

End-point: triggering function was considered as "safe and acceptable" when TD was less than 100 ms.[16].

4. Statistical analysis

Continuous variables were expressed as mean ± SD values averaged from 5 consecutive breaths. These variables were compared using an ANOVA test. The type I significance level was set at 0.05. When the global F was significant, post hoc tests were computed using a student t-test with Bonferroni correction, which sets the level of significance for pairwise differences between the five ventilators at 0.005.

Figure 1. Illustration of bench test to simulate spontaneous breathing to assess trigger performances

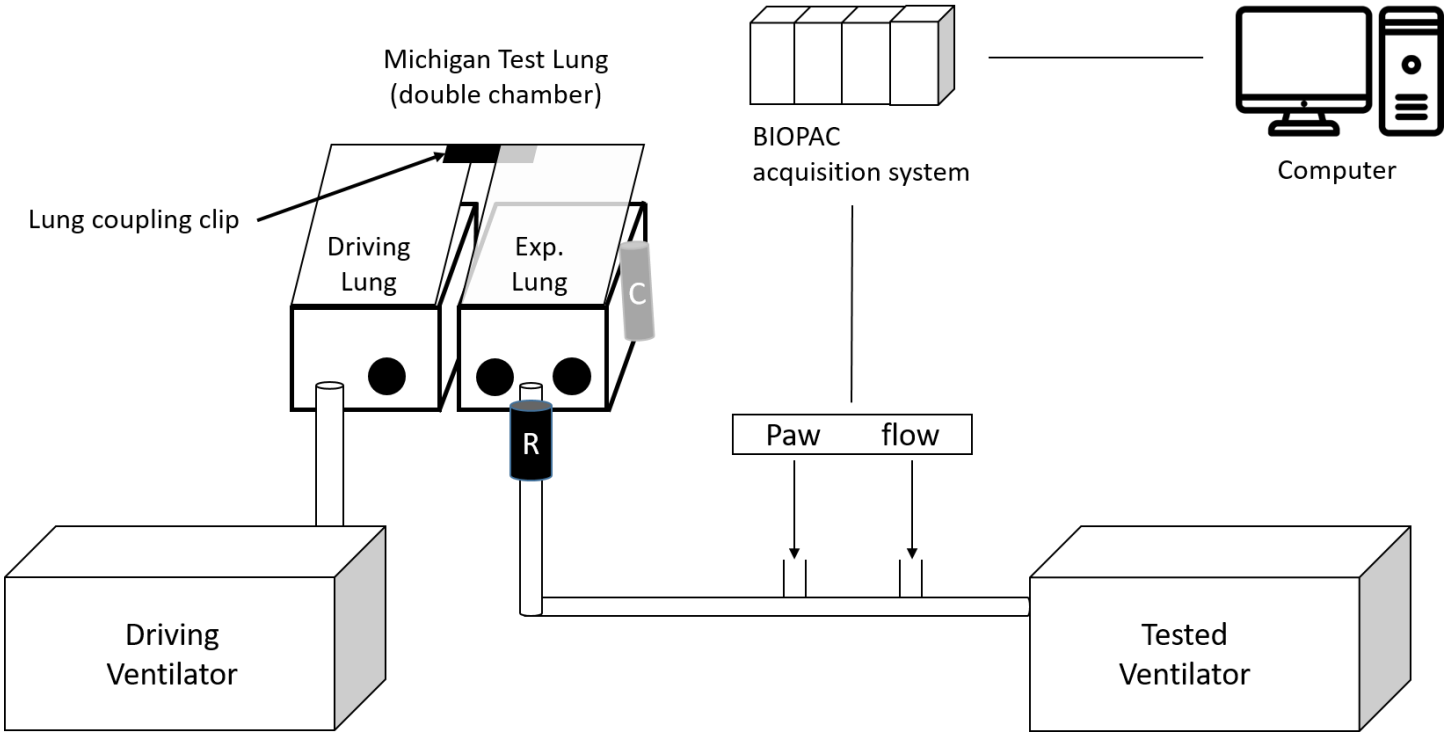

The figure illustrates the bench test used to simulate spontaneous breathing to assess trigger performances.

A double chamber Michigan test lung was used to simulate spontaneous breathing. One chamber of the test lung was defined as the driving lung while the other chamber was connected to the ventilator being tested. A lung-coupling clip allowed a connection between the two chambers, so that a positive pressure created in the driving lung (by the driving ventilator) induced a negative pressure in the experimental lung ("exp. Lung" on the figure), leading to trigger the ventilator tested.

Of note, only one chamber of the test lung (experimental lung) is used to assess Vte error whereas the two chambers (driving lung and experimental lung) are used to simulate spontaneous breathing to assess trigger performances.

Figure 2. Explicative figure of ventilator triggering assessment

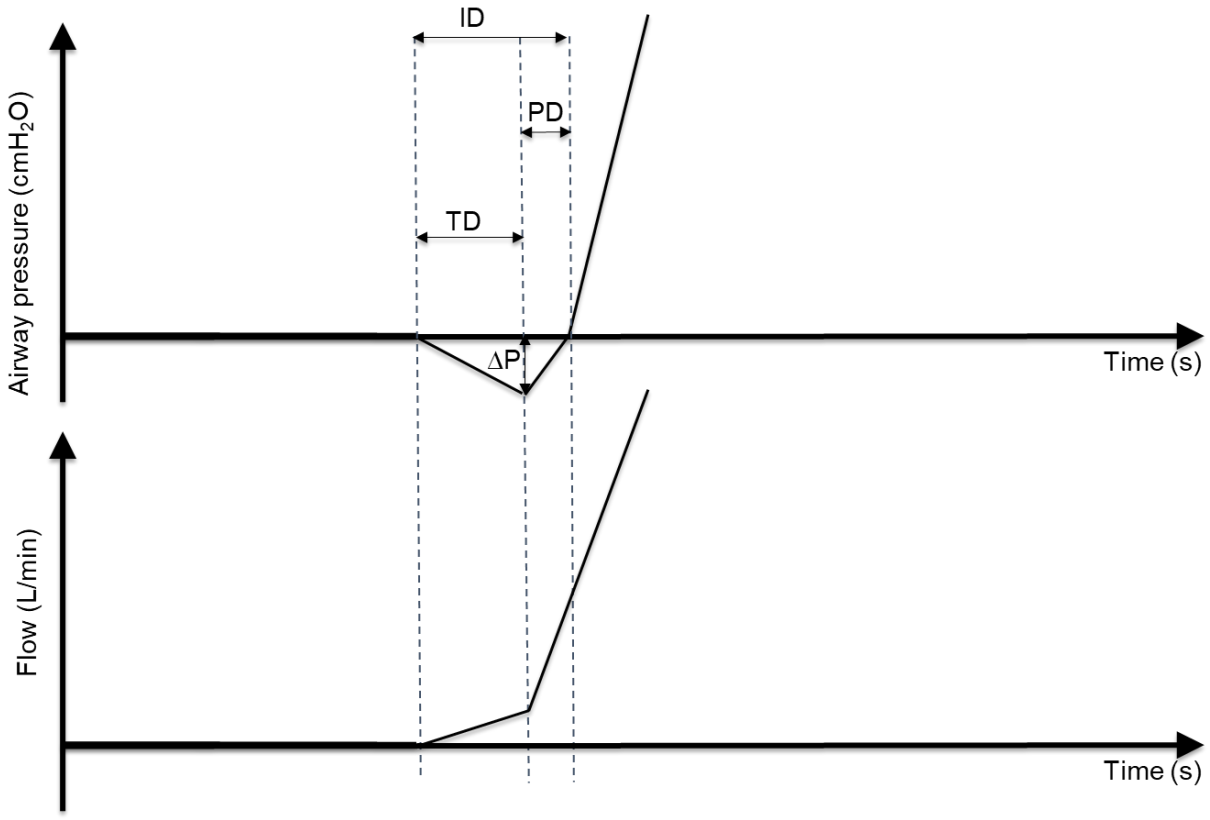

The figure illustrates ventilator triggering assessment. Airway pressure (Paw) and flow are displayed. Triggering delay (TD) is the delay between the onset of airway pressure drop ("patient" effort) and flow delivery by the ventilator. Pressurization delay (PD) is defined by the time at which the airway pressure comes back to the level of PEEP. The addition of TD and PD gives the inspiratory delay (ID). The drop of airway pressure (ΔP) due to patient effort is also shown on the figure.

Results

1. Volume delivered and PEEP measured with different respiratory mechanics

Results obtained with a P0.1 of 4 cmH_2O (moderate effort) are displayed in figure 3 and mean volume errors (Vte_{error}) for each ventilator are shown in Table 2. When all conditions and set volumes were included, the Engström Carestation was the most accurate ventilator, and the Oxylog 3000 was comparable. The performance was considered as acceptable (delta Vt ± 0.5ml/kg PBW) except for one turbine ventilator (Elisee 350). The impact of FiO_2 selection (FiO2 100% or 70%) on volume error was significant considering all ventilators ($p < 0.05$, see table 2). There was no impact of compliance on volume error ($p > 0.05$, table 2). FiO_2 measured on Osiris 3 was 72.3 ± 1.7% across all the conditions tested. Differences between measured PEEP and set PEEP were less than 2 cmH_2O as shown on table 2 (all conditions together).

Volume delivered at a Vt_{set} of 300 ml for the Osiris 3 is shown in the ESM on figure E1. Table E1 summarizes measured inspiratory flow for each ventilator in the different experimental conditions.

2. Impact of inspiratory flow on pneumatic ventilators

The effect of inspiratory flow rates on Vte_{error} for Osiris 3 is shown on figure 4. Considering a Vt_{set} of 450 ml, the lowest values of inspiratory flow were associated with a Vte_{error} higher than 8% (delta Vt ± 0.5ml/kg PBW). Performances were acceptable when inspiratory flow (resulting from the combination of Vt, I:E ratio and respiratory rate) was strictly above 30 L/min, which corresponds to a respiratory rate higher than 18 cycles/min.

Figure 3. Tidal Volume delivery in volume control ventilation in static conditions

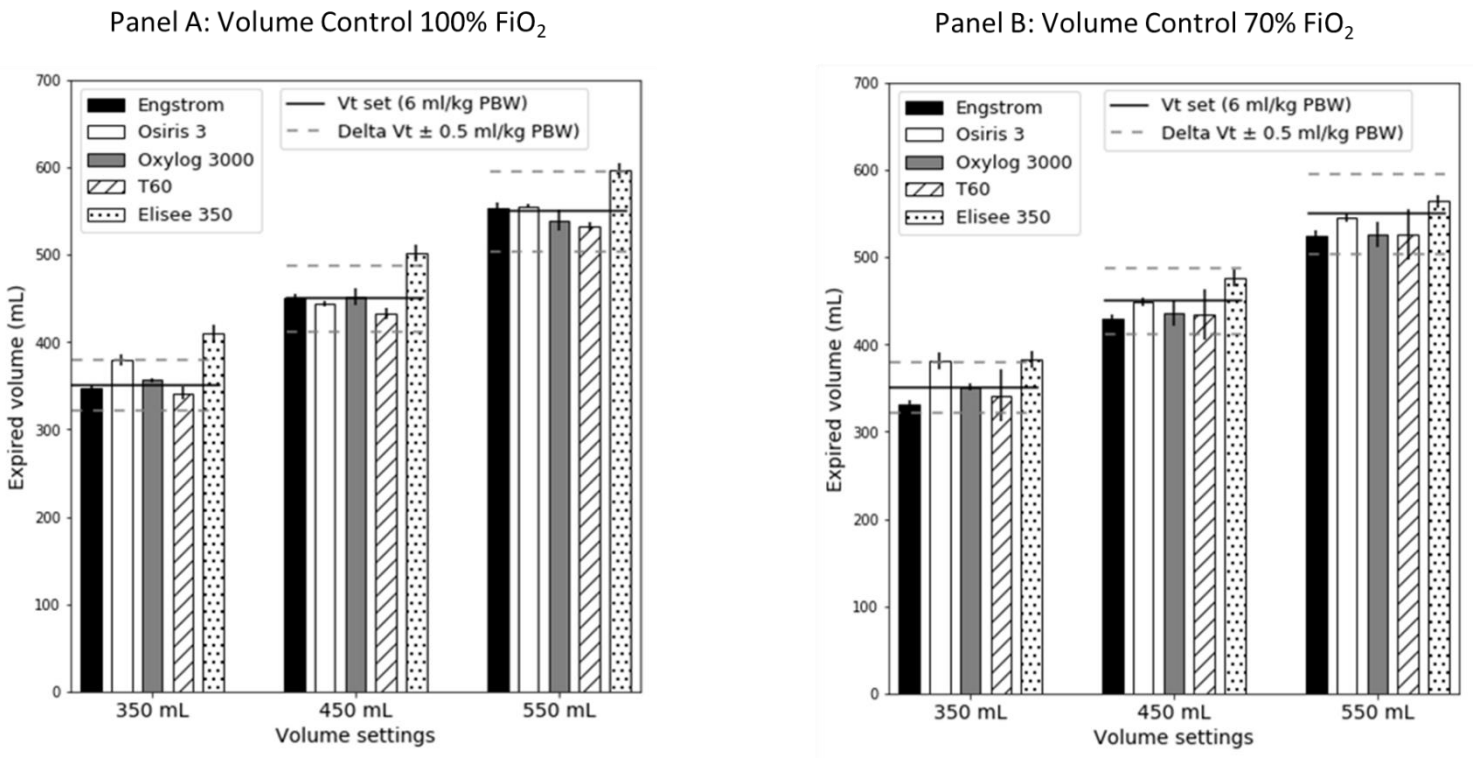

Panel A. *The histogram represents the mean expired volumes measured for each ventilator according to the three Vt set in 100% FiO_2. The average was computed over the four conditions of resistance (15 cmH2O/L/s), compliance (20 - 50 ml/cmH_2O) and PEEP (10 - 15 cmH_2O). The three tidal volumes tested were chosen to cover 6 ml/kg PBW, with 350, 450 and 550 ml corresponding to 6ml/kg PBW for respectively 58, 75 and 92 kg PBW. Limits of acceptable ventilation are displayed with dotted lines and defined as a volume change within ± 0.5 ml/kg PBW, which corresponds to a Vt between 5.5 and 6.5 ml/kg PBW.*

Panel B. *The histogram represents the mean expired volumes measured for each ventilator according to the three Vt set in 70% FiO_2. The average was computed over the four conditions of resistance (15 cmH2O/L/s), compliance (20 - 50 ml/cmH_2O) and PEEP (10 - 15 cmH_2O).*

Figure 4. Impact of flow on effective volume with Osiris 3 ventilator

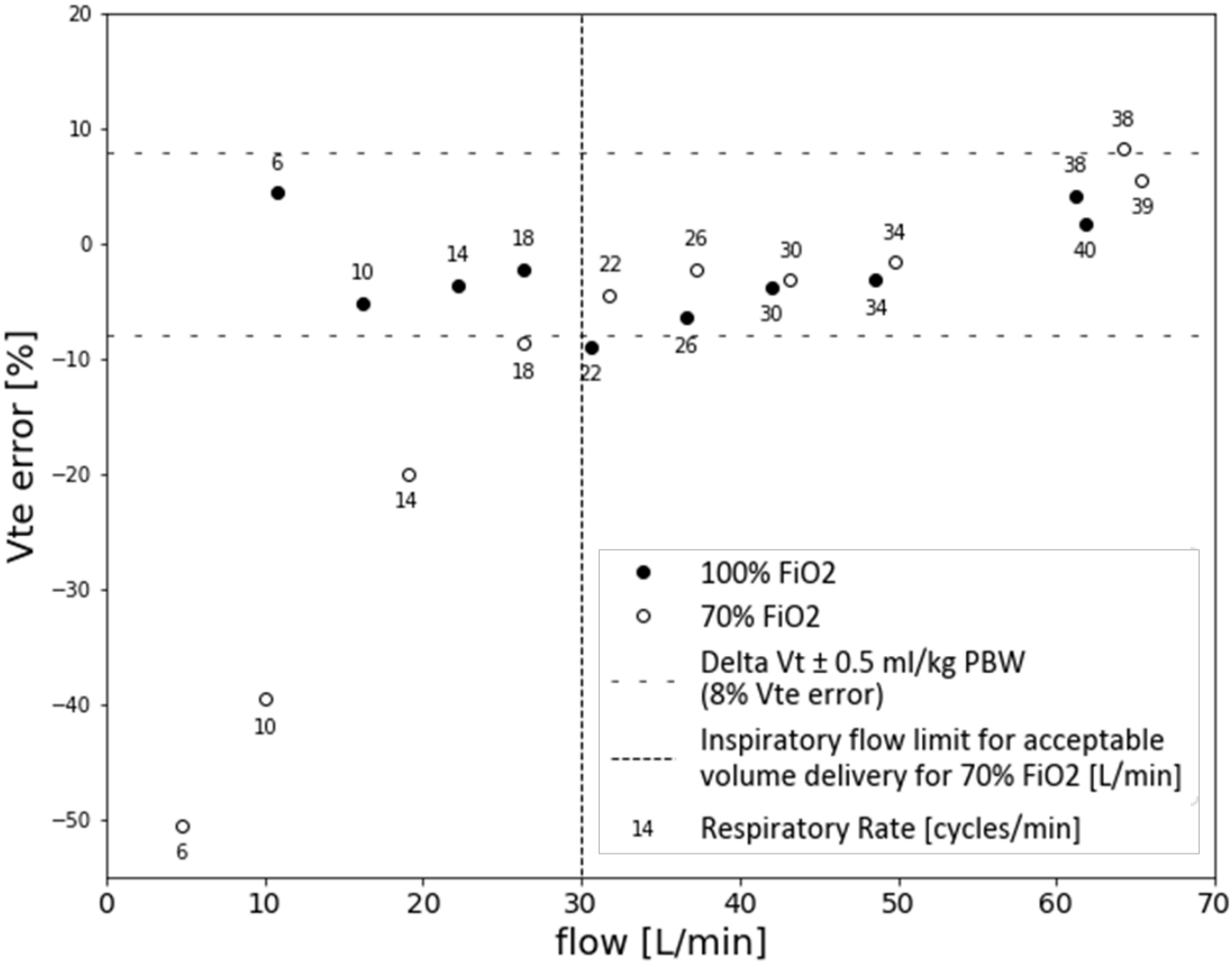

This figure shows the volume error of the Osiris 3 expressed in percentage of Vt set according to different inspiratory flows obtained at a constant 450 ml Vt set. Compliance, resistance and PEEP were set at 20 ml/cmH_2O, 15 cmH2O/L/s and 10 cmH_2O respectively. Black circles were obtained with 100% FiO_2 while the white circles were obtained with 70% FiO_2. Respiratory rate associated with each point is also displayed. This figure illustrates that for an inspiratory flow below 30 L/min, the Vt error is substantial with 70% FiO_2. The Vt error is within ± 0.5 ml/kg PBW (which corresponds to an 8% difference between set and measured Vt) whatever the inspiratory flow when 100% FiO_2 is selected.

3. Trigger performances during ACV

Inspiratory trigger was evaluated for each ventilator and results corresponding to a moderate effort ($P_{0.1}$ = 4 cmH_2O) are displayed on figure 5. All simulated efforts triggered a ventilatory cycle. The Triggering Delay was 42 ± 4 ms, 65 ± 5 ms, 151 ± 14 ms, 51 ± 6 ms and 64 ± 5 ms for Engström Carestation, Osiris 3, Oxylog 3000, Monnal T60 and Elisee 350, respectively (all conditions grouped, $p < 0.05$; pairwise differences between ventilators were all significant with a p-value < 0.005). The Inspiratory Delay (ID) was measured at 54 ± 5 ms for Engström Carestation, 95 ± 5 ms for Osiris 3, 217 ± 21 ms for Oxylog 3000, 72 ± 6 ms for Monnal T60 and 85 ± 7 ms for Elisee 350 and ($p < 0.05$; pairwise differences between ventilators were all significant with a p-value < 0.005).

The airway pressure drop was much larger for Oxylog 3000 (- 4.2 ± 0.3 cmH_2O), than for the others:- 0.9 ± 0.3 cmH_2O for Engström Carestation, - 1.9 ± 0.1 cmH_2O for Osiris 3, - 0.6 ± 0.1 cmH_2O for Monnal T60 and - 0.8 ± 0.1 for Elisee 350 ($p < 0.05$; pairwise differences between ventilators were all significant with a p-value < 0.005, except between Engstrom Carestation – Elisee 350 and Engstrom Carestation – Monnal T60).

Ventilator performances were considered acceptable (TD < 100ms) except for one pneumatic ventilator (Oxylog 3000). Triggering Delays obtained with a strong effort ($P_{0.1}$ = 8 cmH_2O) are available on figure E2 (see ESM). Grouping all conditions ($P_{0.1}$ of 4 cmH_2O and 8 cmH_2O), trigger delay was 50 ± 11 ms, 71 ± 8 ms, 132 ± 22 ms, 60 ± 12 and 67 ± 6 ms for Engström Carestation, Osiris 3, Oxylog 3000, Monnal T60 and Elisee 350, respectively. The effect of set volume, compliance and PEEP on triggering delay performances (at $P_{0.1}$ = 8 cmH_2O) are shown on table E2, E3 and E4 respectively (see ESM).

Figure 5. Triggering characteristics in volume assist-control ventilation for a P0.1 of 4 cmH_2O

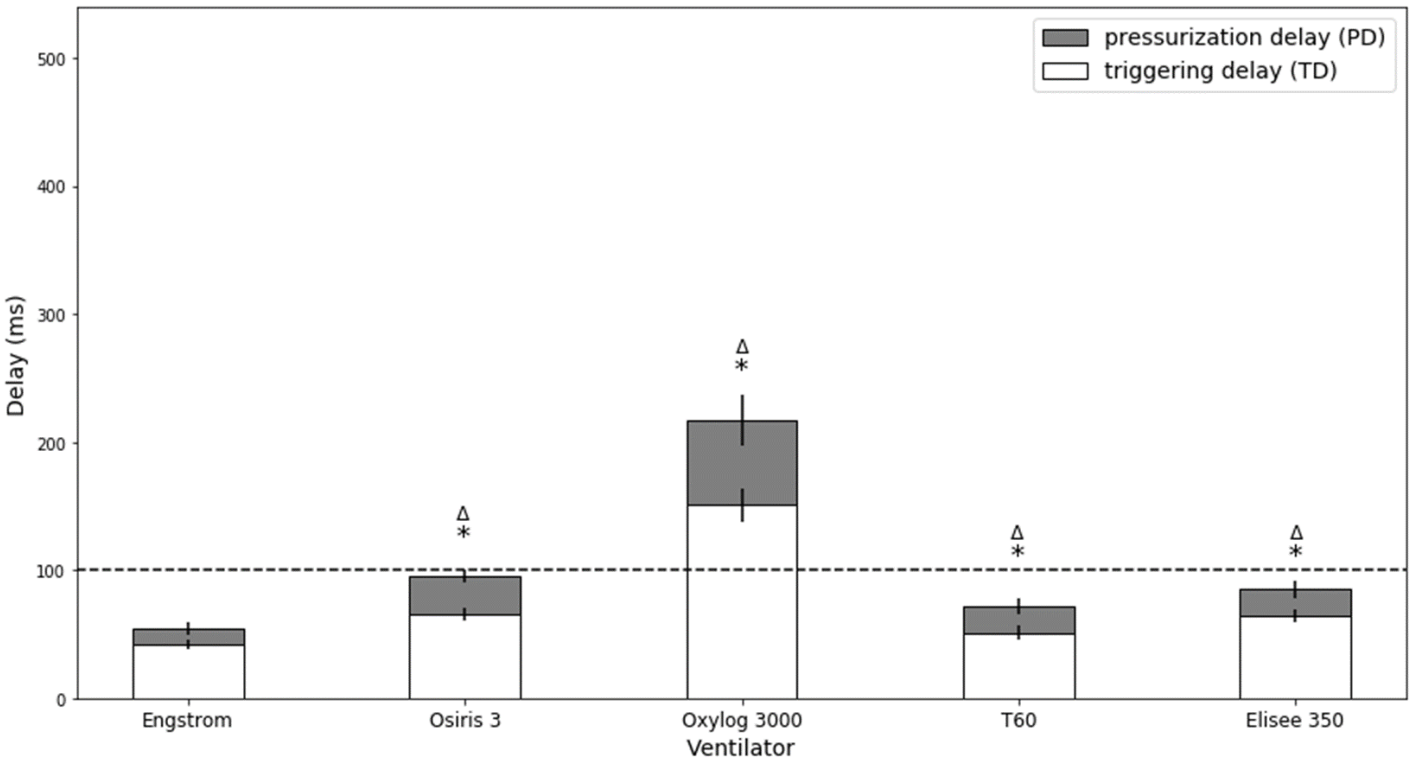

The figure illustrates the triggering efficiency for each ventilator tested during assist-control ventilation using the Michigan test lung to simulate spontaneous breathing. A moderate effort was achieved, corresponding to a decrease in airway pressure 100 ms after occlusion (P0.1) of 4 cmH_2O was achieved. A PEEP of 10 cmH_2O, a compliance of 20 and 50 ml/cmH_2O and a resistance of 15 cmH2O/L/s were selected. Triggering Delay (TD, ms) and Pressurization Delay (PD, ms) were computed. A definition of TD and PD is available on figure 1. Triggering function was considered safe and acceptable when TD was less than 100 ms.

** indicates P < 0.005 for TD when comparing each transport ventilator with the Engstrom ICU ventilator (ANOVA test: global F was significant).*

Δ indicates P < 0.005 for PD when comparing each transport ventilator with the Engstrom ICU ventilator (ANOVA test: global F was significant).

Discussion

The results of the present bench test study comparing turbine and pneumatic transport ventilators to an ICU ventilator, can be summarized as follows: 1. Turbine ventilators' performances in VC and ACV are very close to those of the ICU ventilator tested for most of the settings including volume delivery and reliability of PEEP. 2. For most of the severe respiratory mechanics conditions tested, the volume error does not exceed 0.5 ml/kg PBW except for one turbine ventilator (two conditions) and one pneumatic ventilator (one condition). Volume error delivered by the simplest pneumatic ventilator significantly increased at FiO_2 70%, when inspiratory flow was less than 30 L/min indicating a technological limit of the Venturi system. 3. Inspiratory trigger reactivity was less than 100 ms except for one pneumatic transport ventilator.

The increasing number of patients requiring mechanical ventilation in the context of the COVID-19 worldwide crisis, and the ventilators shortage reported in some severely affected countries, has led to discuss the possibilities to manage intubated patients outside the walls of the ICU [2]. According to this dire scenario, simple and easy to set ventilators that only require one oxygen pressure source to function and able to reliably deliver lung protective ventilation could be considered. In addition, an assisted mode that controls the Vt with PEEP up to 15 cmH_2O and FiO_2 up to 100% is required to manage patients with high elastic load and severe shunt that characterize potentially severe COVID-19 ARDS [1,2].

Performances during controlled ventilation:

Recent turbine transport and emergency ventilators display performances which are very close to conventional ICU ventilators [5,17]. In the context of "mass casualty", as experienced with the COVID-19 crisis, pneumatic transport ventilators could be used to extend the possibility to manage intubated patients in case of ICU beds shortage. The working principle of these pneumatic ventilators is based on a "Venturi system" which is a simple technological solution that permits to manage ventilation generated by the oxygen pressurized source when a position called air-O_2 mix is selected. Interestingly, the simplicity of such pneumatic systems permits to consider massive industrialization faster and at a lower cost. On the opposite, the Venturi system explains the limits observed with low inspiratory flow previously described with this technology [10].

For pneumatic ventilators, in case of high impedance, a low inspiratory flow may increase significantly volume error when the air-O2 mix position is selected “on”. In turn, manipulating I:E ratio, respiratory rate and increasing inspiratory flow above 30 L/min permits to reverse the Vt error that is directly explained by the working principle of this ventilator (see figure 4). The technological adaptations available on Oxylog 3000 (Venturi coupled with proportional inspiratory valve) solve this problem while expired Vt monitoring available on Osiris 3 simplifies settings adaptation if required. Previous bench test studies have reported a Vt error with pneumatic basic transport ventilators that reached 20% of set Vt with resistive load [10,18]. These experiments were performed with very low set inspiratory flow thus explaining the Vt reduction observed. For clinical practice, when FiO_2 70% is used on the Osiris 3, an essential recommendation is to follow these steps: first adjust the I:E ratio at 1:3 (i.e. the minimal available value) and the respiratory rate at 18/min or above. Secondarily, the Vt knob that also controls the inspiratory flow must be adjusted to reach the desired Vt based on Vt expired monitoring. With these recommendations, volume error measured on pneumatic transport ventilators at low compliance is close from turbine performances and acceptable.

Of note, only the ICU and turbine ventilators tested compensate for the loss in Vt due to the compression of gas inside the circuit. Nevertheless, this effect previously quantified in ICU ventilators with inspiratory-expiratory circuits is significantly less in basic transport ventilators since they are equipped with a single limb circuit [4]. Of note, an HEPA filter can be easily adjusted on the expiratory limb to limit risks of viral contamination.

Performances during assisted ventilation:

Recent experience with COVID-19 induced ARDS reports that these patients often exhibit high respiratory drive and asynchrony that may require deep sedation and sometimes paralysis [7]. We therefore evaluated the behavior of the four transport ventilators during triggered breaths, especially pneumatic ones since performances of their trigger have been questioned [5,18]. The triggering performances were acceptable except for the Oxylog 3000 exhibiting the poorest triggering performances. The triggering delay was consistently longer in pneumatic ventilators but acceptable except on the Oxylog 3000, compared to the ICU ventilator [5].

Limitations

The results obtained in vitro necessitate some caution to be translated to the clinical practice, but previous studies showed that this type of simulation predicts the results observed in clinical situations with a high fidelity [4,19,20]. The lung model gives the unique opportunity to

compare ventilator performances according to several simulated but standardized clinical conditions. Bench experiment also permits to accurately depict and understand advantages and limits of the different ventilator's technologies as previously done [10]. The Michigan test lung (Michigan Instruments, Kentwood, MI, USA) used in the present study is a simple model that presents obvious limitations, but its reliability for Vt and trigger performances evaluation has been well demonstrated. Of note, the results have not been corrected in BTPS conditions, which may have slightly underestimated actual expired volumes [17]. Our experiment reported performances of only two pneumatic and two turbine ventilators while several other ventilators with similar technology are available worldwide. We did not evaluate pressure support ventilation while this approach can be useful to manage weaning of COVID-19 patients. Previous studies already showed that turbine-based ventilator significantly outperform pneumatic transport ventilators during pressure mode ventilation [5,17].

Performances of pneumatic ventilators can be viewed as "acceptable" during the initial phase of respiratory failure. For patients with difficulties to be separated from the ventilator, better performances may be expected for assisted ventilation.

Conclusion

The present bench study suggests that turbine technologies may acceptably replace ICU ventilators, at least transiently, to extend ICU beds where only oxygen pressure supply is available, in special surge situations such as COVID-19 crisis. Pneumatic transport ventilators are limited in terms of FiO_2 settings, but provide acceptable volume accuracy in severe simulated conditions. For this purpose, the respiratory rate should be set at or above 18/min (to maintain sufficient inspiratory flow) in the Osiris 3 with a FiO_2 of 70% [21]. A monitoring of expired Vt available on the two pneumatic transport ventilators tested greatly facilitates adequate settings. Performances regarding triggering function are non-acceptable in one of the pneumatic transport ventilators.

List of abbreviations

ACV: Assist-Control Ventilation

ARDS: Acute Respiratory Distress Syndrome

Covid-19: Coronavirus Disease 2019

C_{RS}: Compliance of the respiratory system

FiO_2: Fraction of inspired Oxygen

ICU: Intensive Care Unit

PEEP: set Positive End-Expiratory Pressure

SARS-CoV-2: Severe Acute Respiratory Syndrome Coronavirus – 2

VC : Volume Control

Vt : tidal volume

Declarations

- Ethics approval and consent to participate: not applicable
- Consent for publication : not applicable
- Availability of data and material: the datasets analyzed during the current study are available from the corresponding author on reasonable request
- Competing interests: DS reports grants from Fisher and Paykel and travel fees from Air Liquide Medical Systems. JCR reports part time salary for research activities (Med2Lab) from Air Liquide Medical Systems and Vygon and grants from Creative Air Liquide, outside this work. AL is PhD student in the (Med2Lab) partially funded by Air Liquide Medical Systems. BB is research engineer in the Med2Lab funded by Air Liquide Medical Systems. AB is master student from the Telecom-Physic-Strasbourg Strasbourg University France. FB reports personal fees from Löwenstein Medical, travel fees from Draeger and research support from Covidien, GE Healthcare and Getinge Group, outside this work. AM reports personal fees from Draeger, Faron Pharmaceuticals, Air Liquid Medical Systems, Pfizer, Resmed and Draeger and grants and personal fees from Fisher and Paykel and Covidien, outside this work. All other authors declare no competing interests. This study did not receive any grant or financial support.
- Funding: not applicable
- Authors' contributions: AL, JCR and AM contributed to the study conception and design. AL, JCR performed the experiments, the data collection and the initial data analysis. JCR, LB and AM prepared the first draft of the manuscript. All authors contributed to the data analysis and to the critical revision and approval of the final manuscript.
- Acknowledgements: Authors would like to greatly acknowledge Nathan Prouvez and Bilal Badat for their contribution to the bench experiments. Authors are also grateful to Marie-Laure Evrat for having made ventilators available for the tests despite the COVID crisis.

References

[1] Beitler JR, Mittel AM, Kallet R, Kacmarek R, Hess D, Branson R, et al. Ventilator Sharing During an Acute Shortage Caused by the COVID-19 Pandemic. Am J Respir Crit Care Med. 2020 Jun 9;rccm.202005-1586LE

[2] Emanuel EJ, Persad G, Upshur R, Thome B, Parker M, Glickman A, et al. Fair Allocation of Scarce Medical Resources in the Time of Covid-19. N Engl J Med. 2020 May 21;382(21):2049–55.

[3] Monti G, Cremona G, Zangrillo A, Lombardi G, Sartini C, Sartorelli M, et al. Home ventilators for invasive ventilation of patients with COVID-19. Critical Care and Resuscitation. 2020 Apr 30 :5.

[4] Lyazidi A, Thille AW, Carteaux G, Galia F, Brochard L, Richard J-CM. Bench test evaluation of volume delivered by modern ICU ventilators during volume-controlled ventilation. Intensive Care Med. 2010 Dec;36(12):2074–80.

[5] L'Her E, Roy A, Marjanovic N. Bench-test comparison of 26 emergency and transport ventilators. Critical Care. 2014 Oct;18(5).

[6] Pan C, Chen L, Lu C, Zhang W, Xia J-A, Sklar MC, et al. Lung Recruitability in SARS-CoV-2 Associated Acute Respiratory Distress Syndrome: A Single-center, Observational Study. Am J Respir Crit Care Med. 2020 Mar 23;rccm.202003-0527LE.

[7] Gattinoni L, Coppola S, Cressoni M, Busana M, Rossi S, Chiumello D. Covid-19 Does Not Lead to a "Typical" Acute Respiratory Distress Syndrome. Am J Respir Crit Care Med. 2020 Mar 30;rccm.202003-0817LE.

[8] Gattinoni L, Chiumello D, Caironi P, Busana M, Romitti F, Brazzi L, et al. COVID-19 pneumonia: different respiratory treatments for different phenotypes? Intensive Care Med. 2020 Apr 14;s00134-020-06033–2.

[9] Grasselli G, Zangrillo A, Zanella A, Antonelli M, Cabrini L, Castelli A, et al. Baseline Characteristics and Outcomes of 1591 Patients Infected With SARS-CoV-2 Admitted to ICUs of the Lombardy Region, Italy. JAMA. 2020 Apr 6;323(16):1574.

[10] Breton L, Minaret G, Aboab J, Richard J-C. Fractional inspired oxygen on transport ventilators: an important determinant of volume delivery during assist control ventilation with high resistive load. Intensive Care Med. 2002 Aug;28(8):1181; author reply 1182.

[11] Boussen S, Gainnier M, Michelet P. Evaluation of Ventilators Used During Transport of Critically Ill Patients: A Bench Study. Respir Care. 2013 Jan 11;58(11):1911–22.

[12] Gattinoni L, Marini JJ, Camporota L. The Respiratory Drive: An Overlooked Tile of COVID-19 Pathophysiology. Am J Respir Crit Care Med. 2020 Oct 15;202(8):1079–80.

[13] Beloncle F, Piquilloud L, Olivier P-Y, Vuillermoz A, Yvin E, Mercat A, et al. Accuracy of P0.1 measurements performed by ICU ventilators: a bench study. Ann Intensive Care. 2019 Dec;9(1):104.

[14] Telias I, Junhasavasdikul D, Rittayamai N, Piquilloud L, Chen L, Ferguson ND, et al. Airway Occlusion Pressure As an Estimate of Respiratory Drive and Inspiratory Effort during Assisted Ventilation. Am J Respir Crit Care Med. 2020 May 1;201(9):1086–98.

[15] Richard J-C, Carlucci A, Breton L, Langlais N, Jaber S, Maggiore S, et al. Bench testing of pressure support ventilation with three different generations of ventilators. Intensive Care Med. 2002 Aug;28(8):1049–57.

[16] Aslanian P, El Atrous S, Isabey D, Valente E, Corsi D, Harf A, et al. Effects of Flow Triggering on Breathing Effort During Partial Ventilatory Support. Am J Respir Crit Care Med. 1998 Jan;157(1):135–43.

[17] Thille AW, Lyazidi A, Richard J-CM, Galia F, Brochard L. A bench study of intensive-care-unit ventilators: new versus old and turbine-based versus compressed gas-based ventilators. Intensive Care Med. 2009 Aug;35(8):1368–76.

[18] Zanetta G, Robert D, Guérin C. Evaluation of ventilators used during transport of ICU patients – a bench study. Intensive Care Med. 2002 Apr;28(4):443–51.

[19] Carteaux G, Lyazidi A, Cordoba-Izquierdo A, Vignaux L, Jolliet P, Thille AW, et al. Patient-Ventilator Asynchrony During Noninvasive Ventilation. Chest. 2012 aug;142(2):367-76.

[20] Vignaux L, Tassaux D, Jolliet P. Performance of noninvasive ventilation modes on ICU ventilators during pressure support: a bench model study. Intensive Care Medicine. 2007 jul;33(8):1444-51.

[21] Garnier M, Quesnel C, Fulgencio J-P, Degrain M, Carteaux G, Bonnet F, et al. Multifaceted bench comparative evaluation of latest intensive care unit ventilators. British Journal of Anaesthesia. 2015 Jul;115(1):89–98.

Tables:

Table 1. General characteristics of the ventilators

	Engström Carestation	**Osiris 3**	**Oxylog 3000**	**Monnal T60**	**Elisee 350**
Manufacturer	GE Healthcare	Air Liquide Medical Systems	Draeger	Air Liquide Medical Systems	Resmed
Weight [kg]	31.0	5.0	5.4	3.7	4.0
Working pressure	Pressurized oxygen and air	Pressurized oxygen	Pressurized oxygen	Pressurized oxygen	Pressurized oxygen
Expired volume monitoring	Yes	Yes	Yes	Yes	Yes
Tidal volume (Vt) [ml]	20 - 2000	100 - 2000	50 - 2000	20 - 2000	50 - 2500
Accuracy of Expiratory flow sensor	± 10 %	± 15 %	± 15 %	VTe ≥ 50 ml: +/- (2,5 ml + 15 %)	10 % or 10 ml
PEEP [cmH20]	1 - 50	0 - 15	0 - 20	0 - 20	0 - 25
Peak inspiratory pressure [cmH20]	7 - 100	10 - 80	PEEP + 3 - PEEP + 55	0 - 80	0 - 100
FiO_2 [%]	21 - 100	70 or 100	40 - 100	21 - 100	21 - 100
Battery duration [h]	0.5 - 2	6 - 14	4	2.5 - 5	3 - 6

Abbreviations

- *PEEP* = positive end expiratory pressure
- *FiO2* = fraction of inspired oxygen

Table 2. Mean volume errors and Positive End Expiratory Pressure (PEEP) measured for each ventilator

	Engström Carestation	Osiris 3	Oxylog 3000	Monnal T60	Elisee 350
Vte_{error} global [%]	2.9 ± 2.2	3.6 ± 3.9	2.5 ± 2.1	5.4 ± 2.7 (*)	8.8 ± 4.8 (*)
Vte_{error} 100% FiO_2 [%]	1.0 ± 0.7	3.7 ± 3.7 (*)	2.0 ± 1.2 (*)	3.3 ± 1.4 (*)	11.9 ± 4.1 (*)
Vte_{error} 70% FiO_2 [%]	4.9 ± 1.3	3.5 ± 4.2	2.9 ± 2.7 (*)	7.5 ± 2.0 (*)	5.9 ± 3.5
Vte_{error} C50 [%]	3.3 ± 2.7	3.4 ± 4.0	1.6 ± 1.1 (*)	5.1 ± 3.1 (*)	10.4 ± 5.3 (*)
Vte_{error} C20 [%]	2.6 ± 1.6	3.8 ± 3.8	3.4 ± 2.6	5.7 ± 2.2 (*)	7.0 ± 3.7 (*)
mean PEEP 10 [cmH_2O]	9.9 ± 0.2	10.6 ± 0.6 (*)	11.5 ± 0.3 (*)	9.5 ± 0.5 (*)	10.3 ± 0.1 (*)
mean PEEP 15 [cmH_2O]	15.1 ± 0.2	14.9 ± 0.6 (*)	15.4 ± 2.2	14.7 ± 0.1 (*)	15.4 ± 0.2 (*)

Abbreviations

- *Vte_{error} global* = mean volume error including all conditions of resistance (15 cmH2O/L/s), compliance (20 - 50 ml/cmH_2O) and PEEP (10 - 15 cmH_2O) for both 100% FiO2 and 70% FiO2.
- *Vte_{error} 100% FiO2* = mean volume error including all conditions of resistance (15 cmH2O/L/s), compliance (20 - 50 ml/cmH_2O) and PEEP (10 - 15 cmH_2O) for 100% FiO2.
- *Vte_{error} 70% FiO2* = mean volume error including all conditions of resistance (15 cmH2O/L/s), compliance (20 - 50 ml/cmH_2O) and PEEP (10 - 15 cmH_2O) for 70% FiO2.
- *Vte_{error} C50* = mean volume error including all conditions of resistance (15 cmH2O/L/s), FiO2 (100 - 70 %) and PEEP (10 - 15 cmH_2O) for a compliance of 50 ml/cmH_2O.
- *Vte_{error} C20* = mean volume error including all conditions of resistance (15 cmH2O/L/s), FiO2 (100 - 70 %) and PEEP (10 - 15 cmH_2O) for a compliance of 20 ml/cmH_2O.

- *Mean PEEP 10* = mean PEEP measured when PEEP was set at 10 cmH_2O including all conditions of resistance (15 cmH2O/L/s) and compliance (20 - 50 ml/cmH_2O) for both 100% FiO2 and 70% FiO2.
- *Mean PEEP 15* = mean PEEP measured when PEEP was set at 15 cmH_2O including all conditions of resistance (15 cmH2O/L/s) and compliance (20 - 50 ml/cmH_2O) for both 100% FiO2 and 70% FiO2.

* indicates $P < 0.005$ when comparing each transport ventilator with the Engstrom ICU ventilator (ANOVA test: global F was significant).

Electronic supplementary material

Table E1. Measured inspiratory flow in volume control ventilation

			Engström Carestation	**Osiris 3**	**Oxylog 3000**	**Monnal T60**	**Elisee 350**
Inspiratory flow [L/min]	Vt_{set} = 350 ml	FiO_2 100%	55.2 ± 0.3	40.1 ± 0.7	43.9 ± 0.6	67.2 ± 2.0	81.4 ± 1.1
		FiO_2 70%	53.8 ± 0.4	40.8 ± 1.3	43.3 ± 1.0	68.6 ± 5.4	76.5 ± 2.1
	Vt_{set} = 450 ml	FiO_2 100%	56.1 ± 0.4	47.0 ± 0.6	56.6 ± 0.6	66.4 ± 1.7	77.7 ± 1.0
		FiO_2 70%	54.7 ± 0.3	48.2 ± 1.0	55.3 ± 1.4	67.2 ± 4.0	73.1 ± 2.2
	Vt_{set} = 550 ml	FiO_2 100%	57.0 ± 0.1	59.0 ± 0.7	70.2 ± 1.3	66.3 ± 0.8	74.8 ± 0.9
		FiO_2 70%	55.0 ± 0.3	58.3 ± 1.0	68.9 ± 2.6	66.0 ± 3.2	71 ± 0.8

Abbreviations

- Vt_{set} = set tidal volume on the ventilator.
- *FiO2* = fraction of inspired oxygen

Table E2. Effect of set tidal volume on Trigger Delay

		Engström Carestation	Osiris 3	Oxylog 3000	Monnal T60	Elisee 350
Trigger Delay [ms]	Vt_{set} = 350 ml	53 ± 5	72 ± 4	112 ± 9	70 ± 9	65 ± 7
	Vt_{set} = 450 ml	56 ± 7	78 ± 7	110 ± 7	68 ± 10	65 ± 6
	Vt_{set} = 550 ml	62 ± 12	76 ± 10	110 ± 11	72 ± 4	59 ± 6

Abbreviations

- Vt_{set} = set tidal volume on the ventilator.

Table E3. Effect of compliance on Trigger Delay

		Engström Carestation	**Osiris 3**	**Oxylog 3000**	**Monnal T60**	**Elisee 350**
Trigger Delay [ms]	Compliance = 20 ml/cmH_2O	52 ± 4	75 ± 8	109 ± 8	63 ± 8	62 ± 6
	Compliance = 50 ml/cmH_2O	62 ± 9	78 ± 8	112 ± 9	75 ± 6	66 ± 7

Table E4. Effect of Positive End Expiratory Pressure (PEEP) on Trigger Delay

		Engström Carestation	**Osiris 3**	**Oxylog 3000**	**Monnal T60**	**Elisee 350**
Trigger Delay [ms]	PEEP = 5 cmH_2O	54 ± 5	83 ± 5	104 ± 5	69 ± 9	64 ± 5
	PEEP = 10 cmH_2O	58 ± 10	75 ± 7	112 ± 8	70 ± 8	64 ± 7
	PEEP = 15 cmH_2O	57 ± 7	76 ± 8	113 ± 8	65 ± 13	62 ± 6

Abbreviations

- *PEEP* = Positive End Expiratory Pressure.

Figure E1. Tidal Volume delivery in volume control ventilation in static conditions

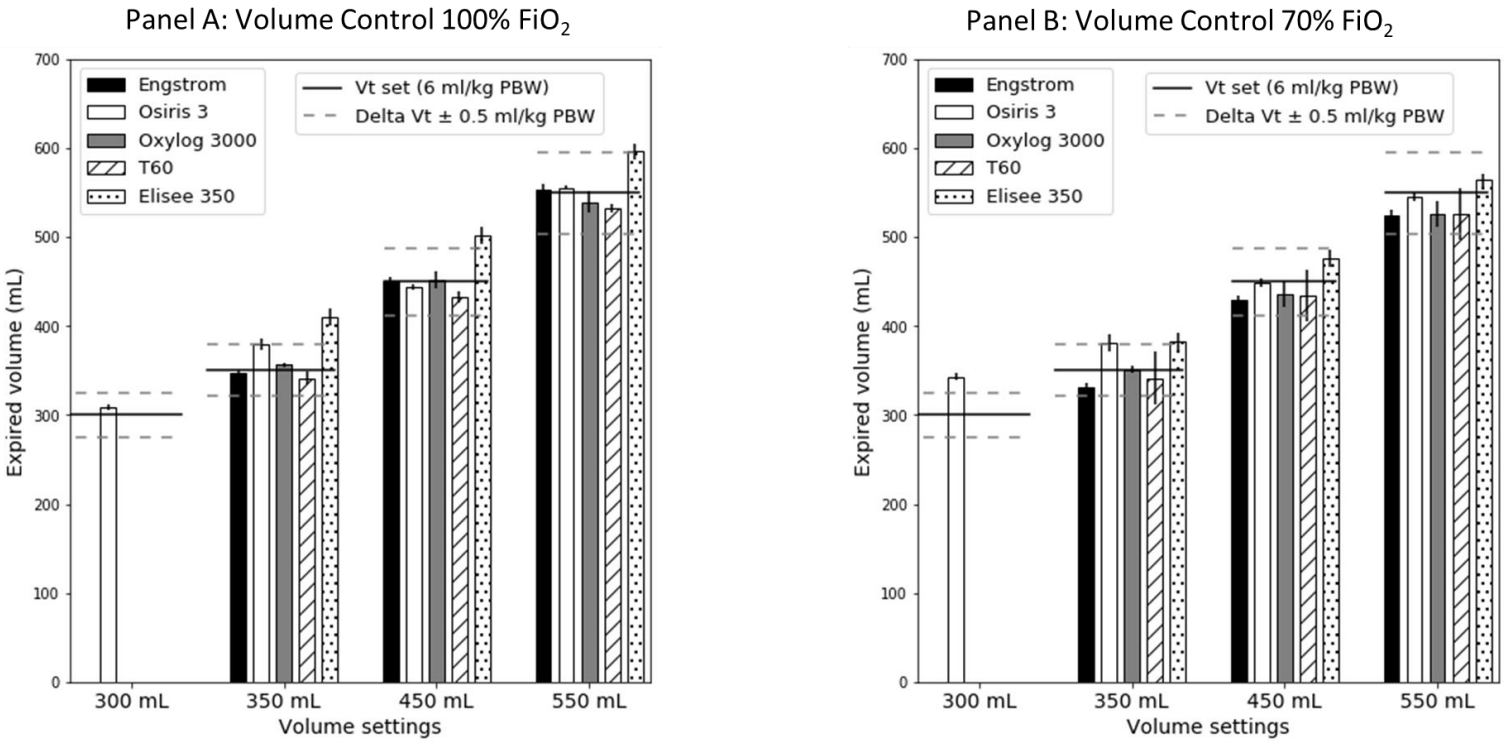

Panel A. The histogram represents the mean expired volumes measured for each ventilator according to the three Vt set (350 - 450 - 550 ml) in 100% FiO_2. The mean expired volume was also measured for a Vt set of 300 ml for the Osiris 3 ventilator. The average was computed over the four conditions of resistance (15 $cmH_2O/L/s$), compliance (20 - 50 ml/cmH_2O) and PEEP (10 - 15 cmH_2O). The four tidal volumes tested were chosen to cover 6 ml/kg PBW, with 300, 350, 450 and 550 ml corresponding to 6ml/kg PBW for respectively 50, 58, 75 and 92 kg PBW. Limits of acceptable ventilation are displayed with dotted lines and defined as a volume change within ± 0.5 ml/kg PBW, which corresponds to a Vt between 5.5 and 6.5 ml/kg PBW.

Panel B. The histogram represents the mean expired volumes measured for each ventilator according to the three Vt set (350 - 450 - 550 ml) in 70% FiO_2. The mean expired volume was also measured for a Vt set of 300 ml for the Osiris 3 ventilator. The average was computed over the four conditions of resistance (15 $cmH_2O/L/s$), compliance (20 - 50 ml/cmH_2O) and PEEP (10 - 15 cmH_2O).

Figure E2. Triggering characteristics in volume assist-control ventilation for a P0.1 of 8 cmH_2O

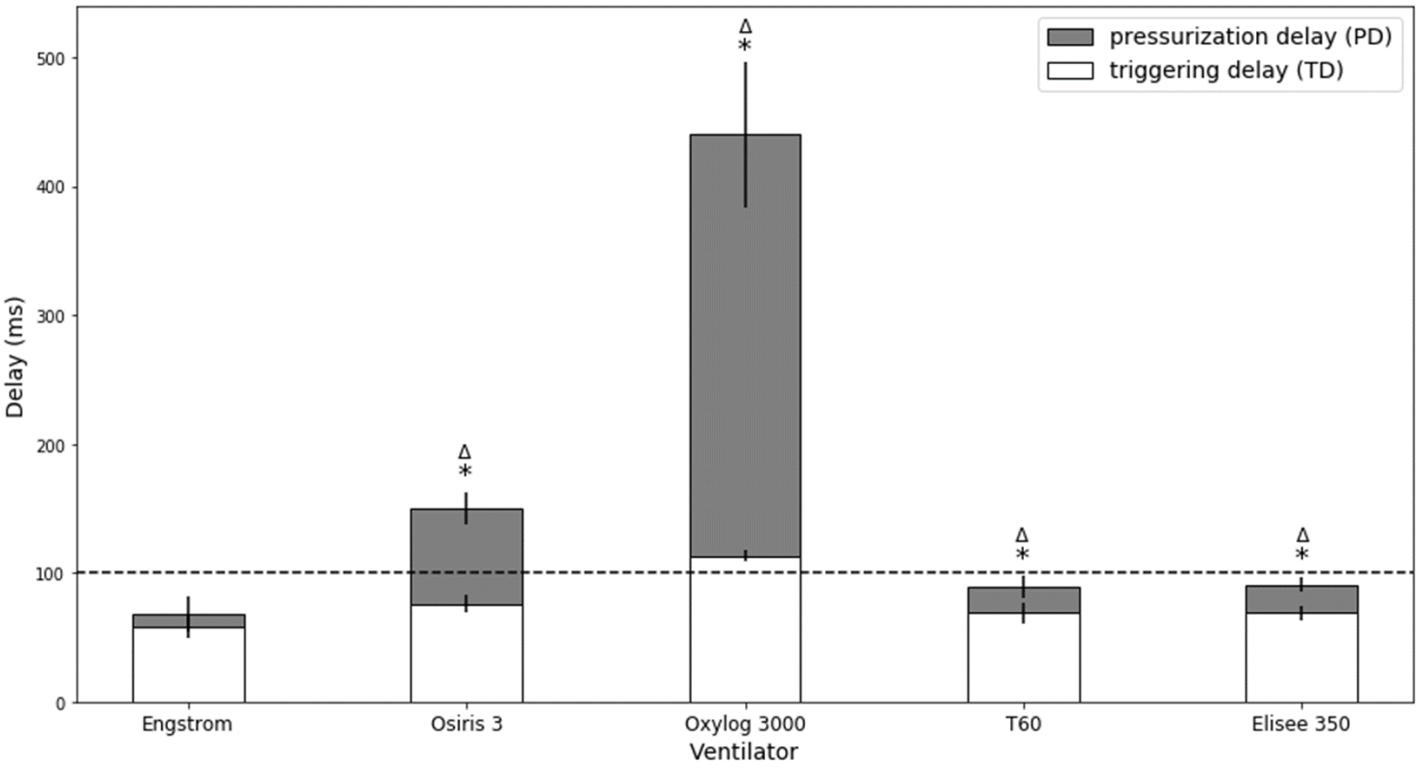

The figure illustrates the triggering efficiency for each ventilator tested during assist-control ventilation using the Michigan test lung to simulate spontaneous breathing. A strong effort was achieved, corresponding to a decrease in airway pressure 100 ms after occlusion (P0.1) of 8 cmH_2O. A PEEP of 10 cmH_2O, a compliance of 20 and 50 ml/cmH_2O and a resistance of 15 $cmH_2O/L/s$ were selected. Triggering Delay (TD, ms) and Pressurization Delay (PD, ms) were computed. A definition of TD and PD is available on figure 1. Triggering function was considered safe and acceptable when TD was less than 100 ms.

* indicates $P < 0.005$ for TD when comparing each transport ventilator with the Engstrom ICU ventilator (ANOVA test: global F was significant).

Δ indicates $P < 0.005$ for PD when comparing each transport ventilator with the Engstrom ICU ventilator (ANOVA test: global F was significant).

2.2. The importance of CO2 signal to guide cardiopulmonary resuscitation

2.2.1. Context

The optimal ventilation strategy during Cardio-Pulmonary Resuscitation (CPR) remains challenging, especially because of the complex interactions between ventilation and circulation. As CO2 is produced in systemic tissues and organs and then transported into the blood by the circulation induced by chest compressions, end-tidal CO2 (EtCO2) has been proposed to assess the quality of CPR and even more so as a prognosis factor. Actually, emerging evidence suggests a positive relationship between EtCO2 and outcome. Nevertheless, EtCO2 also depends on gas exchange and lung function, which complexifies its interpretation, as shown by Leturiondo et al. (9, 10). Based on recent findings, we suggested that the analysis of expired CO2 signal (called capnogram) may help to better assess the quality of ventilation and possibly circulation during CPR. Indeed, we suspect that lung volume at which CPR operates (compared to functional residual capacity) is essential to optimize quality of CPR. We hypothesized that capnogram pattern during chest compressions might permit to detect lung volume above or below the functional residual capacity and as a result may guide ventilation to protect circulation.

During CPR, the application of continuous chest compressions decreases lung volume below the functional residual capacity and may generate intrathoracic airway closure. Conversely, large insufflations can induce thoracic distension and jeopardize circulation by limiting venous return. A previous study showed that the expired CO2 signal (capnogram) recorded during chest compressions allows to identify intrathoracic airway closure associated with a negative impact on lung volumes and gas exchange (11). We hypothesized that the capnogram (CO2 signal) may also reflect thoracic distension associated with lung volume above the FRC during decompression. In this context, the expired CO2 signal could be of great interest and may potentially be considered to guide ventilation during CPR.

In the current study, the objective was to

- evaluate the different CO2 patterns (intrathoracic airway closure - thoracic distension - regular pattern) present in clinical data and reproduce them on different models.
- test whether a specific capnogram may identify thoracic distension during CPR and to assess the impact of thoracic distension on gas exchange and hemodynamics.

2.2.2. CO2 as a reflect of thoracic lung volume?

The application of continuous chest compressions during CPR generates specific CO2 patterns (9, 11) that may reflect thoracic lung volume. Importantly, the functional residual capacity (FRC) is the volume of air present in the lungs at the end of passive expiration. It represents the resting volume of the lung at which the opposing elastic recoil forces of the lungs and chest wall are in equilibrium

CPR close to the FRC.

Both compression and decompression are needed to generate and sustain effective circulation. The increase of intrathoracic pressure during compression has been shown to generate circulation, thus introducing the concept of thoracic pump theory (63). Essentially, according to the thoracic pump theory, the rise in intrathoracic pressure during compression enhances blood flow out of the thorax (i.e. to the brain). During decompression, venous return is facilitated by recoil of the chest creating a negative intrathoracic pressure if lung is placed below the functional residual capacity (FRC) when decompression starts. This situation corresponding to CPR operating close to the FRC with effective venous return could be identified by what we called the regular CO2 pattern with fully oscillating capnogram (more details in the manuscript).

CPR with a reduction of lung volumes way below the FRC: intrathoracic airway closure.

As explained above, the continuous application of chest compressions may result in “intrathoracic airway closure” for some patients. Interestingly, non-oscillating capnograms reported by Grieco et al. (11) reflect intrathoracic airway closure that affects ventilation and occurs when thorax is pushed far below the FRC along the course of CPR.

CPR operating above FRC: thoracic distension

Unlike intrathoracic airway closure, excessive ventilation may place lung volume above the functional residual capacity. We recently identified another capnogram pattern referred to as "thoracic distension”, in which oscillations are not present at the beginning of expiration but appear after a few chest compressions have been generated, while lung volume decreases. We hypothesized that in case of “thoracic distension”, relatively large insufflations place lung volume above the functional residual capacity, therefore losing the inward / inspiratory recoil

of the chest and transiently affecting the circulatory effect of decompression by limiting negative recoil pressure, until returning below FRC.

2.2.3. Methods

This clinical study was conducted in Annecy hospital to obtain capnograms from out of hospital cardiac arrest patients. The cadaver study was performed in the anatomy laboratory of Trois-Rivières in Canada. The animal study was performed in the veterinary laboratory of Maisons-Alfort. For this work, I participated to the definition of protocols for bench, cadaver and animal studies. I was directly involved in these experiments and I developed a specific algorithm to recognize and classify CO2 patterns using mathematical modeling in clinical recordings. This algorithm was adapted to the animal specificities. I performed data analysis, statistics, provided tables and figures, and wrote the preliminary draft of the manuscript. I also contributed afterwards at each steps of the reviewing process.

1. Clinical observations

Capnograms from 202 out-of-hospital cardiac arrest patients were printed just after intubation with the Lifepak 15 monitor defibrillator. Numerical CO2 data was extracted from the scanned capnograms with a dedicated application developed on python using image processing. CO2 signal obtained with chest compressions during the expiratory phase was analyzed and labelled into one of the three CO2 patterns: intrathoracic airway closure, thoracic distension or regular pattern. A specific algorithm was designed to identify them automatically. To quantify thoracic distension CO2 pattern within the algorithm, a distension ratio was defined based on the analysis of the area under the CO2 curve.

2. Experimental observations

To link CO2 patterns with ventilation, we conducted three experiments:

Human Thiel cadavers

CO2 patterns were reproduced in “Thiel” human cadavers. Those cadavers were validated as a robust model to study ventilation during CPR. Experiment was done in the anatomy laboratory of the University of Québec in Trois-Rivières in Canada.

Bench study

The influence of tidal volume and respiratory mechanics on thoracic distension was assessed using a mechanical lung model (POUTAC). This model was designed to allow ventilation either above or below FRC (a unique situation specific to CPR) and permits to simulate a constant production of CO2.

Pig model

The impact of thoracic distension patterns on different circulation parameters during CPR was explored on a pig model. Six animals were enrolled in the main study. Ventricular fibrillation was induced and CPR was organized into three periods associated with a specific tidal volume (period T0 to T5 => 5 min at 6 ml/kg-period T5 to T10 => 5 min at 12 ml/kg-period T10 to T15 => 5 min at 6 ml/kg). This study was approved by the ethics committee for animal research Cometh-016 (project 2018062813205311).

2.2.4. Main results

1. Clinical observations

From the 202 capnograms included in the study, 35% showed airway closure, 22% thoracic distension pattern and 43% regular pattern.

2. Experimental observations

Human Thiel cadavers

Thoracic distension based on capnogram was associated with higher tidal volumes compared with intrathoracic airway closure ($p = 0.008$) or regular pattern ($p = 0.005$)

Bench study

Thoracic distension identified on capnogram was favored by high tidal volumes and high time constants (Resistance × Compliance). The larger the insufflated volume or the longer the time constant, the more likely thoracic distension was present.

Pig model

In the animal experiment, the distension ratio calculated from the capnogram to quantify thoracic distension was inversely correlated with cerebral perfusion and arterial blood pressure, while no correlation was found with tidal volume.

2.2.5. Discussion

During CPR, three distinct CO2 patterns have been detected based on clinical capnogram analysis from out of hospital cardiac arrest patients. Intrathoracic airway closure, thoracic distension or regular pattern can be reliably identified by the capnogram analysis. Interestingly, those three patterns may represent three distinct levels of lung volume at which CPR operates. The distribution observed in the present study seems consistent with capnogram analysis reported by Leturiundo et al. even if intrathoracic airway closure in their study was much more prevalent (10). This may be due to the strategy of manual bag ventilation they used without positive end expiratory pressure (PEEP), while in our study the PEEP of 5 cmH_2O systematically used may have limited intrathoracic airway closure occurrence.

Grieco et al. (11) showed that intrathoracic airway closure identified with the capnogram limited total minute ventilation, potentially impacting negatively gas exchange. The present study identified intrathoracic airway closure in 35% of patients. Interestingly, we recently showed that intrathoracic airway closure identified on patients after cardiac arrest was associated with a reduction of lung volumes, and for almost 50% of them with CRALE (77), thus supporting the study of Magliocca et al. suggesting that intrathoracic airway closure during CPR may be generated by a dramatic reduction of lung volumes below the FRC (5).

A novel interpretation of capnogram was proposed in the current study, and permits to detect “thoracic distension” potentially harmful for circulation. This pattern was associated with higher tidal volumes, while the concomitant analysis of airway and flow signals in case of thoracic distension suggested that lung volume was above the FRC, even during a portion of expiratory time. This could limit the effect of decompression, potentially impacting negatively venous return, as suggested by the decrease in blood pressure and cerebral perfusion.

As both “intrathoracic airway closure” and “thoracic distension” may be easily reversed by ventilation, we believe that these original findings may help to protect circulation from ventilation harmful effects during resuscitation. In fact, increasing positive end expiratory pressure may open the airways, while volume reduction may prevent thoracic distension. The regular CO2 pattern associated with an optimal lung volume could be seen as the targeted situation. We think that this work may help to better address the question of the optimal ventilation during CPR.

2.2.6. The study

Lesimple et al. Critical Care (2022) 26:287
https://doi.org/10.1186/s13054-022-04156-0

Critical Care

RESEARCH Open Access

A novel capnogram analysis to guide ventilation during cardiopulmonary resuscitation: clinical and experimental observations

Arnaud Lesimple[1,3,4†], Caroline Fritz[2†], Alice Hutin[5,6], Emmanuel Charbonney[7,8], Dominique Savary[3,9,10], Stéphane Delisle[11], Paul Ouellet[12], Gilles Bronchti[8], Fanny Lidouren[6,13], Thomas Piraino[14], François Beloncle[3,15], Nathan Prouvez[3,4], Alexandre Broc[3,4], Alain Mercat[15], Laurent Brochard[16,17], Renaud Tissier[6,13†] and Jean-Christophe Richard[3,4,15,18*†] on behalf of the CAVIAR (Cardiac Arrest, Ventilation International Association for Research) Group

Abstract

Background: Cardiopulmonary resuscitation (CPR) decreases lung volume below the functional residual capacity and can generate intrathoracic airway closure. Conversely, large insufflations can induce thoracic distension and jeopardize circulation. The capnogram (CO_2 signal) obtained during continuous chest compressions can reflect intrathoracic airway closure, and we hypothesized here that it can also indicate thoracic distension.

Objectives: To test whether a specific capnogram may identify thoracic distension during CPR and to assess the impact of thoracic distension on gas exchange and hemodynamics.

Methods: (1) In out-of-hospital cardiac arrest patients, we identified on capnograms three patterns: intrathoracic airway closure, thoracic distension or regular pattern. An algorithm was designed to identify them automatically. (2) To link CO_2 patterns with ventilation, we conducted three experiments: (i) reproducing the CO_2 patterns in human cadavers, (ii) assessing the influence of tidal volume and respiratory mechanics on thoracic distension using a mechanical lung model and (iii) exploring the impact of thoracic distension patterns on different circulation parameters during CPR on a pig model.

Measurements and main results: (1) Clinical data: 202 capnograms were collected. Intrathoracic airway closure was present in 35%, thoracic distension in 22% and regular pattern in 43%. (2) Experiments: (i) Higher insufflated volumes reproduced thoracic distension CO_2 patterns in 5 cadavers. (ii) In the mechanical lung model, thoracic distension patterns were associated with higher volumes and longer time constants. (iii) In six pigs during CPR with various tidal volumes, a CO_2 pattern of thoracic distension, but not tidal volume per se, was associated with a significant decrease in blood pressure and cerebral perfusion.

Conclusions: During CPR, capnograms reflecting intrathoracic airway closure, thoracic distension or regular pattern can be identified. In the animal experiment, a thoracic distension pattern on the capnogram is associated with a negative impact of ventilation on blood pressure and cerebral perfusion during CPR, not predicted by tidal volume per se.

Keywords: Cardiopulmonary resuscitation, Thoracic distension, Intrathoracic airway closure, CO_2 pattern, Cardiac arrest

A novel capnogram analysis to guide ventilation during cardiopulmonary resuscitation. From clinical to experimental observations

Arnaud Lesimple [1,3,4] *, Caroline Fritz [2] *, Alice Hutin [5,6], Emmanuel Charbonney [7,8], Dominique Savary [3,9,10], Stéphane Delisle [11], Paul Ouellet [12], Gilles Bronchti [8], Fanny Lidouren[6,13], Thomas Piraino [14], François Beloncle [3,15], Nathan Prouvez [3,4], Alexandre Broc [3,4], Alain Mercat [15], Laurent Brochard [16,17], Renaud Tissier [6,13] *, Jean-Christophe Richard [3,4,15] * on behalf of the CAVIAR (Cardiac Arrest and Ventilation International Association for Research) Group.

[1] - CNRS, INSERM 1083, MITOVASC, University of Angers, Angers, France.

[2] -Anesthesia-Intensive Care department, European Hospital Georges Pompidou APHP, Paris, France

[3] - Vent'Lab, Angers University Hospital, University of Angers, Angers, France.

[4] - Med$_2$Lab, Air Liquide Medical Systems, Antony, France

[5] - SAMU of Paris, Necker Hospital, Paris, France.

[6] - Ecole Nationale Vétérinaire d'Alfort, IMRB, AfterROSC Network, F-94700, Maisons-Alfort, France

[7] - Hospital Center of University of Montréal, Montreal Qc H2X 0C1, Canada.

[8] - Anatomy department, University of Québec at Trois-Rivières, Trois-Rivières, Canada.

[9] - Emergency Department, University Hospital of Angers, Angers, France

[10] - Inserm, EHESP, University of Rennes, Irset (Institut de recherche en santé, environnement et travail) - UMR_S 1085, F-49000, Angers, France

[11] - FCCM University of Montréal, Department of Family and Emergency Medicine, Montréal, Québec, Canada.

[12] - Vitalité Health Network, North West Zone, Edmundston, Canada.

[13] - Univ Paris Est Créteil, INSERM, IMRB, F-94010, Créteil, France

[14] - St. Michael's Hospital Toronto, Ontario, Canada.

[15] - Medical ICU, Angers University Hospital, University of Angers, Angers, France

[16] - Keenan Research Centre for Biomedical Science, Li Ka Shing Knowledge Institute, St. Michael's Hospital, Toronto, Canada

[17] - Interdepartmental Division of Critical Care Medicine, University of Toronto, Toronto, Canada

Corresponding author:

Jean-Christophe Richard, Critical Care Department, Angers University Hospital, 4 rue Larrey 49933 ANGERS, phone number (+33) 622115851, jcmb.richard@gmail.com

Declarations:

Ethics approval and consent to participate

- Capnograms analyzed from the clinical data complied with the Declaration of Helsinki and the study was approved by the ethics committee of the University Hospital of Clermont-Ferrand, France (IRB no. 5891) with waiver of consent.
- The cadaver study was approved by the ethics committee of the University of Quebec at Trois-Rivieres (SCELERA-19-01-PR02).
- The animal study was approved by the ethics committee for animal research Cometh - 016 (project 2018062813205311).

Consent for publication:

Not applicable

Availability of data and materials

The datasets used and/or analyzed during the current study are available from the corresponding author on reasonable request.

Competing interests

- AL is PhD student in the Med2Lab partially funded by Air Liquide Medical Systems.
- DS reports grants from Fisher and Paykel and travel fees from Air Liquide Medical Systems.
- SD consultant for Vitalaire Canada INC
- FB reports personal fees from Löwenstein Medical, travel fees from Draeger and Air Liquide Medical systems and research support from Covidien, GE Healthcare and Getinge Group, outside this work.
- NP reports salary for research activities (Med2Lab) from Air Liquide Medical Systems
- AB is master student from Telecom Physique Strasbourg University France.
- AM reports personal fees from Draeger, Faron Pharmaceuticals, Air Liquide Medical Systems, Pfizer, Resmed and Draeger and grants and personal fees from Fisher and Paykel and Covidien, outside this work.

- LB has received research grants for his research laboratory from Covidien (PAV), Draeger (EIT), and equipment from Fisher Paykel (high flow), Air Liquide, Sentec (PtcCO2) and Philips (sleep), and received fees for lectures from Fisher Paykel.
- RT reports grants from Air Liquide and grants, shares and personal fees from Orixha, all outside of this work.
- JCR reports part time salary for research activities (Med2Lab) from Air Liquide Medical Systems and Vygon and grants from Creative Air Liquide.
- All other authors declare no competing interests.

C. Fritz* and A. Lesimple* equally contributed to this work as first authors.

R. Tissier* and JC. Richard* equally contributed to this work as senior authors.

Funding

CF received a research grant from French society of intensive care medicine (SRLF).

Authors' contributions

AL, DS, LB, RT and JCR contributed to the study conception and design. CF, AL, AH, EC, PO, SD, FL, YL, NP, AB and JCR performed the experiments, the data collection and the initial data analysis. JCR, AL, RT, CF and LB prepared the first draft of the manuscript. All authors contributed to the data analysis and to the critical revision and approval of the final manuscript. The study was performed in Veterinary school of Maisons-Alfort (France), Anatomy laboratory of University of Quebec at Trois Rivieres (Canada) and University Hospital of Angers (France).

Acknowledgments

Authors are very grateful to Bilal Badat for his active participation in the discussions and cadavers experiments. Also the contribution of Manon Hannoucene and Clémence Gilbert for helping in cadavers experiments.
Authors would like to greatly acknowledge Yaël Levy for her active participation in the discussions and pigs experiments.
Authors are very grateful to the technicians of the anatomy laboratory at UQTR, namely Johanne Pellerin, Marie-Eve Lemire and Sophie Plante.

Collaboration group:

CAVIAR (Cardiac Arrest and Ventilation International Association for Research).

Arnaud Lesimple, Caroline Fritz, Emmanuel Charbonney, Dominique Savary, Stéphane Delisle, Paul Ouellet, Gilles Bronchti, Thomas Piraino, François Beloncle, Nathan Prouvez, Alain Mercat, Laurent Brochard, Jean-Christophe Richard.

Word count

- the body of the manuscript: 3618
- the abstract: 300

List of abbreviations

- *CPR*: Cardio-Pulmonary Resuscitation
- *FRC*: Functional Residual Capacity
- *RR*: Respiratory Rate
- *FiO_2*: Inspired Fraction of Oxygen
- *PEEP*: Positive End Expiratory Pressure
- *ROSC*: Return Of Spontaneous Circulation
- *R*: resistance
- *C*: compliance

ABSTRACT

Background: Cardio-Pulmonary Resuscitation (CPR) decreases lung volume below the functional residual capacity and can generate intrathoracic airway closure. Conversely, large insufflations can induce thoracic distension and jeopardize circulation. The capnogram (CO_2 signal) obtained during continuous chest compressions can reflect intrathoracic airway closure and we hypothesized here that it can also indicate thoracic distension.

Objectives: to test whether a specific capnogram may identify thoracic distension during CPR and assess its impact on gas exchange and hemodynamics.

Methods:

1. In out-of-hospital cardiac arrest patients, we identified on capnograms three patterns: intrathoracic airway closure, thoracic distension or regular pattern. An algorithm was designed to identify them automatically.
2. To link CO2 patterns with ventilation, we conducted three experiments:

    i) Reproducing the CO2 patterns in human cadavers.

    ii) Assessing the influence of tidal volume and respiratory mechanics on thoracic distension using a mechanical lung model.

    iii) Exploring the impact of thoracic distension patterns on different circulation parameters during CPR on a pig model.

Measurements and main results:

Clinical data: 202 capnograms were collected. Intrathoracic airway closure was present in 35%, thoracic distension in 22% and regular pattern in 43%.

Experiments:

i) Higher insufflated volumes reproduced thoracic distension CO_2 patterns in 5 cadavers.

ii) In the mechanical lung model, thoracic distension patterns were associated with higher volumes and longer time constants.

iii) In six pigs during CPR with various tidal volumes, a CO_2 pattern of thoracic distension, but not tidal volume *per se*, was associated with a significant decrease in blood pressure and cerebral perfusion.

Conclusions: During CPR, capnograms reflecting intrathoracic airway closure, thoracic distension or regular pattern can be identified. In the animal experiment, a thoracic distension pattern on the capnogram is associated with a negative impact of ventilation on blood pressure and cerebral perfusion during CPR, not predicted by tidal volume *per se*.

Keywords: cardiopulmonary resuscitation, thoracic distension, intrathoracic airway closure, CO_2 pattern, cardiac arrest

INTRODUCTION

In the management of cardiac arrest, it is recommended to perform high quality chest compressions (1). The optimal ventilation strategy during Cardio-Pulmonary Resuscitation (CPR) remains to be determined (2). CO_2 monitoring is recommended in clinical practice by International guidelines (1, 3). However, the application of chest compressions during CPR influences CO_2 waveform and complicates its interpretation (4, 5). We previously showed that the actual recommended rate and depth of chest compressions are such that CPR tends to operate below the functional residual capacity (FRC) (6). During each chest decompression, the recoil of the chest creates a negative intrathoracic pressure with a beneficial circulatory effect. We also showed that the reduction of lung volume due to continuous chest compressions can result in “intrathoracic airway closure” that influences the capnogram waveform (7). We recently identified in out-of-hospital cardiac arrest patients, another capnogram pattern referred to as "thoracic distension”, in which oscillations are not present at the beginning of expiration but appear after a few chest compressions have been generated, while lung volume decreases. We hypothesized that in case of “thoracic distension”, relatively large insufflations place lung volume above the functional residual capacity, therefore losing the inward / inspiratory recoil of the chest and transiently affecting the circulatory effect of decompression by limiting negative recoil pressure, until returning below FRC. The significance of this “thoracic distension” CO_2 pattern, as representing a potentially harmful condition for circulation, was investigated in the present study.

The objectives of this study were: i) to design an algorithm permitting to classify and assess the occurrence of the different CO_2 patterns observed during CPR in a series of out-of-hospital cardiac arrest patients; ii) to reproduce the CO_2 pattern associated with thoracic distension on different experimental models; iii) to evaluate the impact of a thoracic distension capnogram pattern on ventilation and circulation in pigs during CPR performed with continuous chest compressions.

METHODS

CO2 patterns detection

Capnogram classification: the three patterns.

Capnograms were analyzed as illustrated on figure 1 using a simple classification algorithm detailed below. CO_2 signal obtained with chest compressions during the expiratory phase of the ventilatory cycle was labelled into one of the three patterns defined as follows:

i) intrathoracic airway closure: oscillations due to chest compressions and decompressions are small or absent. Lung volume reduction far below the FRC and complete or partial intrathoracic airway closure explain this capnogram.

ii) *thoracic distension*: oscillations due to chest compressions and decompressions are limited or absent at the beginning of the expiration phase, and resume after a few chest compressions. Increase of lung volume above FRC explains this capnogram.

iii) regular pattern: oscillations due to chest compressions and decompressions are clearly visible during the entire duration of the expiration phase. This pattern corresponds to the situation when neither thoracic distension nor intrathoracic airway closure is identified.

Distension ratio, definition and calculation.

To quantify thoracic distension, a distension ratio was defined based on the analysis of the area under the CO_2 curve (see figure 2). In case of thoracic distension, one, two or sometimes more CO_2 oscillations disappear at the beginning of expiration due to the thorax still transitorily above FRC, preventing the negative recoil pressure during decompression (that only occurs below the FRC). As a result, "thoracic distension" is visible on the capnogram since it prevents several chest compression-induced CO_2 oscillations. We computed the distension ratio as the ratio between the initial area under the CO2 curve without oscillation (AUC1) and the area of the consecutive normal CO2 oscillation (AUC2) as illustrated in figure 2. A distension ratio of 2 (AUC_1 is two times superior to AUC_2) was arbitrarily defined as a cut-off value; considering that the loss of oscillations in case of thoracic distension includes at least two inefficient chest decompressions (distension ratio >= 2). Calculations details are available in the supplementary methods (additional file 1).

Figure 1: Capnograms classification from clinical observations

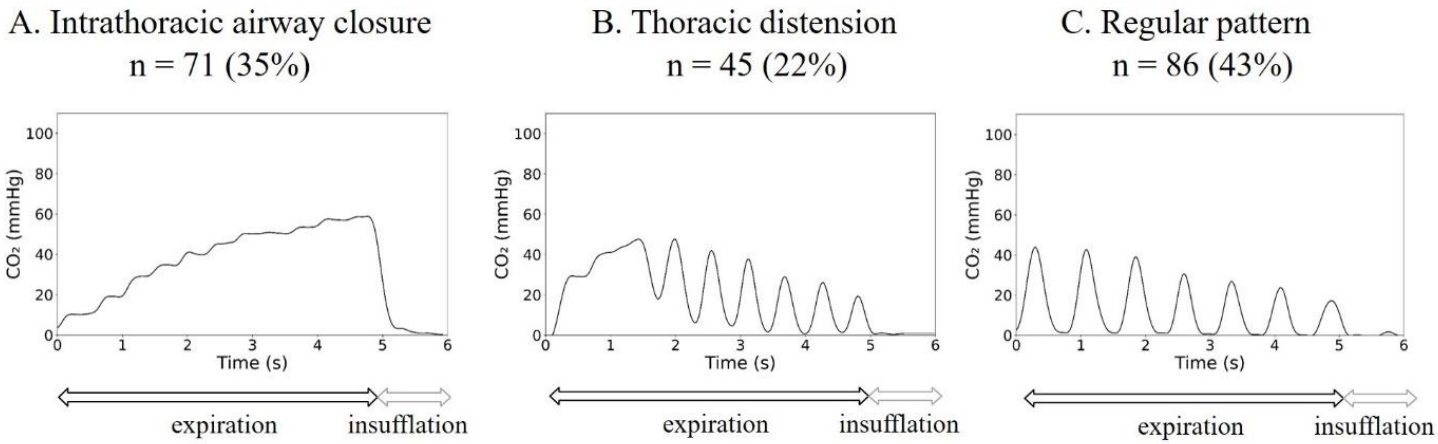

The figure illustrates the distribution of capnograms according to the classification. Each panel shows a typical CO2 pattern obtained from clinical observations after numerical treatment from raw capnogram data (python, Python Software Foundation, Wilmington, Delaware, USA). X-axis represents inspiratory and expiratory time.

***A) intrathoracic airway closure**: oscillations due to chest compressions and decompressions are small or absent. Lung volume reduction far below the FRC and complete or partial intrathoracic airway closure explain this specific capnogram.*

***B) thoracic distension**: oscillations due to chest compressions and decompressions are limited or absent at the beginning of the expiration phase, and resume after a few chest compressions. Increase of lung volume due to large Vt insufflation before returning to FRC explains this specific capnogram.*

***C) regular pattern**: oscillations due to chest compressions and decompressions are clearly visible during the entire duration of the expiration phase. The regular pattern corresponds to the situation when neither thoracic distension nor intrathoracic airway closure is identified.*

Figure 2: Quantification of thoracic distension: the distension ratio

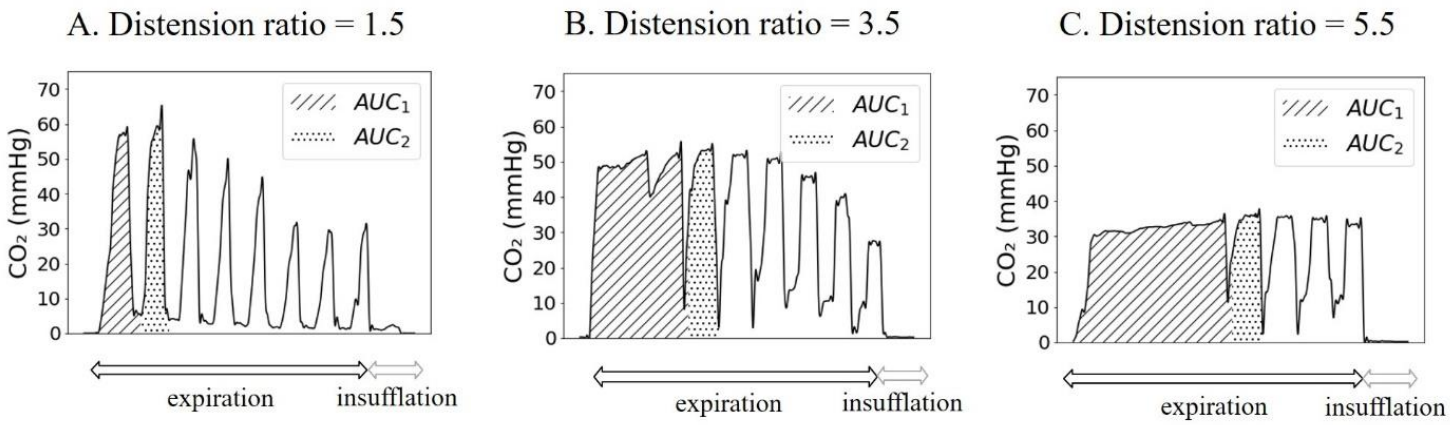

The figure shows examples of capnograms representing different distension ratios (used to quantify thoracic distension) calculated as a continuous variable. Typical capnograms from the animal experiment are displayed for three values of "distension ratio": 1.5 on panel A, 3.5 on panel B and 5.5 on panel C. X-axis corresponds to inspiratory and expiratory time.

AUC1 represents the area under the CO_2 curve between the beginning of the expiratory CO_2 signal and the first local minimum (the first local minima having an amplitude two times lower than the mean amplitude of all peaks are discarded).

AUC2 represents the area under the CO_2 curve of the first "normal" oscillation corresponding to an efficient compression decompression phase around FRC.

The distension ratio corresponds to the ratio AUC_1 / AUC_2. It is used as a surrogate marker of the level of thoracic distension.

Capnogram classification: algorithm

1. Maximum and minimum values of CO_2 peaks corresponding to chest compressions-induced oscillations during the expiratory phase were identified.

2. Airway Opening Index (AOI) was calculated as defined by Grieco et al. (7) to quantify the magnitude of chest compressions-induced expired CO_2 oscillations. An AOI lower than 30% was considered as intrathoracic airway closure. The threshold of 30% was defined based on the results of the Grieco et al. study showing that below an AOI of 30%, the impact on ventilation and as result on CO2 washout was substantial.

3. When AOI was above 30%, the "distension ratio" defined as AUC_1 / AUC_2 was then calculated (see figure 2 and supplementary methods - additional file 1 for details). Thoracic distension was considered when "distension ratio" was greater than 2.

4. Capnogram was considered as regular pattern if AOI was above 30% and distension ratio less than or equal to 2.

Clinical observations

The main objective of the present clinical series was to confirm the existence of the three CO2 patterns at a given time of the CPR process. Capnograms were obtained from patients enrolled in the French RENAU network registry for Out of Hospital Cardiac Arrest (OHCA) (authorization number CNIL 046461). All patients who were receiving manual continuous chest compressions after intubation according to international recommendations (1) with available capnograms (recorded systematically provided there were no technological issues) were consecutively enrolled in the study. Of the patients included in the present study (n=202), capnograms of 89 patients were already reported in a previous study (7). The CO2 pattern was determined based on the classification algorithm described above, using a single representative ventilatory cycle for each patient. Patients were ventilated with a transport ventilator (Monnal T60, Air Liquide Medical Systems Antony, France) using a bilevel pressure mode called CPV, with standardized ventilator settings: respiratory rate (RR) 10 breaths/min; inspiratory time 1 second and expiratory time 5 seconds (I/E=1/5); inspired oxygen fraction (FiO2) 100%; inspiratory pressure 20 cmH_2O; positive end expiratory pressure (PEEP) 5 cmH_2O. Soon after intubation, CO_2 signal was recorded and printed at airway opening from LifePak monitor/defibrillator (LIFEPACK 15, Physio-Control, Redmond, WA 98052, USA) with a sidestream sensor placed between the Y-piece and the endotracheal tube. Data were

prospectively collected without any interference with care. The study complied with the Declaration of Helsinki and was approved by the ethics committee of the University Hospital of Clermont-Ferrand, France (IRB no. 5891) with waiver of consent.

Human cadavers with simulation of CO_2 production.

To validate observations obtained from clinical data, the different conditions (*i.e.*, intrathoracic airway closure, thoracic distension and regular pattern) were reproduced with Thiel embalmed human cadavers with simulation of CO_2 production in the Anatomy Laboratory of the Université Québec à Trois Rivières (UQTR) in Canada with five bodies (authorization number CER-14-201-08-06-17). Those cadavers were validated as a robust model to study ventilation during CPR (8). The objective of the study was to reproduce on a same human body the three CO2 patterns by changing PEEP and tidal volume. The study was approved by the ethics committee of the University of Quebec at Trois-Rivieres (SCELERA-19-01-PR02). Methods used to ventilate the cadavers and to simulate CO_2 production have already been described; airway pressure, flow and esophageal pressure were recorded (8, 9) (see supplementary methods - additional file 1). Manual continuous chest compressions were applied. The Airway Opening Pressure (AOP) was determined in each cadaver as previously reported (10). Regular pattern and thoracic distension were obtained with a PEEP set above AOP while intrathoracic airway closure was obtained with a PEEP set below AOP. Using pressure-controlled ventilation, we adapted different inspiratory pressures (20, 30, 40 cmH_2O) to generate a high range of tidal volumes. Ventilation cycles were classified according to the same algorithm used for the clinical study as intrathoracic airway closure, thoracic distension or regular pattern based only on the CO_2 signal.

Mechanical bench with simulation of CO_2 production.

The objective of the bench study was to address the influence of respiratory mechanics and volume on thoracic distension CO2 pattern. An original thoracic lung model (POUTAC - non patented prototype reported in the Grieco et al. study (7)) permitting to add a constant production of CO2 was used (6) (see supplementary methods - additional file 1). The model was designed to allow ventilation either above or below FRC (a unique situation specific to CPR) under different combinations of resistance and compliance. Manual chest compressions

were applied continuously on the POUTAC using different compliances (C= 20 – 40 – 60 ml/cmH_2O) and resistances (R = 5 – 10 cmH_2O/L/s); capnograms were recorded under a large range of Vt (0.3 to 1L). For each combination of RxC and tidal volume, capnogram was analyzed to detect thoracic distension as described for both the clinical and cadaver study.

Animal study

Ethical statement.

This study was approved by the ethics committee for animal research Cometh - 016 (project 2018062813205311). The procedure for the care and sacrifices of study animals was in accordance with the European Community Standards on the Care and Use of Laboratory Animals. A reporting checklist regarding animal preparation and study design is provided in the additional file 2, in compliance with the ARRIVE guidelines.

Experimental protocol

We tested 7 female pigs weighing 28±1 kg. A first animal was tested over a large range of tidal volumes (from 6 ml/kg to 20 ml/kg) to illustrate what can be expected in terms of circulation impact and capnogram patterns.

Six animals were enrolled in the main study. Ventricular fibrillation was induced by a pacing wire inserted in the right ventricular through the femoral vein catheter. Fibrillation was left untreated during 4 min (no-flow period). Then continuous mechanical chest compression was started at a rate of 100 per minute and a depth of 5 cm with ventilation as recommended (100 % oxygen fraction, respiratory rate 10/min, I/E 1/5, tidal volume 6 ml/kg). The LUCAS 3^{TM} (Physio-control, Lund, Sweden) chest compression device could exert a mild active decompression effect due to the suction cup. CPR was organized into three periods associated to a specific tidal volume (period T0 to T5 => 5 minutes at 6 ml/kg - period T5 to T10 => 5 minutes at 12 ml/kg - period T10 to T15 => 5 minutes at 6 ml/kg). Blood gases were measured at each tidal volume change. Animals were sacrificed at the end of the protocol (*i.e.,* low-flow period of 15 minutes) with a lethal dose of pentobarbital (60 mg.kg^{-1}). Details of animal preparation are available in the supplementary methods (additional file 1).

***Capnogram analysis and thoracic distension*.**

Thoracic distension was defined based on the “distension ratio” calculated as a continuous variable as illustrated in figure 2. This ratio was computed and averaged for each tidal volume

period. Correlations between the “distension ratio”, tidal volume, time and hemodynamic parameters were performed.

Statistical analysis

Statistical analysis was performed with Python Software (Python version 3.9.5, Wilmington - USA). Data are summarized as mean (± SD) for continuous variables and count (%) for categorical variables. In the cadaver experiment, comparisons of tidal volumes between CO2 patterns were performed using a repeated measures ANOVA test. Normality of the data was assessed with a Shapiro-Wilk test. Concerning bench experiments, results were averaged over three ventilation cycles for every condition. For the pig experimentation, correlation was assessed using a random effects linear model with each pig’s id as the random effect. All statistical tests were two-sided and results with $p < 0.05$ were considered statistically significant.

RESULTS

Clinical observations.

Capnography was available in 202 patients soon after intubation during chest compressions and all were included in the study. Patients' characteristics and outcomes are described in table 1. Return of spontaneous circulation (ROSC) and rates of survival at hospital admission were 20.5% and 12.9% respectively.

From the 202 capnograms included in the study, 35% showed airway closure, 22% thoracic distension pattern and 43% regular pattern (see figure 1). The mean distention ratio was 2.23 ± 2.19 (median 1.55) for all patients, 4.24 ± 2.61 (median 3.43) for thoracic distension patients and 1.16 ± 0.64 (median 1.00) for regular pattern patients.

Human Thiel Cadavers

The characteristics of the cadavers are given in the supplementary table 1 (additional file 2). Figure 3 shows an illustration of the three CO_2 patterns obtained with the Thiel cadavers. Thoracic distension based on capnogram was associated with higher tidal volumes compared with intrathoracic airway closure ($p = 0.008$) or regular pattern ($p = 0.005$) (after ANOVA). Mean tidal volume was 130 ± 136 ml for intrathoracic airway closure, 453 ± 222 ml for thoracic distension and 141 ± 82 ml for regular pattern. The mean distention ratio was 2.85 ± 1.56 (median 2.65) for all cadavers, 3.72 ± 1.21 (median 3.50) for thoracic distension, and 1.23 ± 0.42 (median 1.22) for regular pattern.

Bench study

Table 2 shows that thoracic distension was favored by high tidal volumes and high time constants (R x C). The larger the insufflated volume or the longer the time constant, the more likely thoracic distension was present. Thoracic distension was identified on capnograms with a frequency of 0%, 0%, 33%, 33%, 66%, 83%, 83% and 100% for insufflated volumes of respectively 300 ml, 400 ml, 500 ml, 600 ml, 700 ml, 800 ml, 900 ml and 1000 ml. Thoracic distension was detected on capnograms with a frequency of 13%, 50%, 38%, 50%, 75% and 75% for RC values of respectively 0.10 s, 0.2 s, 0.25, 0.40 s, 0.5 and 0.80 s.

Figure 3: Reproduction of CO_2 patterns on Thiel cadaver model

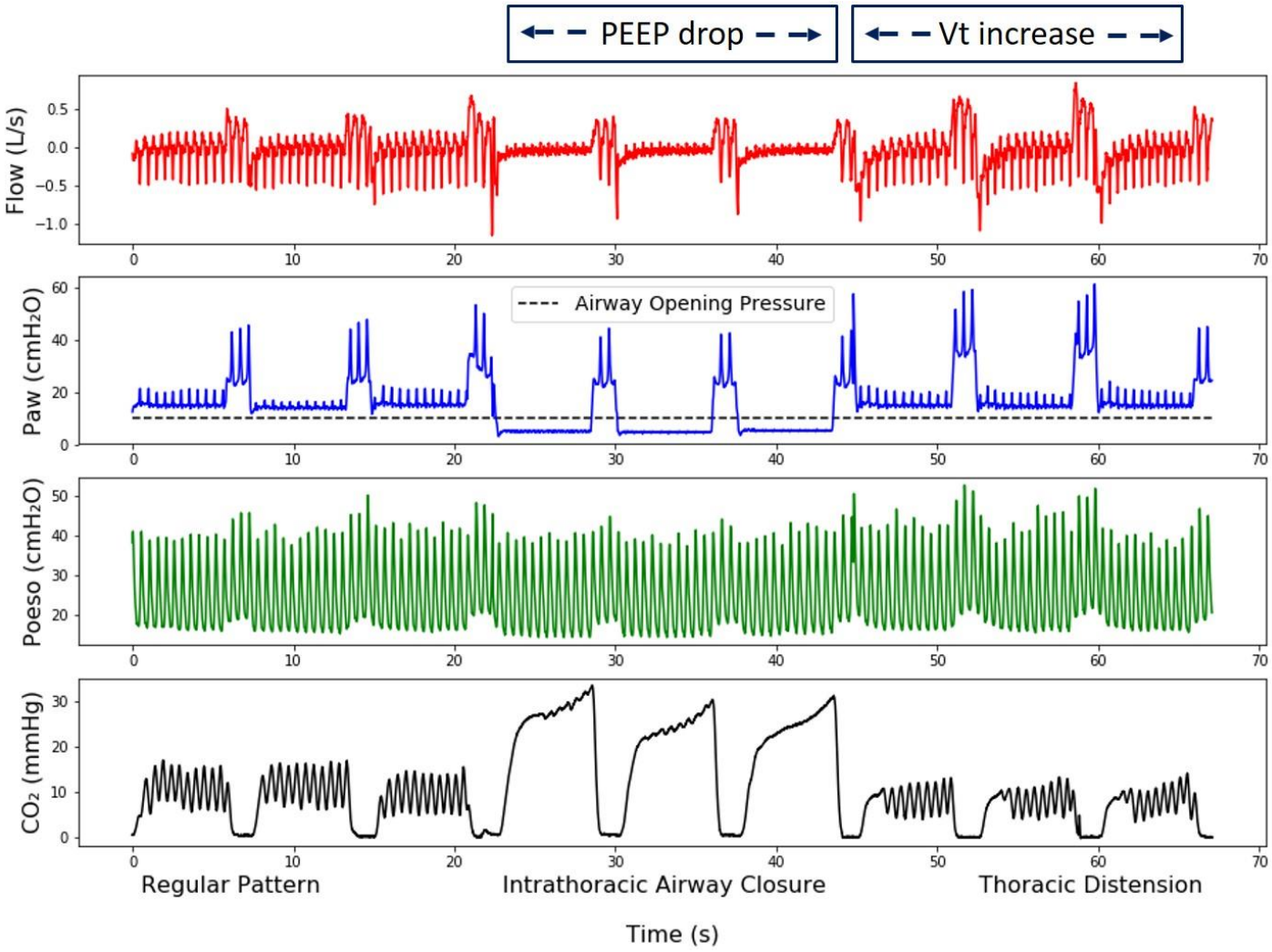

Reproduction of CO_2 patterns: illustration in one cadaver.

From top to bottom recordings of flow at airway opening (Flow), airway pressure (Paw), esophageal pressure (Poeso) and expired CO_2 (CO_2). The tilted line on the Paw tracing represents the Airway Opening Pressure (AOP). The recording is divided into three configurations:

*1. **Regular pattern**: Positive End Expiratory Pressure (PEEP) was set above the AOP to simulate airway patency.*

*2. **Intrathoracic airway closure**: PEEP was set below the AOP to simulate airway closure.*

*3. **Thoracic distension**: PEEP was set above the AOP to simulate airway patency and peak airway pressure set on the ventilator was increased to generate higher tidal volumes compared to step 1.*

Pig model

Intrathoracic airway closure was not observed in the animals enrolled in the experiment. Pigs' characteristics are given in the supplementary table 2 (additional file 2).

Test Animal.

Figure 4 illustrates in one animal the increasing variations induced by ventilation of aortic blood pressure, right atrial pressure, intracranial pressure, coronary and cerebral perfusion pressure as Vt increased. The capnogram depicted a change of the CO_2 pattern from regular pattern to thoracic distension as Vt increased.

Experiment in six animals.

The "distension ratio", expressing the level of thoracic distension based on the capnogram, (figure 5) was significantly and inversely correlated with cerebral perfusion pressure ($p = 0.002$), mean blood pressure ($p=0.006$), systolic blood pressure ($p=0.007$), and diastolic blood pressure ($p=0.009$). There was no significant effect on coronary perfusion pressure and carotid blood flow.

The different hemodynamic parameters recorded were not significantly impacted by tidal volume per se. There was no significant correlation between Vt and any recorded circulation parameter: coronary ($p = 0.283$) and cerebral ($p = 0.998$) perfusion pressure, mean ($p = 0.839$), systolic ($p = 0.962$) and diastolic ($p = 0.882$) blood pressure as well as carotid blood flow ($p = 0.713$).

A time effect was present on the different hemodynamic parameters recorded except for coronary perfusion pressure, cerebral perfusion pressure and diastolic blood pressure.

Figure 4: Impact of a stepwise increase of tidal volume on airway pressure, circulation and capnograms in a pig during cardiopulmonary resuscitation

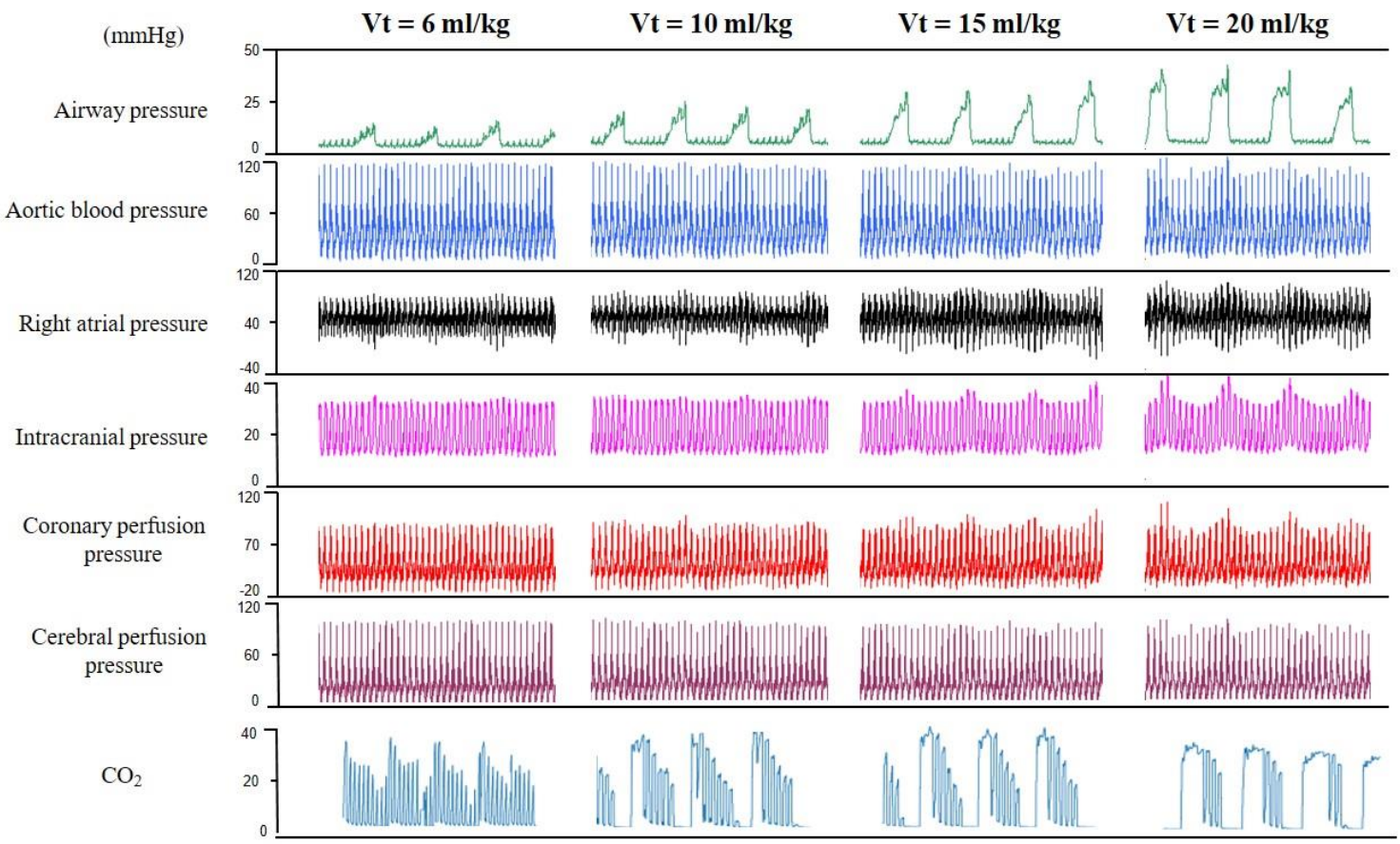

From top to bottom, recording tracings of airway pressure, aortic blood pressure, right atrial pressure, intracranial pressure, coronary perfusion pressure (aortic blood pressure minus right atrial pressure), cerebral perfusion pressure (mean arterial pressure minus intracranial pressure) and capnogram during tidal volume (Vt) trial. Vt was increased as follows: 6 - 10 - 15 - 20 ml/kg. Coronary perfusion pressure waveforms should be interpreted cautiously and read only at end of decompression.

Figure 5: Relationship between CO_2 pattern analyzed by the distension ratio and coronary perfusion, cerebral perfusion, mean, systolic, diastolic blood pressure and carotid blood flow in pigs during cardiopulmonary resuscitation

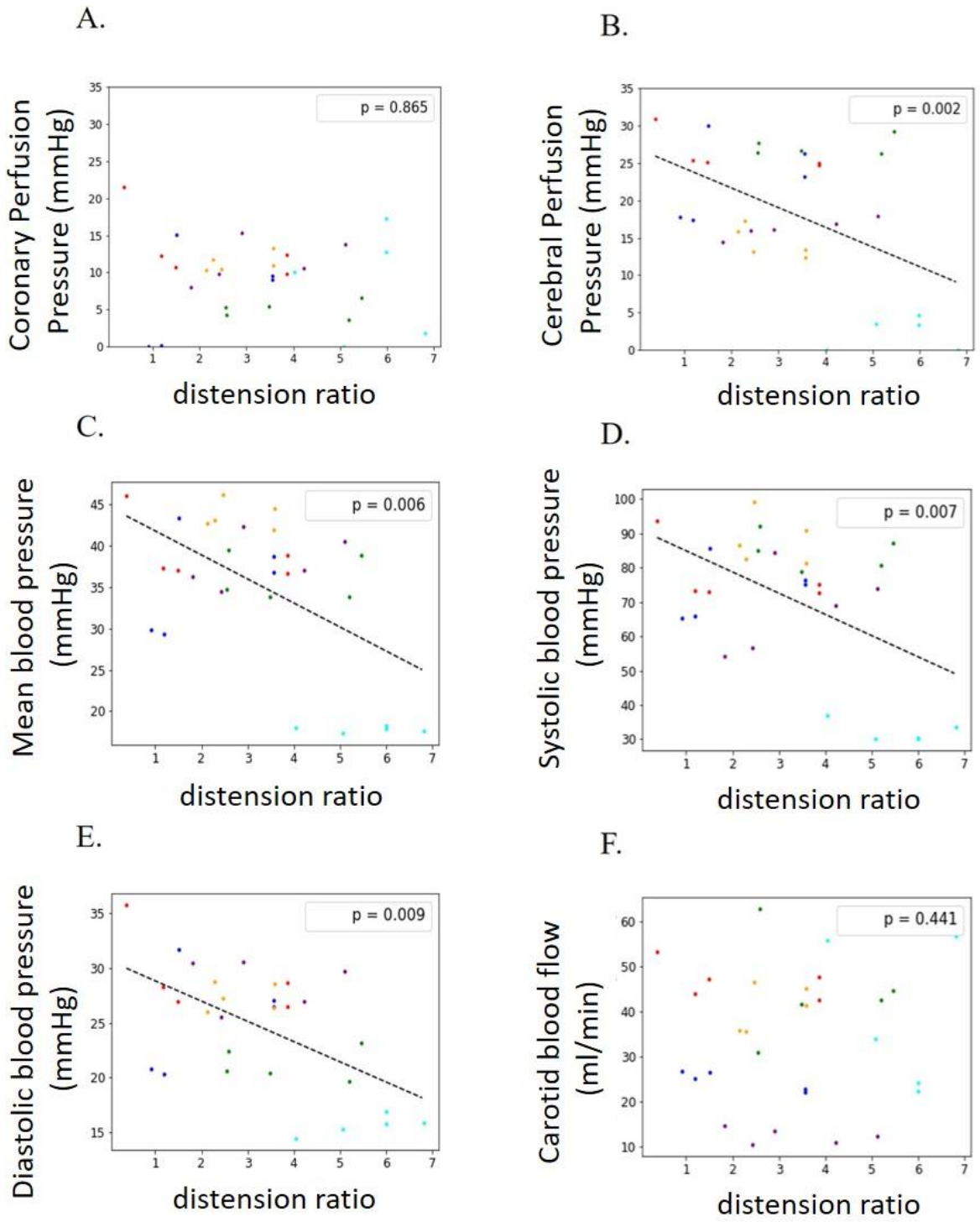

A. *Coronary Perfusion Pressure (measured at end-decompression) depending on "distension ratio".*

B. *Cerebral Perfusion Pressure (mean value throughout chest compression / decompression cycles) depending on "distension ratio".*

C. *Mean blood pressure depending on "distension ratio".*

D. *Systolic blood pressure depending on "distension ratio".*

E. *Diastolic blood pressure depending on "distension ratio".*

F. *Carotid blood flow depending on "distension ratio".*

Correlations were assessed using a mixed linear model. The p-values are displayed. Each pig is represented by a different color.

DISCUSSION

The main results of the present study could be summarized as follows:

1. In the present series of capnograms, intrathoracic airway closure, thoracic distension and regular pattern concerned respectively 35%, 22% and 43% of 202 OHCA patients after intubation.
2. The capnogram indicating thoracic distension was associated with higher tidal volumes on Thiel cadavers. Capnogram indicating thoracic distension on a CPR bench model was also more likely to occur with higher insufflated volumes or longer time constants (RxC).
3. In the animal experiment, the distension ratio calculated from the capnogram to quantify thoracic distension was inversely correlated with cerebral perfusion and arterial blood pressure while no correlation was found with tidal volume.

Theoretical optimal thoracic volume for effective chest compressions

The application of continuous chest compressions during CPR complicates CO2 waveform interpretation and generates specific CO2 patterns (4, 5, 6, 7). Both compression and decompression are needed to generate and sustain effective circulation. The increase of intrathoracic pressure during compression has been shown to generate circulation, thus introducing the concept of thoracic pump theory (11). Venous return is facilitated by recoil of the chest creating a negative intrathoracic pressure if lung is placed below the functional residual capacity (FRC) when decompression starts. CPR close to the FRC with effective venous return could be identified by the regular CO2 pattern with fully oscillating capnogram. Interestingly, non-oscillating capnograms reported by Grieco et al. (7) reflect intrathoracic airway closure that affects ventilation and occurs when thorax is pushed far below the FRC along the course of CPR.

"Thoracic distension" pattern of the capnogram

We hypothesized that the specific capnogram called "thoracic distension" may indicate the risk associated with excessive ventilation inflating the thorax above FRC. It may jeopardize circulation (venous return) by limiting negative intrathoracic pressure during decompression (12, 13). Expired CO2 oscillations which result from the combination of compression and decompression may transiently disappear when the time during which thoracic volume above FRC is prolonged, indicating this risk (see figure 6 and additional file 2).

Figure 6: Illustration of thoracic distension mechanism based on airway pressure, flow and CO2 analysis

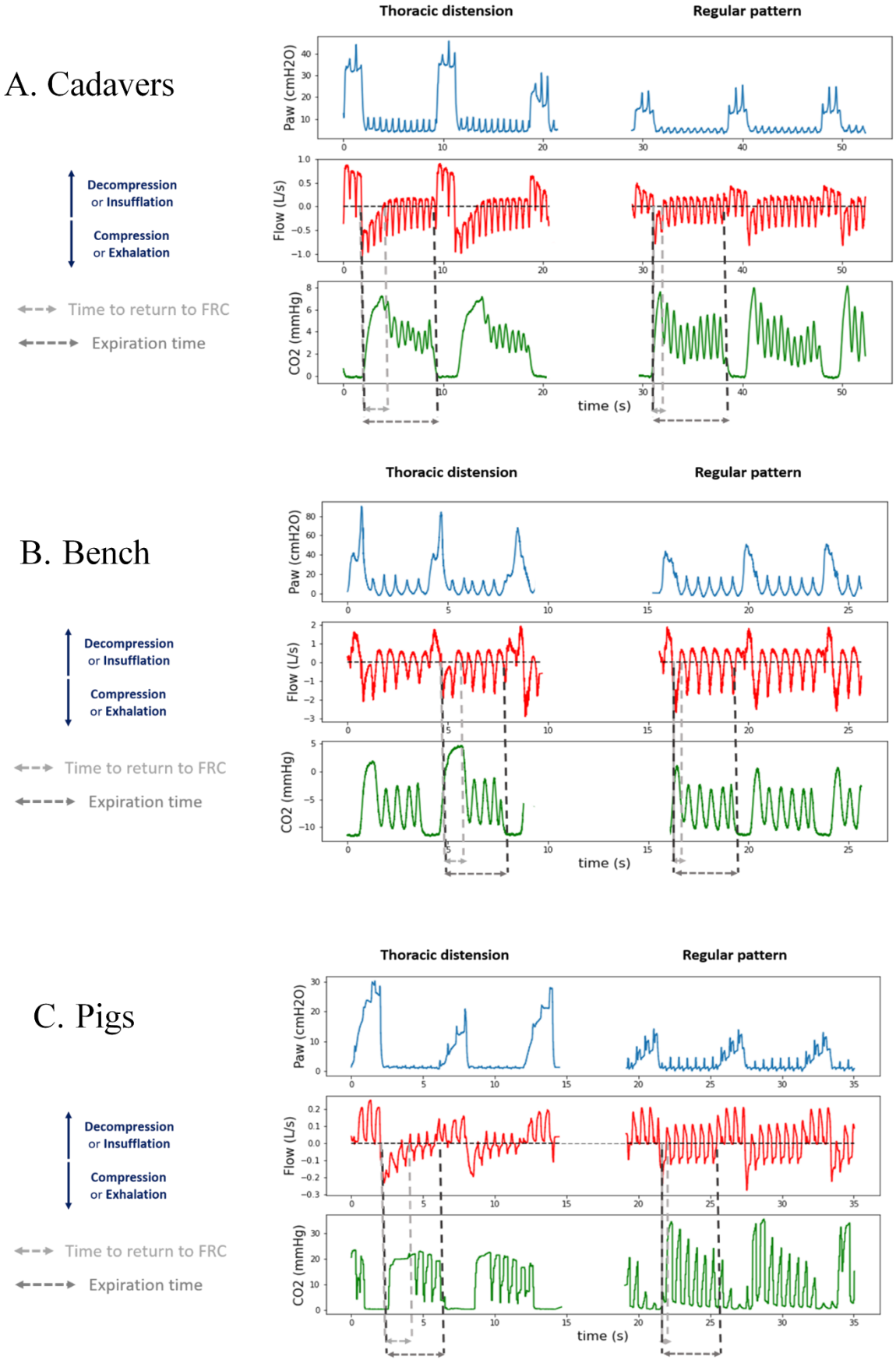

This figure illustrates from top to bottom, airway pressure (Paw), flow at airway opening (Flow) and expired CO2 (CO2) tracings obtained in cadavers (panel A), bench (panel B) and animals (panel C). The left column illustrates thoracic distension while the right column represents regular pattern.

For each situation, the two grey vertical tilted lines define the time for the lung volume to return to FRC (time with thorax above FRC) while the two black vertical tilted lines define the expiration time (time between two insufflations).

Positive flow indicates decompression or insufflation. Negative flow indicates compression or exhalation. Please note the exact time correspondence between flow and CO2 oscillations whatever the situation.

During expiration, in case of thoracic distension (left column), the flow does not return to zero line during a couple of CC indicating that the thorax is still above FRC even during the decompression phase. CO2 oscillations resume only once the flow crosses the zero line, thus indicating the return of lung volume to FRC.

On the contrary, the right column obtained with a smaller Vt illustrates that the flow induced by CC crosses the zero line immediately after insufflation generating CO2 full oscillations. This specific full oscillating CO2 pattern indicates that chest compressions operate close to FRC.

This is also markedly visible in the pig model (test animal), where we observed that the stepwise increase of Vt from 6 to 20 ml/kg magnified coronary and cerebral circulation oscillations related to ventilation and modified capnogram from regular to thoracic distension in parallel (figure 4).

Is the CO_2 pattern associated with thoracic distension more informative than the Vt to detect any impact on circulation?

Thoracic distension CO_2 pattern was reproduced on cadaver, bench and porcine models. This phenomenon was associated on average with higher insufflated volumes compared to intrathoracic airway closure or regular patterns. We found in the pig model that thoracic distension assessed by distension ratio was significantly and negatively correlated to mean arterial blood pressure and cerebral perfusion pressure, suggesting its potential negative impact on circulation during resuscitation.

Unlike the capnogram, Vt absolute values were not significantly associated with a negative effect on blood pressure, coronary perfusion and cerebral perfusion. Those results may suggest that the capnogram may be more relevant than Vt per se to predict a circulatory impact induced by ventilation.

The bench study provides a possible explanation for the previous observed result. Indeed, prolonged time constant that characterizes the time required to return to FRC may favor thoracic distension even with low Vt, as we observed in some animals.

Occurrence of thoracic distension, intrathoracic airway closure and regular capnogram

In our series of 202 OHCA patients, thoracic distension and intrathoracic airway closure concerned 22% and 35% of patients respectively. Interestingly, very similar capnograms have been reported during CPR, without specifically identifying the phenomenon of thoracic distension (4, 5).

An important methodological point is that capnograms from the present study were captured soon after intubation with a respiratory rate of 10/min and a protective pressure mode of ventilation limiting Vt. One cannot exclude that thoracic distension may be much more frequently observed with manual bag ventilation during which Vt and respiratory rate are poorly controlled thus favoring the risk of hyperventilation. In addition, a moderate level of PEEP was used in our series, which could have minimized the occurrence of intrathoracic airway closure, favored by low airway pressures. Although our brief periods of recordings with one to ten cycles displayed similar patterns for all breaths, it is likely that CO_2 patterns evolve along the course

of CPR, and that the classification could change depending on the time of intervention, thus precluding any interpretation of its significance in terms of outcome.

Of note, intrathoracic airway closure was not observed during the animal experiment. It is possible that the pig thorax anatomy may limit the reduction of lung volumes we observe in humans during resuscitation and thus occurrence of intrathoracic airway closure. Besides, pig bronchial tree presents lateral connections that may also limit occurrence of distal airway closure (14). In addition, the mechanical chest compression device used in the swine study was operated with a mild active decompression due to the suction cup, which may limit the reduction of lung volume below the FRC potentially responsible for intrathoracic airway closure.

Clinical perspectives

Excessive ventilation during cardiac arrest has already been shown to be associated with poor outcomes (15, 16). Nevertheless, it is definitively challenging to control and monitor Vt delivered during manual bag ventilation (17).

Based on these observations, a capnogram-based ventilation strategy may permit to optimize ventilation during CPR, using real-time identification of capnograms (intrathoracic airway closure, thoracic distension or regular pattern). As previously shown, PEEP increase may be considered in case of intrathoracic airway closure to open the airways, while Vt reduction could be proposed in case of thoracic distension. Further evidence is needed before developing such ventilatory approach on a ventilator but these findings may be of potential additional value for bag valve mask ventilation during which hyperventilation is likely to occur.

Study limitations

First, the capnogram analysis proposed in the present study is based on continuous chest compression; and whether it is generalizable to an interrupted chest compression strategy ideally needs further assessment. But thoracic distension may also be present during interrupted chest compressions.

Second, capnogram from one ventilatory cycle recorded soon after intubation (according to the local routine procedure) was analyzed for each patient. This relatively limits the possibility to generalize CO2 pattern distribution to different CPR strategies (chest compression frequency, depth or other); and renders hazardous outcomes' interpretation.

Third, the specific set up in cadavers experiment to administer CO2 via a catheter placed in the endotracheal tube resulted in significant additional resistance that favored early occurrence of thoracic distension as suggested by the observations obtained on the bench.

In the animal study, since each animal was its own control, several time related factors might have also impacted circulation. Further studies comparing animals with different ventilation strategies are needed to confirm our observations.

CONCLUSION

During CPR, intrathoracic airway closure, thoracic distension or regular pattern can be reliably identified by the capnogram analysis. We describe a novel CO2 pattern indicating relative thoracic distension, which may be associated with a negative impact on blood pressure and cerebral perfusion, irrespective of tidal volume per se. This original capnogram classification has the potential to help optimizing ventilation during CPR.

REFERENCES

1. Soar J, Böttiger BW, Carli P, Couper K, Deakin CD, Djärv T, et al. European Resuscitation Council Guidelines 2021: Adult advanced life support. *Resuscitation*. 2021;161:115–51.

2. Chang MP, Idris AH. The past, present, and future of ventilation during cardiopulmonary resuscitation. *Curr Opin Crit Care*. 2017;23:188–92.

3. Sutton RM, French B, Meaney PA, Topjian AA, Parshuram CS, Edelson DP, et al. Physiologic monitoring of CPR quality during adult cardiac arrest: A propensity-matched cohort study. *Resuscitation*. 2016;106:76–82.

4. Leturiondo M, Ruiz de Gauna S, Gutiérrez JJ, Alonso D, Corcuera C, Urtusagasti JF, et al. Chest compressions induce errors in end-tidal carbon dioxide measurement. *Resuscitation*. 2020;153:195–201.

5. Leturiondo M, Ruiz de Gauna S, Ruiz JM, Julio Gutiérrez J, Leturiondo LA, González-Otero DM, et al. Influence of chest compression artefact on capnogram-based ventilation detection during out-of-hospital cardiopulmonary resuscitation. *Resuscitation*. 2018;124:63–8.

6. Cordioli RL, Lyazidi A, Rey N, Granier J-M, Savary D, Brochard L, et al. Impact of ventilation strategies during chest compression. An experimental study with clinical observations. *J Appl Physiol* (1985). 2016;120:196–203.

7. Grieco DL, J Brochard L, Drouet A, Telias I, Delisle S, Bronchti G, et al. Intrathoracic Airway Closure Impacts CO2 Signal and Delivered Ventilation during Cardiopulmonary Resuscitation. *Am J Respir Crit Care Med*. 2019;199:728–37.

8. Charbonney E, Grieco DL, Cordioli RL, Badat B, Savary D, Richard J-CM, et al. Ventilation During Cardiopulmonary Resuscitation: What Have We Learned From Models? *Respir Care*. 2019;64:1132–8.

9. Charbonney E, Delisle S, Savary D, Bronchti G, Rigollot M, Drouet A, et al. A new physiological model for studying the effect of chest compression and ventilation during cardiopulmonary resuscitation: The Thiel cadaver. *Resuscitation*. 2018;125:135–42.

10. Chen L, Del Sorbo L, Grieco DL, Junhasavasdikul D, Rittayamai N, Soliman I, et al. Potential for Lung Recruitment Estimated by the Recruitment-to-Inflation Ratio in Acute Respiratory Distress Syndrome. A Clinical Trial. *Am J Respir Crit Care Med*. 2020;201:178–87.

11. Rudikoff MT, Freund P, Weisfeldt ML. Mechanisms of blood flow during cardiopulmonary resuscitation. 1980;61:8.

12. Ditchey RV. Potential adverse effects of volume loading on perfusion of vital organs during closed-chest resuscitation. *LABORATORY INVESTIGATION*. 1984;69:9.

13. Guerci AD, Shi AY, Levin H, Tsitlik J, Weisfeldt ML, Chandra N. Transmission of intrathoracic pressure to the intracranial space during cardiopulmonary resuscitation in dogs. *Circ Res*. 1985;56:20–30.

14. Maina JN, van Gils P. Morphometric characterization of the airway and vascular systems of the lung of the domestic pig, Sus scrofa: comparison of the airway, arterial and venous systems. *Comp Biochem Physiol A Mol Integr Physiol*. 2001;130:781–98.

15. Cordioli RL, Grieco DL, Charbonney E, Richard J-C, Savary D. New physiological insights in ventilation during cardiopulmonary resuscitation. *Curr Opin Crit Care*. 2019;25:37–44.

16. Adhiyaman V, Adhiyaman S, Sundaram R. The Lazarus phenomenon. *J R Soc Med*. 2007;100:552–7.

17. Gordon L, Pasquier M, Brugger H, Paal P. Autoresuscitation (Lazarus phenomenon) after termination of cardiopulmonary resuscitation - a scoping review. *Scand J Trauma Resusc Emerg Med*. 2020;28:14.

Tables

Table 1: Patients characteristics (n=202)

Age (year)	68 (± 15)
Sex male (n)	162 (80%)
BMI (kg/m^2)	25.6 (± 7.2)
Initial rhythm (n) • Non - shockable • Shockable	 153 (73%) 57 (27%)
Low-flow time (min)	20 (± 15)
$EtCO_2$ at the beginning of ALS (mmHg)	31 (± 18)
Maximal $EtCO_2$ during ALS (mmHg)	38 (± 20)
ROSC (n)	43 (20.5%)
Survival at hospital admission (n)	27 (12.9%)

Data are presented as means (± SD) for continuous variables and count (%) for categorical variables.

- BMI: body mass index calculated as weight/height^2;
- $EtCO_2$: end tidal CO_2;
- ALS: advanced life support;
- ROSC: return of spontaneous circulation;

Table 2: Thoracic distension reproduced on lung model

Vt (ml) / RC(s)	300	400	500	600	700	800	900	1000
0,1	regular	regular	regular	regular	regular	regular	regular	distension
0,2	regular	regular	regular	regular	distension	distension	distension	distension
0,25	regular	regular	regular	regular	regular	distension	distension	distension
0,4	regular	regular	regular	regular	distension	distension	distension	distension
0,5	regular	regular	distension	distension	distension	distension	distension	distension
0,8	regular	regular	distension	distension	distension	distension	distension	distension

- Vt: tidal volume
- RC: time constant corresponding to the multiplication of resistance and compliance

The thoracic distension pattern was reproduced on the thoracic lung model called POUTAC. This table displays CO_2 pattern depending on time constant RC (multiplication of resistance and compliance) and the set tidal volume using the classification algorithm described in the methods. Each combination of time constant and tidal volume was identified into either regular pattern (called “regular”), or thoracic distension (called “distension”).

Additional files:

Additional file 1: supplementary methods (format = ".doc")

- Distension ratio: calculation details
- Human cadavers with simulation of CO2 production
- Mechanical bench with simulation of CO2 production
- Pig study: animal preparation.

Additional file 2: supplementary results (format = ".doc")

- Clinical study from Grieco et al.
- Illustration of thoracic distension mechanism based on airway pressure, flow and CO2 analysis
- Supplementary table 1: Cadavers' characteristics
- Supplementary table 2: Baseline pigs' characteristics
- Compliance to the ARRIVE Guidelines of the pigs' experiment

Additional file 1: supplementary methods

Distension ratio: calculation details.

Distension ratio was defined based on the analysis of the area under the CO2 curve in order to quantify thoracic distension. Thoracic distension is characterized by the absence of several CO2 oscillations at the beginning of expiration despite the delivery of chest compressions. This reflects the displacement of the thorax above the Functional Residual Capacity (FRC) due to the insufflation, preventing the negative recoil pressure during decompression (that only occurs below the FRC).

The distension ratio is the ratio between two areas under the capnogram curve (see figure 1):
1. The area 1 under the CO2 curve (AUC1) from the beginning of expiration to the first local minimum.
2. The area 2 under the CO2 curve (AUC2) of the first “normal” oscillation corresponding to an efficient compression decompression phase around FRC.

Of note, the point of transition from the first oscillation (AUC1) to the first "normal" oscillation (AUC2) corresponds to the first local minimum with one condition:

- The first CO2 peaks (including local minima) with an amplitude much lower than the mean amplitude of all the peaks are discarded from the analysis.
- Amplitude is calculated as $\frac{(\mathrm{CO2\ max} - CO2\ \mathrm{min})}{CO2\ max}$ where CO2max and CO2min are respectively the local maximum and minimum CO2 values of each oscillation.

To better illustrate this condition, a capnogram from one ventilatory cycle was displayed in the figure below. The local maxima and minima of chest compressions-induced CO2 peaks are displayed in red points and blue points respectively. In this case, the CO2 peak associated with the first local minimum has a lower amplitude (orange arrow) compared to the mean amplitude of all the peaks. Consequently, this oscillation is discarded from the analysis. The point of transition from the first oscillation (AUC1) to the first "normal" oscillation (AUC2) corresponds to the second local minimum.

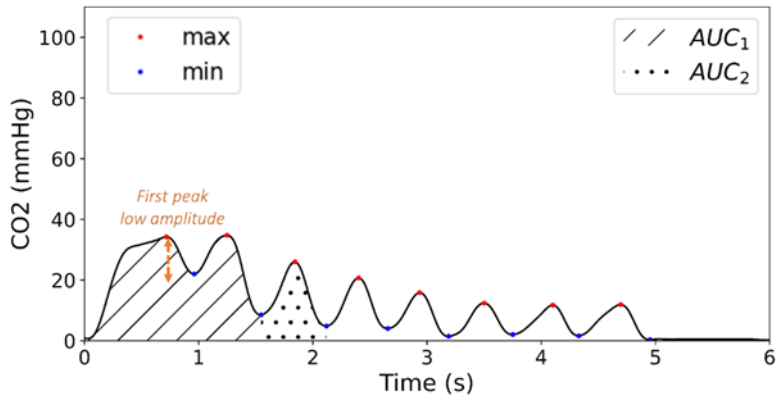

Human cadavers with simulation of CO_2 production

Constant CO_2 flow was inserted via the intubation probe to simulate CO_2 production. Data were recorded with Biopac acquisition system. A pneumotachograph (Fleisch n◦2, Lausanne, Switzerland), a pressure transducer (SD160 series: Biopac systems, Goleta, CA, USA) and an infrared-based CO_2 sensor (CO_2-100C: Biopac systems, Goleta, CA, USA) were used to measure flow, airway pressure and CO_2. Signals were converted with an analog digital converter (MP150; Biopac systems, Goleta, CA, USA) at a sample rate of 200Hz, and stored in a laptop using a dedicated software (Acknowledge, Biopac Systems, Goleta, CA, USA). The cadavers were ventilated with an emergency ventilator (Monnal T60, Air Liquide Medical Systems Antony, France) using pressure mode with standardized settings (RR=10 breaths/min, I/E=1/5, PEEP=5 cmH_2O, FiO_2 100%). Airway Opening Pressure (AOP) was assessed using a pressure time curve recorded during a low flow insufflation (10). The AOP was defined as the pressure level where the pressure time curve abruptly changes from a very steep to a smoother slope.

Mechanical bench with simulation of CO_2 production

A thoracic lung model called POUTAC was used to reproduce the mechanical properties of the respiratory system during CPR as described previously (6). The model is designed to allow ventilation either above (as allowed by all lung models) or below FRC (a unique situation specific to CPR). A bellow on which chest compressions can be applied mimics the lung with an adjustable equilibrium volume representing the Functional Residual Capacity (FRC). A wide range of respiratory mechanics (resistance and compliance) can be tailored. By providing CO_2 to the base of the bellow, our model simulates the production of CO_2, which allows capnograms to be recorded. An infrared-based CO_2 sensor (CO_2-100C: Biopac systems, Goleta, CA, USA)

was used to measure CO_2. During our experiment, ventilation was delivered through an emergency ventilator (Monnal T60, Air Liquide Medical Systems) in Assis Control Ventilation (ACV) mode with a frequency of 10/min and a positive end expiratory pressure (PEEP) of 5 cmH_2O.

Pig study: animal preparation.

We tested 7 female pigs weighing 28±1 kg, including 1 animal for the initial test and 6 animals for the main study. They were anesthetized with a mixture of tiletamine (10 $mg.kg^{-1}$ i.v.), zolazepam (10 $mg.kg^{-1}$, i.v.), propofol (10 $mg.kg^{-1}.h^{-1}$ i.v.) and methadone (0.3 mg/kg^{-1} i.m.). Animals were intubated and mechanically ventilated (Monnal T60, Air Liquide, Antony, France) in ACV mode (30% Oxygen, tidal volume 9 ml/kg, RR=20). Body temperature was controlled for a core temperature at 38°C. Animals were monitored by a five-lead electrocardiogram. Oxygen saturation (SpO_2) and CO_2 using the Monnal system (Irma CO_2 probe Monnal, Masimo Corporation CA, USA) were recorded. Catheters were inserted into femoral artery and vein for the evaluation of aortic and right atrial pressure, respectively. The central catheters were inserted into the femoral artery and vein and then mounted to the aortic and right atrial levels, respectively. Catheters are then positioned at those levels but not by chest opening or laparotomy. An intracranial pressure probe was inserted after trepanation (Millar®, Houston, USA). A flow probe was implanted around the carotid artery for the continuous evaluation of the carotid blood flow (PS-Series Probes, Transonic, NY, USA). After a period of stabilization, animals were paralyzed by rocuronium (1 $mg.kg^{-1}$). The mechanical compression device, a LUCAS 3^{TM} (Physio-control, Lund, Sweden) was placed in a controlled and secured position and was operated with default settings. Hemodynamic parameters were continuously recorded throughout the experimental protocol (HEM version 4.2, Notocord, Croissy-sur-Seine, France). Parameters continuously recorded were: airway pressure (mmHg), aortic blood pressure (mmHg), right atrial pressure (mmHg), intracranial pressure (mmHg), carotid blood flow (ml/min) and CO_2 (mmHg). Coronary perfusion pressure was calculated as aortic blood pressure minus right atrial pressure at end-decompression. Cerebral perfusion pressure was calculated as the mean value of arterial pressure minus intracranial pressure throughout chest compression and decompression cycles.

Additional file 2: supplementary results

Clinical study from Grieco et al.

Interestingly, we applied the present capnogram classification to the previous series (7). The results are very consistent since they show airway closure 36%, thoracic distention 19%, regular pattern 45% versus 35%, 22%, and 43% respectively in the present entire series. The median value of the AOI in the previous series was 50 % versus 52 % in the present series.

Illustration of thoracic distension mechanism based on airway pressure, flow and CO2 analysis

We hypothesized that thoracic distension results from insufflations that place lung volume above functional residual capacity, even at the beginning of expiration. It transiently affects chest decompression by limiting negative recoil pressure, until returning below FRC.

The examination in the animal, bench and cadaver models of concomitant changes of airway flow, airway pressure and CO2 during chest compressions may help to better understand this point regarding the position of the thorax. As illustrated on figure 5, there is an exact correspondence between the flow signal and the CO2.

During expiration, in case of thoracic distension (left column), the flow does not return to zero line during a couple of CC indicating that the thorax is still above FRC (exhalation time) even during the decompression phase. CO2 oscillations resume only once the flow crosses the zero line, thus indicating the return of lung volume to FRC.

On the contrary, the right column obtained with a smaller Vt illustrates that the flow induced by CC crosses the zero line immediately after insufflation generating CO2 full oscillations. This specific full oscillating CO2 pattern indicates that chest compressions operate close to FRC.

Supplementary table 1: *Cadavers' characteristics*

Age (years)	**68.6 (± 4.7)**
Sex male	**4 (80%)**
Height (cm)	**169 (± 9)**
Weight (kg)	**62.7 (± 9.5)**

Data are presented as means (± SD) for continuous variables and count (%) for categorical variables.

Supplementary table 2: *Baseline pigs' characteristics*

Weight (kg)	28 (± 1)
Heart Rate (bpm)	87 (± 32)
Systolic blood pressure (mmHg)	86 (± 12)
Diastolic blood pressure (mmHg)	56 (± 10)
Mean arterial pressure (mmHg)	70 (± 11)
Right atrial pressure (mmHg)	13 (± 1)
Coronary arterial pressure (mmHg)	53 (± 13)
Systolic Intracranial pressure (mmHg)	9 (± 6)
Diastolic Intracranial pressure (mmHg)	7 (± 6)
Mean Intracranial pressure (mmHg)	8 (± 6)

Data are presented as means (± SD)

Compliance to the ARRIVE Guidelines of the pigs' experiment

TITLE	**A novel capnogram analysis to guide ventilation during continuous chest compressions resuscitation. From clinical to experimental observations**
METHODS	
- *Ethical statement*	This study was approved by the ethics committee for animal research Cometh - 016 (project 2018062813205311). The procedure for the care and sacrifices of study animals was in accordance with the European Community Standards on the Care and Use of Laboratory Animals.
- *Study design*	In a first animal, we tested the effect of a large range of tidal volumes during cardiopulmonary resuscitation (from 6 ml/kg to 20 ml/kg) to illustrate what can be expected in terms of circulation impact and capnogram patterns. The six other animals were enrolled in the main study. Ventricular fibrillation was induced by a pacing wire inserted in the right ventricular through the femoral vein catheter (no specific technical issues were observed during cardiac arrest induction). Fibrillation was left untreated during 4 min (no-flow period). Then continuous mechanical chest compression was started at a rate of 100 per minute and a depth of 5 cm with ventilation as recommended (100 % oxygen fraction, respiratory rate 10/min, I/E 1/5, tidal volume 6 ml/kg). CPR was organized into three periods associated to a specific tidal volume (period T0 to T5 => 5 minutes at 6 ml/kg - period T5 to T10 => 5 minutes at 12 ml/kg - period T10 to T15 => 5 minutes at 6 ml/kg). Blood gases were measured at each tidal volume change. Animals were sacrificed at the end of the protocol (i.e., low-flow period of 15 minutes) with a lethal dose of pentobarbital (60 mg.kg-1).
- *Sample size*	1 animal for initial tests and 6 animals for the main study
- *Inclusion and exclusion criteria*	A first animal was used to test different levels of tidal volume. The six others were included in the main study and data analysis.
- *Randomization*	There was only one arm in the study with variation of tidal volumes during cardiopulmonary outcome.

- *Blinding*	The investigators were not blinded for the changes in tidal volumes during cardiopulmonary resuscitation. However, hemodynamic parameters were calculated automatically by a dedicated hemodynamic software (HEM version 4.2, Notocord, Croissy-sur-Seine, France).
- *Outcome measures*	Hemodynamic parameters were continuously recorded throughout the experimental protocol (HEM version 4.2, Notocord, Croissy-sur-Seine, France). Parameters continuously recorded were: airway pressure (mmHg), aortic blood pressure (mmHg), right atrial pressure (mmHg), intracranial pressure (mmHg), carotid blood flow (ml/min), CO2. Coronary perfusion pressure was calculated as aortic blood pressure minus right atrial pressure at end-decompression. Cerebral perfusion pressure was calculated as the mean value of arterial pressure minus intracranial pressure throughout cardiac compression.
- *Statistical methods*	Correlation was assessed between hemodynamic parameters and tidal volumes or distension ratio using a random effects linear model with each pig's id as the random effect. All statistical tests were two-sided and results with $p < 0.05$ were considered statistically significant.
- *Experimental animals*	Female pigs weighing 28±1 kg)
- *Experimental protocol*	We used 7 female pigs weighing 28±1 kg, including 1 animal for the initial test and 6 animals for the main study. They were hosted in Individual and contiguous boxes, allowing interaction between animals. A period of 7 to 10 days of acclimation was allowed before inclusion in the study. Then, swine were anesthetized with a mixture of tiletamine (10 mg.kg-1 i.v.), zolazepam (10 mg.kg-1, i.v.), propofol (10 mg.kg-1.h-1 i.v.) and methadone (0.3 mg/kg-1 i.m.). Animals were intubated and mechanically ventilated (Monnal T60, Air Liquide, Antony, France) in ACV mode (30% Oxygen, tidal volume 9 ml/kg, RR=20). Body temperature was controlled for a core temperature at 38°C. Animals were monitored by a five-lead electrocardiogram. Oxygen saturation (SpO2) and CO2 using the Monnal system (Irma CO2 probe Monnal, Masimo Corporation CA, USA) were recorded. Catheters were inserted into femoral vein and artery for the evaluation of aortic and right atrial pressure, respectively. An intracranial pressure probe was inserted after trepanation (Millar®, Houston, USA). A flow probe was implanted around the carotid artery for the continuous evaluation of the carotid blood flow (PS-Series Probes, Transonic, NY, USA). After a period of stabilization, animals were paralyzed by rocuronium (1 mg.kg-1). The mechanical compression device, a

	LUCASTM (Physio-control, Lund, Sweden) was placed in a controlled and secured position and was operated with default settings with a small active decompression (due to the suction cup. Cardiac arrest and cardiopulmonary resuscitation were then started as described above.
RESULTS	Data are reported in Tables (baseline data) and figures for all investigated parameters.

2.3. SAM: development of a new CPR bench model to evaluate ventilation devices

2.3.1. Context

The optimal ventilation strategy during CPR remains unclear, due to the complex interactions between ventilation and circulation. Over the years, different ventilation strategies and devices have been proposed during cardiac arrest. For instance, some solutions aim to optimize airway pressure to improve circulation efficiency while maintaining optimal oxygenation, such as the impedance threshold device (ITD). Other systems intend to enhance passive ventilation induced by chest compressions, such as continuous flow insufflation devices. Other strategies focus on active ventilation by developing specific modes on the ventilator with the purpose to facilitate ventilation and to limit its harmful effects on circulation. The potential benefit of those innovative developments are not easily assessed. Animal model is not simply available and conveys ventilation information which is difficult to transpose to human physiology due to their substantial anatomic differences. Bench testing may be one important element in the equation to confirm expectations and to estimate the added value of a specific strategy/ventilation device. However, available bench models are not designed for this specific purpose and need to be redesigned based on CPR respiratory physiology to obtain solid conclusions. Of note, results collected on the bench are not easily transposable to the clinical practice, but can be considered as an essential initial step to better understand the mechanisms of the CPR strategy studied, to confirm expected effects before clinical applications and eventually future randomized controlled trials.

Several studies have demonstrated the importance of high quality chest compressions and the challenge to deliver adequate ventilation during Cardio-Pulmonary Resuscitation (CPR). Interestingly, simulation manikins are extensively used and perfectly adapted to train healthcare practitioners to manage cardiac arrest patients with the objective to increase the adherence to international guidelines for both chest compressions and ventilation. In addition, there is a need to develop systems that are able to accurately evaluate the performances of medical devices ranging from ventilation systems to automatic chest compression devices. But there is a lack of CPR bench allowing to reproduce CPR physiological behavior since none of them present lung volume and FRC, which is highly important to assess recoil and thoracic pressure changes as well as passive ventilation during chest compressions as previously discussed. In this context, a physiological manikin dedicated for CPR was developed with Angers university hospital with

the intention to meet those needs. A grant was obtained from this project, which is carried by the SAM network that gathers professionals, researchers and industries from the healthcare systems in the west of France. I had the opportunity to lead this project today still in process.

The objective of this project is to emphasize the importance of such bench systems to evaluate performances of ventilation devices in the context of CPR, based on a deep understanding of specific physiological mechanisms observed during CPR.

2.3.2. Development of the CPR manikin (still in process)

A CPR manikin was designed to reproduce the specific physiological behavior of a patient under cardiac arrest. This development was greatly inspired by observations previously gathered on the POUTAC system initially developed by professors Jean-Christophe Richard, Ricardo Cordioli and Laurent Brochard in Geneva. The system is composed of several components described below:

Lung Volume

As explained previously, cardiopulmonary resuscitation is a unique situation where lung volume goes below the FRC with the application of chest compressions. Chest compressions can be separated into two phases: the compression and the decompression. During compression, the thorax is pushed below the FRC resulting in an increase of intrathoracic pressure. According to the thoracic pump theory, this pressure increase generates circulation and allows the blood to be expulsed from the heart. Then, during decompression, the natural recoil of the chest generates a negative intrathoracic pressure with a beneficial circulatory effect called venous return. It allows the blood to return from the different tissues and organs to the heart. Consequently, it is paramount to design a bench model with an FRC, as lung volume plays an important physiological role during CPR to permit circulation with both compression and decompression. On the SAM manikin, a functional residual capacity (FRC) was implemented to represent thoracic lung volume. A monocompartment bellow was designed with an internal volume mimicking the FRC at the equilibrium state (static condition). The model permits the generation of chest compression starting from FRC, thus simulating a nonbreathing patient under cardiac arrest. A spring was inserted within the bellow to simulate the thoracic elastic properties above and below FRC. After chest compression, the spring allows the passive recoil

of the bellow that returns to FRC during decompression, simulating venous return. In addition, the application of chest compressions generates passive ventilation during expiration. Adjustment of the mechanical properties of the thoracic model is possible by implementing additional parabolic resistance ranging from 5 to 50 $cmH_2O/L/s$ (PneuFlo® Parabolic Resistor, Michigan Instruments).

Intrathoracic airway closure

During CPR, the application of chest compressions tends to reduce lung volume below the FRC. This phenomenon may generate what has recently been described as intrathoracic airway closure. It is associated with reduced minute ventilation, and can be identified by the analysis of capnograms (CO2 signal). It represents approximately 30% of out of hospital cardiac arrest patients. That is why this phenomenon may impact a non-negligible proportion of patients, and that its integration within a bench model simulating patients under cardiac arrest would represent an interesting added-value.

Within our SAM manikin, a starling resistor was added to simulate intrathoracic airway closure. This device consists of an elastic collapsible tube mounted inside a chamber filled with air. The static pressure inside the chamber is used to control the degree of collapse of the tube, thus providing a variable resistor. Our model here can be seen as a flow limitation system, that can limit the flow during chest compressions to quasi-null values to simulate complete intrathoracic airway closure. Our Starling resistor (see figure 18) consists of a cylindrical waterproof tube made of Plexiglas (Ø4cm and length 14cm), in which a latex tube (AirComp, Michelin, France) with a diameter of 18mm has been inserted. The pressure in the chamber can be controlled by different ways to compress the latex tube:

- An electric syringe pump can be managed by a microprocessor, able to deliver pressures up to 60 cmH_2O within the chamber to simulate intrathoracic airway closure.
- A Continuous Positive Airway Pressure (CPAP) system can be used to control the pressure within the chamber.

Figure 18: The Starling resistor

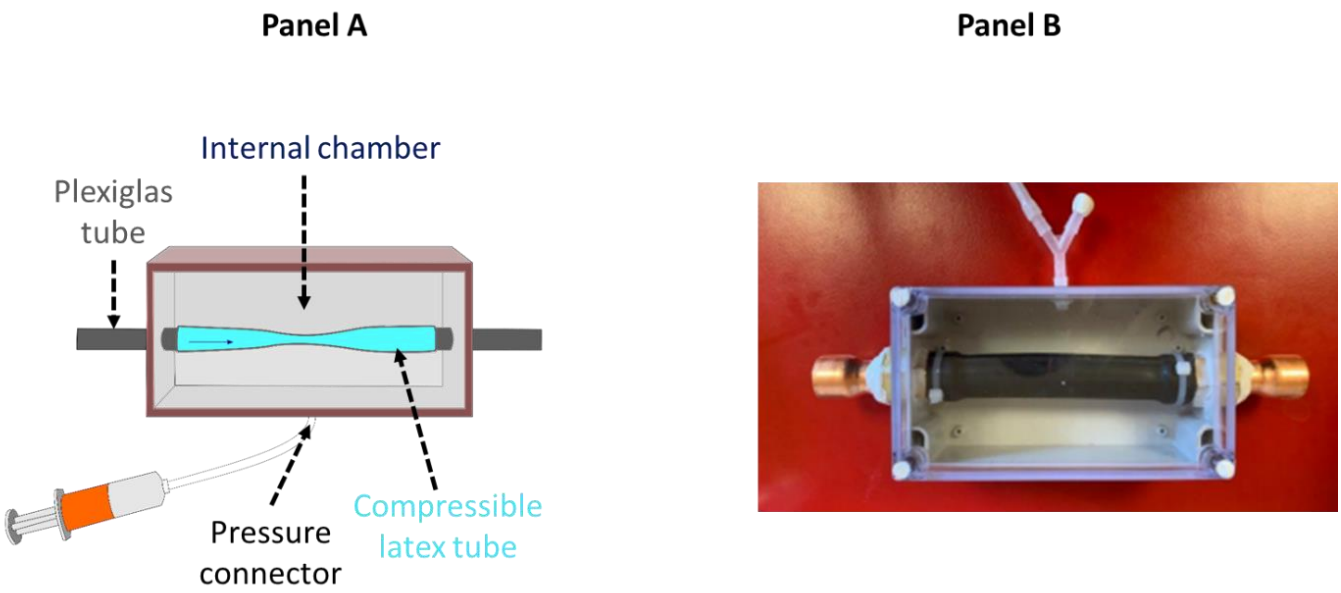

Figure 18: illustration (panel A) and photo (panel B) of the Starling resistor used in the SAM manikin. It consists of an elastic collapsible latex tube mounted inside a chamber filled with air. Pressure can be applied within the internal chamber through the pressure connector, to compress the latex tube thus resulting in flow limitation necessary to simulate intrathoracic airway closure. This pressure may be simply generated manually with a syringe (as shown in panel A), or automatically using an electric syringe pump or a continuous positive airway pressure (CPAP) device.

CO2 production and CO2 monitoring

During CPR, ventilation is delivered to provide gas exchange. During compression, oxygenated blood is transported from the heart to the systemic circulation mainly to permit cellular respiration of the different tissues and organs. The main by-product of cellular respiration is CO2, that is transported back to the heart by the blood during decompression to be eliminated at the lungs. Thus, CO2 plays an important physiological role, and its regulation may impact outcomes. Importantly, different physiological events can be identified by the analysis of CO2 patterns. Both intrathoracic airway closure and thoracic distension can be easily identified on the capnograms, making CO2 an additional tool interesting to include for CPR bench models.
The SAM manikin allows CO2 to be administered within the lungs (bellow) to simulate CO2 production. A CO2 cylinder can be connected to a flowmeter allowing the continuous injection and control of the flow of gas entering at the base of the manikin's thorax. With that system, various levels of CO2 production can be simulated. For instance, a return of spontaneous circulation (ROSC) can be easily reproduced by programing a sudden increase of CO2 production. Thanks to a CO2 sensor, capnograms can be recorded and analyzed.

Realistic manikin head

Cardiopulmonary resuscitation can be performed either under non-invasive ventilation using a mask, or under invasive ventilation using an endotracheal tube. Consequently, a CPR bench should permit to test different strategies and devices, either in invasive or non-invasive settings. In this context, a validated manikin head with realistic upper airways was chosen as the interface with the ventilation devices in the SAM manikin. The model has a dead space of 152ml and a resistance of 2.4 $cmH_2O/L/s$. The airways and nasal cavities were designed based on data from computerized tomography (CT) scans of healthy subjects. Composite 3D printing was performed using rigid material for the endoskeleton and flexible material for the airways; while the skin is made of medical silicon. Consequently, this manikin head allows endotracheal intubation or mask ventilation. It simulates realistic leaks around the mask sealing. The mouth can be open or closed depending on the chosen setting. Importantly, the trachea of the model can be connected to the Starling resistor, itself connected to the thorax of the manikin. A manuscript describing the system and illustrating recordings obtained with different medical devices on it compared to a conventional manikin will be submitted.

2.3.3. Illustration of preliminary results obtained with the SAM manikin

Preliminary tests have been performed with a first version of the SAM manikin. The functioning of the impedance threshold device (ITD) was evaluated. Automatic chest compressions were applied at a frequency of 100/min, using the Life-Stat CPR system (Michigan Instruments) as shown on figure 19, without delivering active ventilation. The ITD was inserted between a bag valve mask set at PEEP 0 and the SAM manikin. A linear pneumotachograph (PNT 3700 series, Shawnee, USA) and a pressure transducer (SD160 series: Biopac systems, Goleta, CA, USA) were used to measure flow and airway pressure. Signals were converted with an analog digital converter (MP150; Biopac systems, Goleta, CA, USA) at a sample rate of 2000 Hz, and stored in a laptop using a dedicated software (Acknowledge, Biopac Systems).

Figure 19: Experimental setting to evaluate ITD working principle

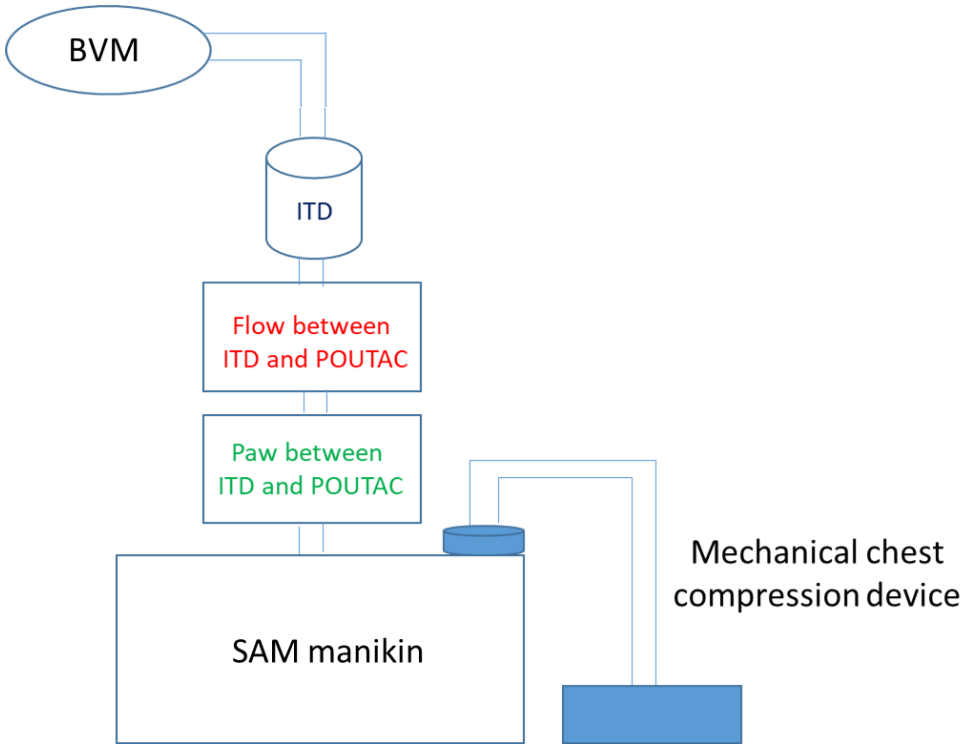

Figure 19: Schematic representing the experimental setting used to evaluate the ITD with the SAM manikin. The ITD was inserted between a bag valve mask (Monnal MI3 - Air Liquide Medical Systems) and the SAM manikin. A mechanical chest compression device was used to generate chest compressions. Airway pressure and flow were recorded.

Results are shown on figure 20. When ITD is used (orange curve), the negative pressure generated by decompression is enhanced with values around -10 to -15 cmH_2O, compared to decompressions without ITD (blue curve) where airway pressure reaches minimum values of -5 cmH_2O during decompression. However, the impact of ITD on Paw during compression does not seem significant. Flow values are very low with the use of the ITD, associated with a dramatic decrease of passive ventilation, almost null.

Figure 20: impact of ITD device on airway pressure and flow during continuous chest compressions

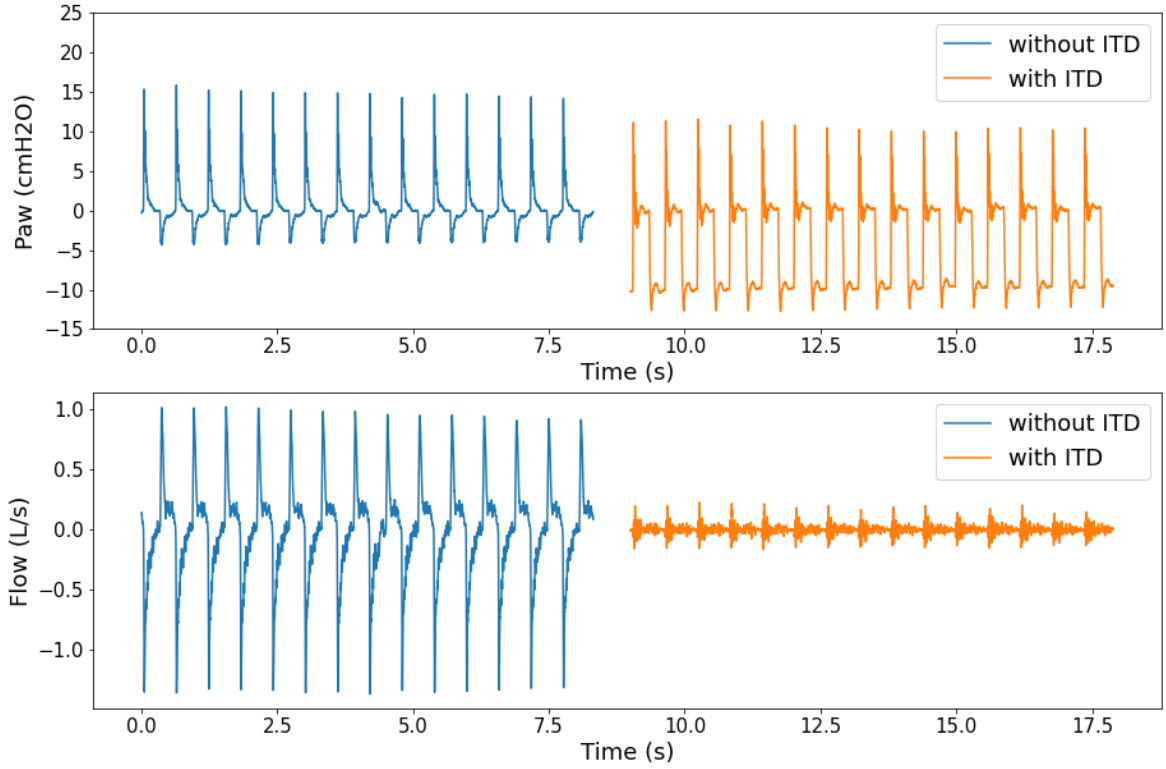

Figure 20: From top to bottom airway pressure and flow curves obtained during continuous chest compressions without (left - blue curves) and with (right – orange curves) ITD.

Those results make sense as ITD aims to increase the negativity induced by decompression, with the objective to improve venous return. To do that, resistance during decompression is significantly increased, limiting passive ventilation and even preventing the opening of the ITD. Those preliminary results illustrate the possibility of the SAM manikin to better understand the working principles of ventilation devices.

2.3.4. Discussion

Combined with a realistic manikin head already validated, a bellow simulating physiological functional residual capacity on which chest compressions can be applied, the presence of a Starling resistor to simulate intrathoracic airway closure and the continuous production of CO2 allowing capnograms to be recorded, the SAM manikin could allow an accurate assessment of the performances of ventilation strategies and devices used in the context of CPR.

Part 3: Perspectives and further steps on CO2 to guide ventilation during cardiopulmonary resuscitation

3.1. Automatic detection of CO2 patterns on a ventilator

3.1.1. Context

The analysis of expired CO2 signal during chest compressions may permit the detection of specific CO2 patterns related to physiological mechanisms, that potentially provide indications on harmful effect of ventilation on circulation (11, 70). A recent study (70) showed that during CPR, intrathoracic airway closure, thoracic distension and regular pattern can be reliably identified using a classification algorithm based on capnogram analysis. We hypothesized that a real time capnogram identification may be implemented as a monitoring tool on an emergency ventilator. The idea behind this concept is to guide the healthcare provider to optimize ventilation and protect circulation during CPR. Of note, this novel monitoring allowing real time evaluation of CO2 patterns on the ventilator has been patented.

3.1.2. Implementation of the algorithm on an emergency ventilator

The objective of this work was to implement the CO2 patterns classification algorithm within an emergency ventilator. A monitoring tool on the ventilator's screen was designed to display in real time the classification of CO2 patterns, in order to give a feedback to the clinician. For this purpose, the algorithm developed for the scientific publication (70) was revised to transfer it on the ventilator. A first version of this monitoring tool is available on a prototype. Two screenshots of the Monnal T60 transport ventilator (Air Liquide Medical Systems, Antony, France) with this specific software are shown on figure 21.

Figure 21: CO2 patterns classification software implemented on the Monnal T60 ventilator

Panel A: Intrathoracic airway closure *Panel B: Regular pattern*

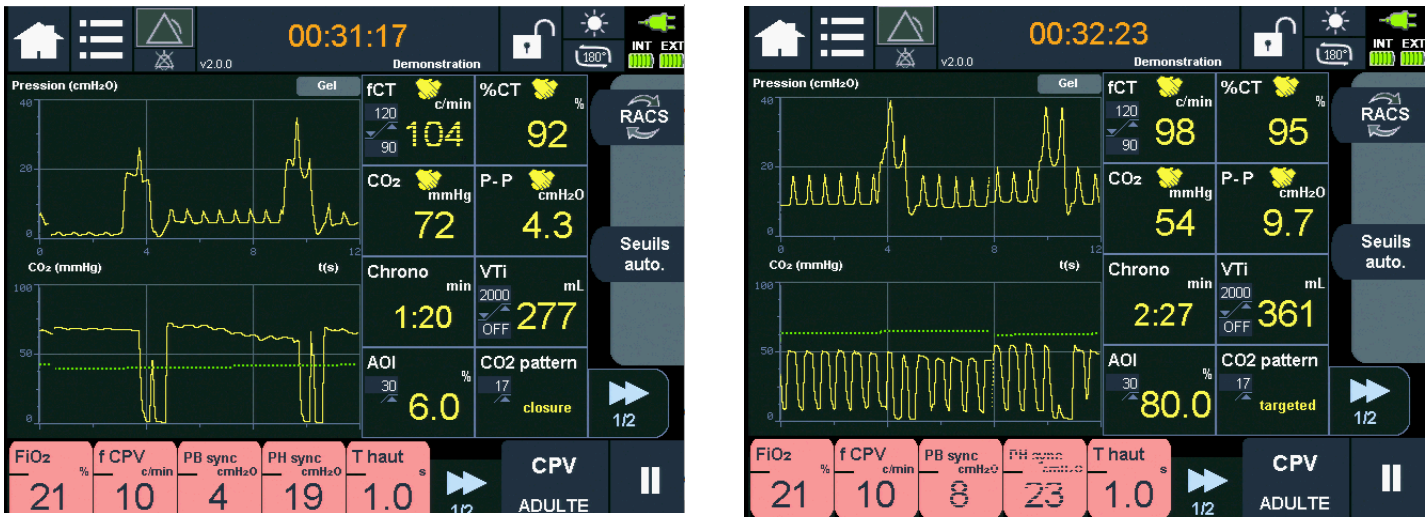

Figure 21: this figure displays images of the Monnal T60 ventilator's screen. This ventilator was implemented with a specific software allowing automatic detection of CO2 patterns based on the classification algorithm recently described (70). The CPV mode of ventilation dedicated for cardiac arrest was launched. Ventilation settings can be seen in red in the lower part of the screen. Monitoring blocks are arranged on the right side of the screen. Monitoring curves are present at the center of the screen, with the airway pressure (Paw) on the upper part and the CO2 signal (or capnogram) on the lower part. Continuous chest compressions were performed on the POUTAC bench model while ventilation was delivered with the T60 ventilator.

- **Panel A**: Intrathoracic airway closure was simulated on the bench using a Starling resistor. Expired CO2 does not oscillate despite the application of chest compressions, suggesting airway closure. The monitoring block at the lower right part called "*CO2 pattern*" displays the type of CO2 pattern analyzed by the ventilator. In this situation, "*closure*" is detected.
- **Panel B**: Regular pattern was simulated on the bench. Expired CO2 fully oscillates, suggesting regular pattern. The monitoring block at the lower right part called "*CO2 pattern*" displays the type of CO2 pattern analyzed by the ventilator. In this situation, "*targeted*" is detected, which represents the regular CO2 pattern.

The working principle of this software is as follows and is repeated at each ventilatory cycle:

During expiration

- *Store expired CO2*
  - From the start to the end of expiration, extract and save the expiratory part of the capnogram.

During insufflation

- *Capnogram classification from the expired CO2*
  - Maximum and minimum values of CO2 peaks corresponding to chest compressions-induced oscillations during the expiratory phase are calculated.
  - Airway opening index (AOI) is computed as defined by Grieco et al. (11) to quantify the magnitude of chest compressions-induced expired CO2 oscillations. An AOI lower than 30% is considered as intrathoracic airway closure. The threshold of 30% was defined based on the results of the Grieco et al.'s study showing that below an AOI of 30%, the impact on ventilation and as result on CO2 washout was substantial.

$$AOI = \frac{\sum_{i=1}^{n} \frac{\Delta CO2(i)}{CO2\max(i)}}{n}$$

  - When AOI is above 30%, the "distension ratio" is calculated. It was defined to objectively quantify the thoracic distension pattern. This ratio was already described (70) and is based on the analysis of the area under the CO2 curve. Thoracic distension is considered when "distension ratio" is greater than 2.
  - Capnogram is considered as regular pattern if AOI is above 30% and distension ratio less than or equal to 2.

- *CO2 pattern display*
  - Based on the capnogram classification, the corresponding CO2 pattern is displayed on the monitoring block of the ventilator:
    - Classification result: intrathoracic airway closure => the display is "*closure*"
    - Classification result: thoracic distension => the display is "*distension*"
    - Classification result: regular pattern => the display is "*targeted*"

This algorithm is repeated at each ventilatory cycle, allowing a real time assessment of CO2 pattern. The capnogram evolution and classification from the ventilator was evaluated on different models.

3.1.3. Bench evaluation

Objectives

The objective of this experiment was to reproduce the different CO2 patterns on the bench in order to evaluate the ability of the emergency ventilator to detect those CO2 patterns and their evolution along time.

Methods

Simulated patient

The POUTAC bench model was used to simulate a patient under cardiac arrest. As with the SAM manikin, a starling resistor was added to replicate intrathoracic airway closure. Depending on the pressure applied within the resistor's chamber, different airway opening pressure (AOP) can be tailored. The AOP represents the airway pressure value threshold below which airways are closed and above which airways are open. Consequently, airways remain open while a positive end expiratory pressure (PEEP) is set above the AOP.

Ventilation and data recording

During our experiment, ventilation was delivered through an emergency ventilator (Monnal T60, Air Liquide Medical Systems) in a pressure-controlled mode dedicated for cardiac arrest patients called CPV. This ventilator was modified and implemented with the classification algorithm recently described (70) allowing an automatic detection of the different CO2 patterns observed during CPR. In addition, four parameters from the ventilator were recorded in real time on a computer using a dedicated application called spydata: CO2, airway opening index (AOI), inspired tidal volume (VTi) and CO2 pattern. CO2 pattern can take three values: intrathoracic airway closure, thoracic distension or regular pattern. As a reminder, AOI was calculated as defined by Grieco et al. (11) to quantify the magnitude of chest compressions-induced expired CO2 oscillations, and thus to determine the presence or absence of intrathoracic airway closure. An AOI lower than 30% was considered as intrathoracic airway closure.

Protocol

Two different situations were tested:

1. Intrathoracic airway closure was simulated using the starling resistor with an AOP at 8 cmH2O. Positive End Expiratory Pressure (PEEP) was gradually increased from 3 cmH2O to 11 cmH2O. Settings were as follows: FiO2 = 100%, Ti = 1 s, RR = 10, Delta between low and high pressure = 15 cmH2O.
2. Thoracic distension was simulated by gradually increasing ventilator high pressure (Phigh) to generate higher inspiratory tidal volumes (Vti). Settings were as follows: FiO2 = 100%, Ti = 1 s, RR = 10, PEEP = 5 cmH2O. No pressure was provided inside the starling resistor's chamber to replicate open airways (AOP = 0 cmH_2O).

Results

1. Figure 22 shows the results obtained when simulating a patient with an AOP at 8cmH2O. Two behaviors are visible

   - *PEEP below the AOP of 8 cmH2O*: the expired CO2 signal is not oscillating, suggesting a low AOI associated with intrathoracic airway closure. Interestingly, AOI calculated by the ventilator is below 30% and the pattern indicated on the ventilator is intrathoracic airway closure. The mean tidal volume is around 200 ml.

   - *PEEP above the AOP of 8 cmH2O*: the expired CO2 signal is fully oscillating, suggesting a high AOI associated with regular pattern. Interestingly, AOI calculated by the ventilator is above 80% and the pattern indicated on the ventilator is regular pattern. The mean tidal volume is around 300 ml.

Figure 22: CO2 patterns detection on the POUTAC bench model simulating a cardiac arrest patient with intrathoracic airway closure

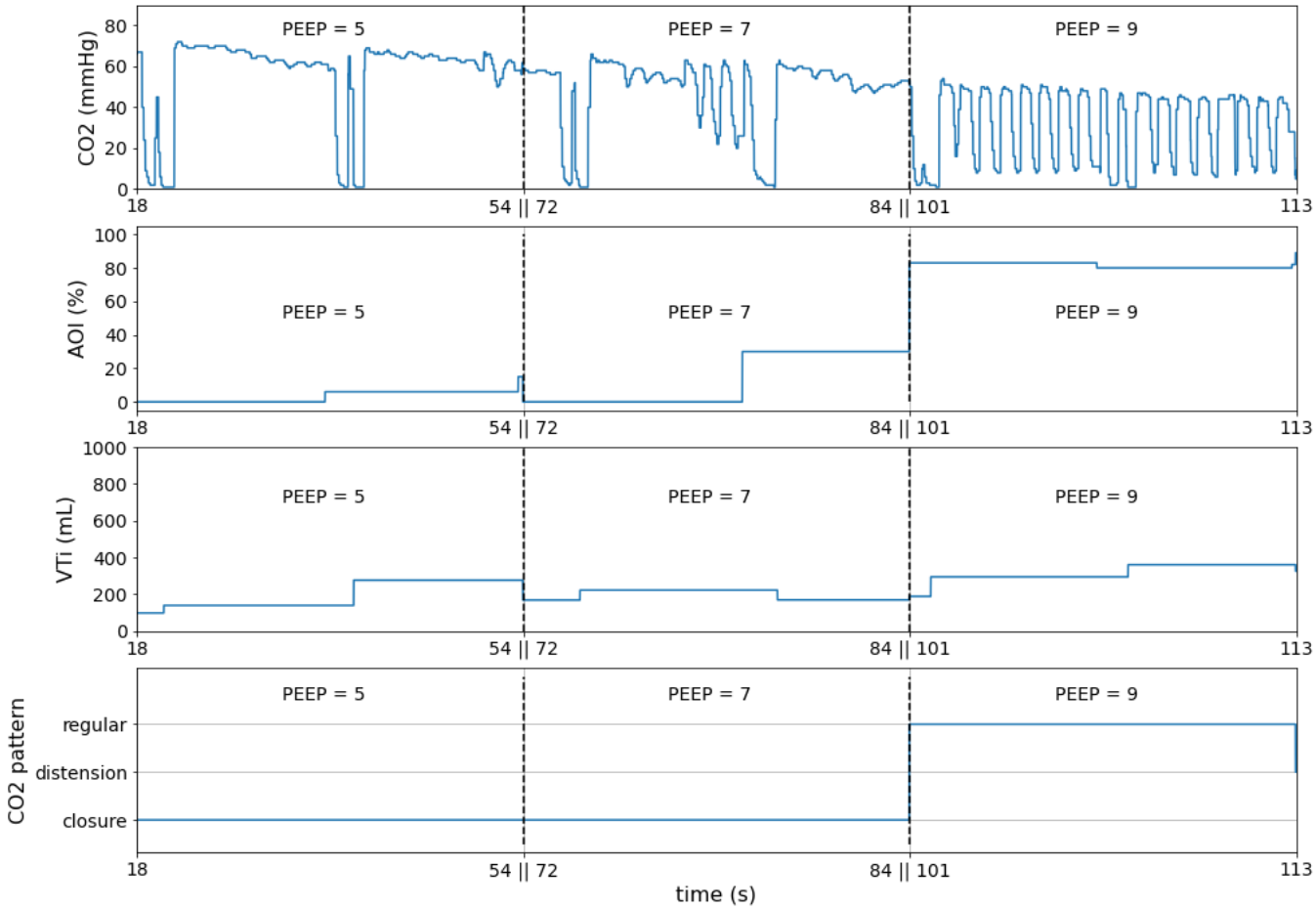

Figure 22: From top to bottom recordings of CO2, Airway Opening Index (AOI), inspired tidal volume (VTi) and CO2 pattern obtained on the POUTAC bench model. Intrathoracic airway closure with an AOP of 8 cmH2O was simulated. Manual continuous chest compressions were applied and ventilation was delivered with the Monnal T60 ventilator in a pressure-controlled mode dedicated for cardiac arrest patients called CPV. Three different PEEP settings are displayed: from left to right, a PEEP of 5, 7 and 9 cmH2O are represented. The black tilted vertical lines illustrate a PEEP change. Of note, CO2 pattern can take three categorical values: “regular pattern”, “thoracic distension” or “airway closure”.

2. Figure 23 shows the results obtained when simulating a patient with open airways, but with increasing insufflated volumes (Vti) to simulate thoracic distension. Two behaviors are visible

- *Vti below 400 ml* (Phigh = 10 cmH2O): the expired CO2 signal is fully oscillating, suggesting a high AOI associated with regular pattern. Interestingly, AOI calculated by the ventilator is above 80% and the pattern indicated on the ventilator is regular pattern.

- *Vti above 400 ml* (Phigh = 20 cmH2O): oscillations on the CO2 signal are limited or absent at the beginning of the expiration phase and resume after a few chest compressions, suggesting a high AOI associated with thoracic distension. Interestingly, AOI calculated by the ventilator is above 80% and the pattern indicated on the ventilator is thoracic distension.

Figure 23: CO2 patterns detection on the POUTAC bench model simulating a cardiac arrest patient with various insufflated volumes

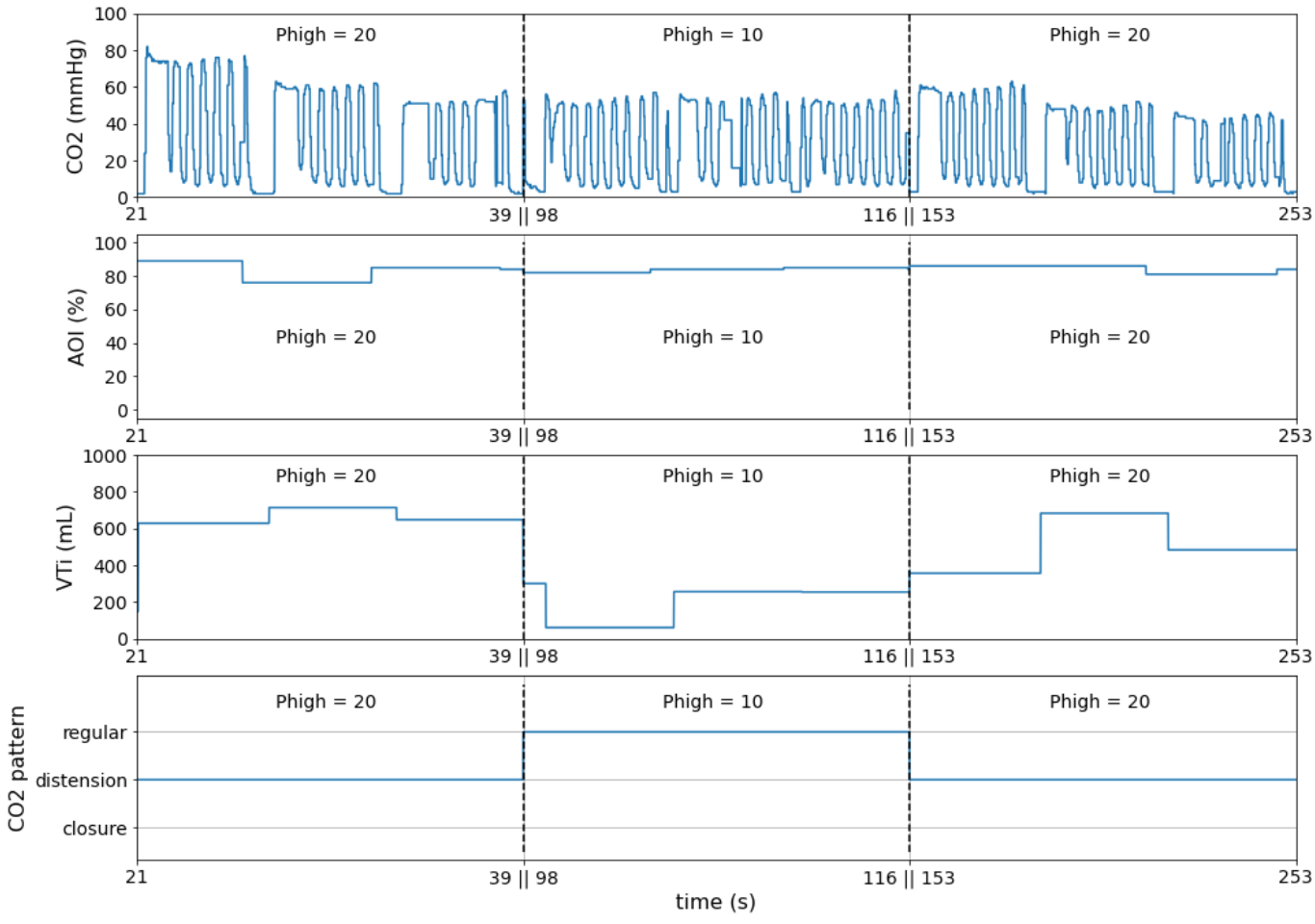

Figure 23: From top to bottom recordings of CO2, Airway Opening Index (AOI), inspired tidal volume (VTi) and CO2 pattern obtained on the POUTAC bench model. Manual continuous chest compressions were applied and ventilation was delivered with the Monnal T60 ventilator in a pressure-controlled mode dedicated for cardiac arrest patients called CPV. Three different high-pressure settings are displayed: from left to right, a high pressure set on the ventilator of 20, 10 and 20 cmH2O are represented. The black tilted vertical lines illustrate a high-pressure change (and consequently a tidal volume change). In fact, a high-pressure increase generates higher tidal volumes. Of note, CO2 pattern can take three categorical values: “regular pattern”, “thoracic distension” or “airway closure”.

Conclusion

The capnogram classification algorithm implemented in the Monnal T60 ventilator is capable to provide a real time analysis of expired CO2 signal and to determine CO2 patterns on the bench in the conditions tested.

3.1.4. First animal experience

Objectives

The objective of this experiment was to reproduce the different CO2 patterns on one animal in order to evaluate the ability of the emergency ventilator to detect the different CO2 patterns depending on ventilation settings. Of note, intrathoracic airway closure was not observed in animal experiments. It is possible that the pig thorax anatomy may limit the reduction of lung volumes we observe in humans during resuscitation and thus occurrence of intrathoracic airway closure. Besides, pig bronchial tree presents lateral connections that may also limit occurrence of distal airway closure (97).

Methods

The animal test

One male pig weighing 28 kg was used in the study. It was anesthetized with a mixture of tiletamine (10 mg.kg-1 i.v.), zolazepam (10 mg.kg-, i.v.), propofol (10 mg.kg-1.h-1 i.v.) and methadone (0.3 mg/kg-1 i.m.). The animal was intubated and mechanically ventilated (Monnal T60, Air Liquide, Antony, France) in CPV pressure mode.

Ventilation and data recording

As in the bench experiment, the ventilator was modified and implemented with the classification algorithm recently described (70) allowing an automatic detection of the different CO2 patterns observed during CPR. Four parameters from the ventilator were recorded in real time using the spydata: CO2, airway opening index (AOI), inspired tidal volume (VTi) and CO2 pattern.

Protocol

Thoracic distension has been shown to be associated with higher insufflated volumes (Vti). Thus, the high pressure (Phigh) was gradually increased from 7 cmH2O to 15 cmH2O to generate higher inspiratory tidal volumes (Vti). Settings were as follows: FiO2 = 100%, Ti = 1 s, RR = 10, PEEP = 5 cmH2O. No pressure was provided inside the starling resistor's chamber to simulate open airways (AOP = 0 cmH_2O).

Results

Figure 24 shows the results obtained on a pig model with increasing insufflated volumes (Vti). Two behaviors are visible:

- *Vti below 150 ml* (Phigh = 11 cmH2O): the expired CO2 signal is fully oscillating, suggesting a high AOI associated with regular pattern. Interestingly, AOI calculated by the ventilator is above 80% and the pattern indicated on the ventilator is regular pattern.

- *Vti above 150 ml* (Phigh = 11 cmH2O or Phigh = 15 cmH2O): oscillations on the CO2 signal are limited or absent at the beginning of the expiration phase and resume after a few chest compressions, suggesting a high AOI associated with thoracic distension. Interestingly, AOI calculated by the ventilator is above 80% and the pattern indicated on the ventilator is thoracic distension.

Figure 24: CO2 patterns detection on a CPR pig model simulating a cardiac arrest patient with various insufflated volumes

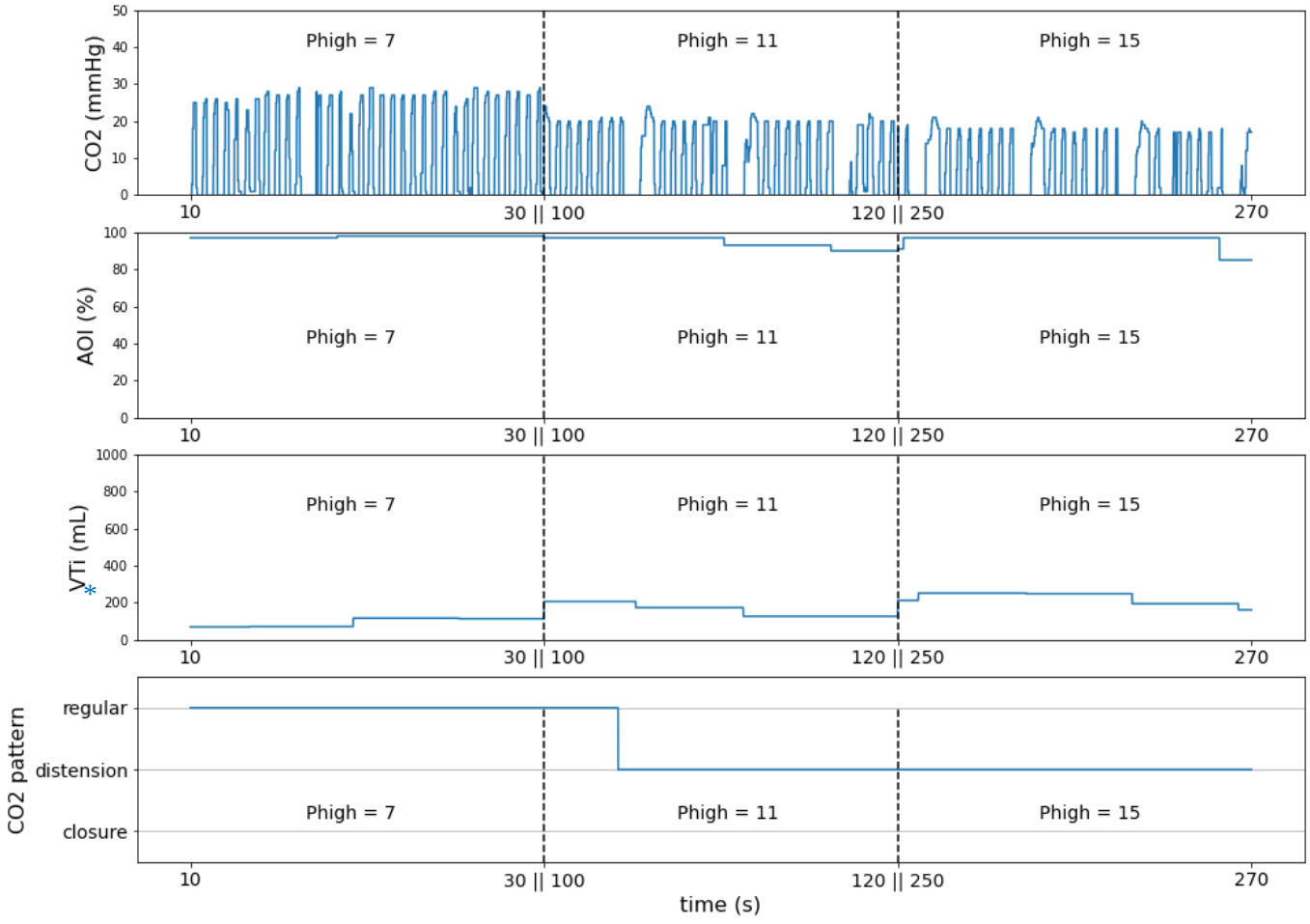

Figure 24: From top to bottom recordings of CO2, Airway Opening Index (AOI), inspired tidal volume (VTi) and CO2 pattern obtained on one pig. Manual continuous chest compressions were applied and ventilation was delivered with the Monnal T60 ventilator in a pressure-controlled mode dedicated for cardiac arrest patients called CPV. Three different high-pressure settings are displayed: from left to right, a high pressure set on the ventilator of 7, 11 and 15 cmH2O are represented. The black tilted vertical lines illustrate a high-pressure change (and consequently a tidal volume change). In fact, a high-pressure increase generates higher tidal volumes. Of note, CO2 pattern can take three categorical values: "regular pattern", "thoracic distension" or "airway closure".

Conclusion

The capnogram classification algorithm implemented in the Monnal T60 ventilator is capable to provide a real time analysis of expired CO2 signal and to determine CO2 patterns on an animal model in the conditions tested.

3.2. Future perspectives

The optimal ventilation strategy during CPR is still debated. Recent studies introduced a novel approach based on the analysis of expired CO2 signal during chest compressions resulting in the identification of specific CO2 patterns (11, 70). We showed that intrathoracic airway closure, thoracic distension or regular pattern can be reliably identified by the capnogram analysis.

On the one hand, intrathoracic airway closure results from the decrease in lung volume below the FRC due to the application of chest compressions. This phenomenon is associated with impaired ventilation, more precisely a decrease in total minute ventilation resulting from the dramatic reduction or absence of passive ventilation. Intrathoracic airway closure is defined by an airway opening pressure (AOP), representing the airway pressure value threshold below which airways are closed and above which airways are open. Consequently, a PEEP set above this AOP may prevent airway closure. As presence of airway closure is uncertain and AOP differs among patients, an individualized method to characterize this phenomenon such as CO2 analysis may be important.

On the other hand, excessive ventilation during cardiac arrest has already been shown to be associated with poor outcomes. Nevertheless, it is definitively challenging to control and monitor Vt delivered during manual bag ventilation (106). We hypothesized that the specific capnogram called “thoracic distension” may indicate the risk associated with excessive ventilation inflating the thorax above FRC. It may jeopardize circulation (venous return) by limiting negative intrathoracic pressure during decompression. This novel CO2 pattern indicating relative thoracic distension may be associated with a negative impact on blood pressure and cerebral perfusion. Interestingly, a decrease in the insufflated volume may prevent thoracic distension.

The regular CO2 pattern with fully oscillating capnogram could identify CPR close to the FRC with effective venous return, illustrating the theoretical optimal thoracic volume for effective chest compressions. Based on these observations, a capnogram-based ventilation strategy may permit to optimize ventilation during CPR, using real-time identification of capnograms (intrathoracic airway closure, thoracic distension or regular pattern). This strategy is illustrated on figure 25. As previously shown, PEEP increase may be considered in case of intrathoracic

airway closure to open the airways, while Vt reduction could be proposed in case of thoracic distension. Further evidence is needed before developing such ventilatory approach on a ventilator, but these findings may be of potential additional value, especially for bag valve mask ventilation during which hyperventilation is likely to occur. A clinical observational study may help to address the real benefit or not of a ventilatory strategy based on CO2 analysis. Interestingly, preliminary investigations showed that it was feasible to implement the CO2 algorithm within a ventilator to detect in real time the different CO2 patterns.

Figure 25: Ventilatory strategy based on capnogram analysis during CPR

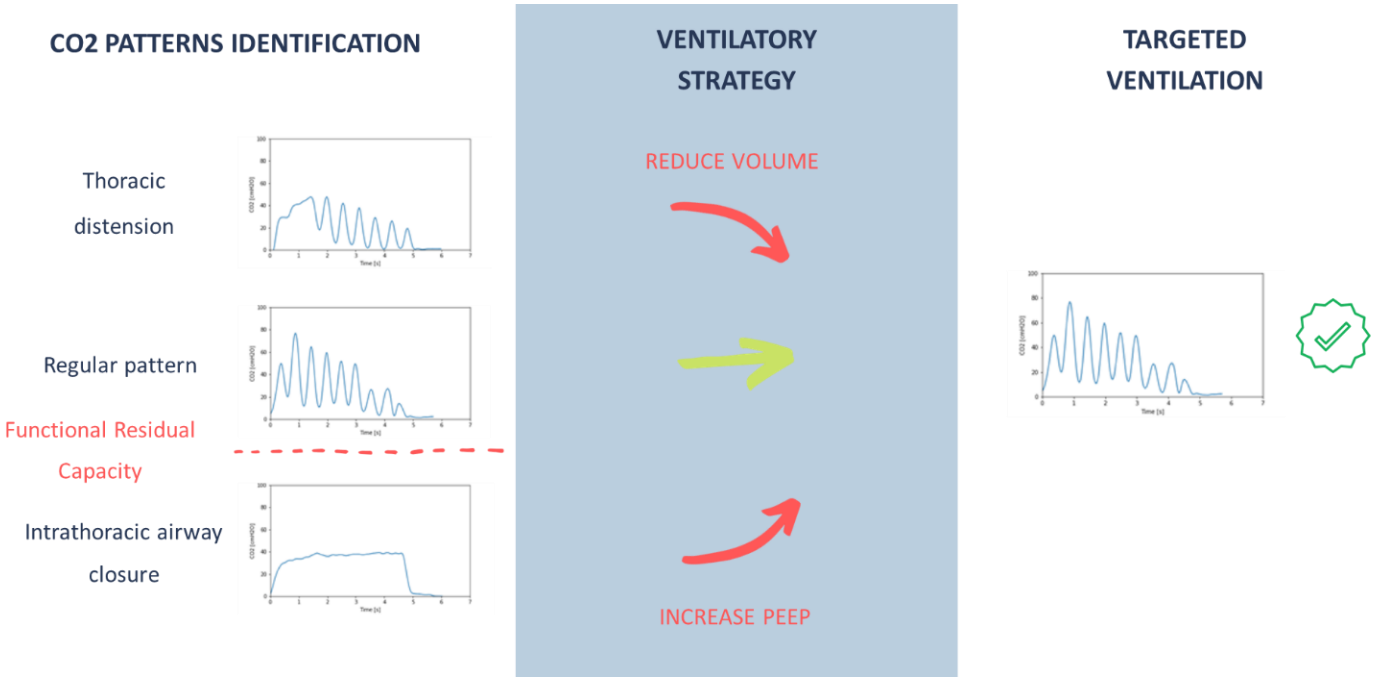

Figure 25: This figure illustrates a ventilatory strategy during CPR based on the analysis of CO2 patterns associated to lung volumes.

1. The first component of this strategy refers to the real time identification of CO2 patterns, using the algorithm recently described (70).
2. Based on the type of CO2 pattern, an adaptation of the ventilation settings could be proposed to the physician. Both thoracic distension (associated with a lung volume above FRC) and intrathoracic airway closure (associated with a significant reduction of lung volumes below FRC) are considered as potentially harmful for the patient, and should be avoided. On the contrary, regular pattern may be considered as the optimal situation (and optimal lung volume) that should be targeted in the current strategy. Consequently, if thoracic distension is identified, a reduction of the tidal volume could be suggested to recover a regular pattern. If intrathoracic airway closure is recognized, an increase of PEEP could be proposed to open the airways and obtain a regular pattern.
3. To summarize, the objective of the capnogram-based ventilatory strategy is to adapt in real time ventilation settings to keep the patient as much as possible within the targeted ventilation associated with the regular CO2 pattern.

Conclusion

Critically ill patients with the need for mechanical ventilation show complex interactions between respiratory and cardiovascular physiology. In the context of the covid crisis, transport ventilators have been used to extend intensive care units, that are based on different working principles that may potentially impact the quality of ventilation delivered to the patient. The present bench study suggests that turbine technologies may acceptably replace ICU ventilators in this context. Pneumatic transport ventilators are limited in terms of FiO2 settings, but provide acceptable volume accuracy in severe simulated conditions.

The optimal ventilation strategy during CPR remains unclear, possibly due to the complexity of interactions between ventilation and circulation during CPR. We hypothesized that expired CO2 could reflect the quality of ventilation during CPR, and reveal at which lung volume CPR operates. Three CO2 patterns have been identified on clinical data and reproduced on animal, cadaver and bench models. Intrathoracic airway closure may be associated with low lung volumes and a reduction of total minute ventilation. A novel CO2 pattern indicating relative thoracic distension may be associated with a negative impact on blood pressure and cerebral perfusion, irrespective of tidal volume per se. Based on these observations, a capnogram-based ventilation strategy may permit to optimize ventilation during CPR, using real-time identification of capnograms. Further evidence is needed before developing such ventilatory approach on a ventilator, but this work has shown that it is feasible. Specific bench models are needed to accurately evaluate such strategies. The SAM manikin is an example of bench model based on physiology, allowing to reproduce intrathoracic airway closure with an FRC. These findings may be of potential additional value to better understand ventilation during CPR.

References

1. L'Her E, Roy A, Marjanovic N. Bench-test comparison of 26 emergency and transport ventilators. Critical Care. 2014;18.

2. El Sayed M, Tamim H, Mailhac A, N Clay M. Ventilator use by emergency medical services during 911 calls in the United States. Am J Emerg Med. 2018;36:763–8.

3. Xu L, Tang F, Wang Y, Cai Q, Tang S, Xia D, et al. Research progress of pre-hospital emergency during 2000-2020: a bibliometric analysis. Am J Transl Res. 2021;13:1109–24.

4. Bucher JT, Vashisht R, Ladd M, Cooper JS. Bag Mask Ventilation. StatPearls. Treasure Island (FL): StatPearls Publishing; 2022.

5. Magliocca A, Rezoagli E, Zani D, Manfredi M, De Giorgio D, Olivari D, et al. Cardiopulmonary Resuscitation-associated Lung Edema (CRALE). A Translational Study. Am J Respir Crit Care Med. 2021;203:447–57.

6. Sutherasan Y, Raimondo P, Pelosi P. Ventilation and gas exchange management after cardiac arrest. Best Pract Res Clin Anaesthesiol. 2015;29:413–24.

7. Chang MP, Idris AH. The past, present, and future of ventilation during cardiopulmonary resuscitation: Current Opinion in Critical Care. 2017;23:188–92.

8. Soar J, Böttiger BW, Carli P, Couper K, Deakin CD, Djärv T, et al. European Resuscitation Council Guidelines 2021: Adult advanced life support. Resuscitation. 2021;161:115–51.

9. Leturiondo M, Ruiz de Gauna S, Gutiérrez JJ, Alonso D, Corcuera C, Urtusagasti JF, et al. Chest compressions induce errors in end-tidal carbon dioxide measurement. Resuscitation. 2020;153:195–201.

10. Leturiondo M, Ruiz de Gauna S, Ruiz JM, Julio Gutiérrez J, Leturiondo LA, González-Otero DM, et al. Influence of chest compression artefact on capnogram-based ventilation detection during out-of-hospital cardiopulmonary resuscitation. Resuscitation. 2018;124:63–8.

11. Grieco DL, J. Brochard L, Drouet A, Telias I, Delisle S, Bronchti G, et al. Intrathoracic Airway Closure Impacts CO2 Signal and Delivered Ventilation during Cardiopulmonary Resuscitation. Am J Respir Crit Care Med. 2019;199:728–37.

12. Cordioli RL, Lyazidi A, Rey N, Granier J-M, Savary D, Brochard L, et al. Impact of ventilation strategies during chest compression. An experimental study with clinical observations. Journal of Applied Physiology. American Physiological Society; 2016;120:196–203.

13. Carvalho AR, Zin WA. Respiratory system dynamical mechanical properties: modeling in time and frequency domain. Biophys Rev. 2011;3:71.

14. Higginson R, Parry A. Emergency airway management: common ventilation techniques. Br J Nurs. 2013;22:366–8, 370–1.

15. Coppadoro A, Bellani G. A novel Venturi system to generate high flow with titratable FiO2. AboutOpen. 2021;8:88–91.

16. Lyazidi A, Thille AW, Carteaux G, Galia F, Brochard L, Richard J-CM. Bench test evaluation of volume delivered by modern ICU ventilators during volume-controlled ventilation. Intensive Care Med. 2010;36:2074–80.

17. Weisfeldt ML, Becker LB. Resuscitation after cardiac arrest: a 3-phase time-sensitive model. JAMA. 2002;288:3035–8.

18. Ornato JP, Peberdy MA. Measuring Progress in Resuscitation. Circulation. American Heart Association; 2006;114:2754–6.

19. Weisfeldt ML. A three phase temporal model for cardiopulmonary resuscitation following cardiac arrest. Trans Am Clin Climatol Assoc. 2004;115:115–22.

20. Goto Y, Funada A, Maeda T, Goto Y. Time boundaries of the three-phase time-sensitive model for ventricular fibrillation cardiac arrest. Resusc Plus. 2021;6:100095.

21. Gilmore CM, Rea TD, Becker LJ, Eisenberg MS. Three-phase model of cardiac arrest: time-dependent benefit of bystander cardiopulmonary resuscitation. Am J Cardiol. 2006;98:497–9.

22. Stiell IG, Nichol G, Leroux BG, Rea TD, Ornato JP, Powell J, et al. Early versus later rhythm analysis in patients with out-of-hospital cardiac arrest. N Engl J Med. 2011;365:787–97.

23. Olasveengen TM, Mancini ME, Perkins GD, Avis S, Brooks S, Castrén M, et al. Adult Basic Life Support: 2020 International Consensus on Cardiopulmonary Resuscitation and Emergency Cardiovascular Care Science With Treatment Recommendations. Circulation. 2020;142:S41–91.

24. Kouwenhoven WB, Jude JR, Knickerbocker GG. Closedchest cardiac massage. JAMA 1960; 173: 1064–7.

25. Cipani S, Bartolozzi C, Ballo P, Sarti A. Blood flow maintenance by cardiac massage during cardiopulmonary resuscitation: Classical theories, newer hypotheses, and clinical utility of mechanical devices. Journal of the Intensive Care Society. 2019;20:2–10.

26. Georgiou M, Papathanassoglou E, Xanthos T. Systematic review of the mechanisms driving effective blood flow during adult CPR. Resuscitation. Elsevier; 2014;85:1586–93.

27. Porter TR, Ornato JP, Guard CS, Roy VG, Burns CA, Nixon JV. Transesophageal echocardiography to assess mitral valve function and flow during cardiopulmonary resuscitation. Am J Cardiol. 1992;70:1056–60.

28. Shaw DP, Rutherford JS, Williams MJ. The mechanism of blood flow in cardiopulmonary resuscitation--introducing the lung pump. Resuscitation. 1997;35:255–8.

29. Ma MH, Hwang JJ, Lai LP, Wang SM, Huang GT, Shyu KG, et al. Transesophageal echocardiographic assessment of mitral valve position and pulmonary venous flow during cardiopulmonary resuscitation in humans. Circulation. 1995;92:854–61.

30. Andreka P, Frenneaux MP. Haemodynamics of cardiac arrest and resuscitation. Curr Opin Crit Care. 2006;12:198–203.

31. Sandroni C, Cronberg T, Sekhon M. Brain injury after cardiac arrest: pathophysiology, treatment, and prognosis. Intensive Care Med. 2021;47:1393–414.

32. Lurie KG, Nemergut EC, Yannopoulos D, Sweeney M. The Physiology of Cardiopulmonary Resuscitation. Anesthesia & Analgesia. 2016;122:767–83.

33. Weil MH, Bisera J, Trevino RP, Rackow EC. Cardiac output and end-tidal carbon dioxide. Crit Care Med. 1985;13:907–9.

34. Aufderheide TP, Pirrallo RG, Yannopoulos D, Klein JP, von Briesen C, Sparks CW, et al. Incomplete chest wall decompression: a clinical evaluation of CPR performance by EMS personnel and assessment of alternative manual chest compression-decompression techniques. Resuscitation. 2005;64:353–62.

35. Ornato JP. Hemodynamic monitoring during CPR. Annals of Emergency Medicine. 1993;22:289–95.

36. Nishiwaki C, Kotake Y, Yamada T, Nagata H, Tagawa M, Takeda J. Response Time of Different Methods of Cardiac Output Monitoring During Cardiopulmonary Resuscitation and Recovery. Journal of Cardiothoracic and Vascular Anesthesia. Elsevier; 2010;24:306–8.

37. Teboul J-L, Saugel B, Cecconi M, De Backer D, Hofer C, Monnet X, et al. Less invasive hemodynamic monitoring in critically ill patients. Intensive Care Med. 2016;42.

38. Argueta EE, Paniagua D. Thermodilution Cardiac Output: A Concept Over 250 Years in the Making. Cardiology in Review. 2019;27:138.

39. Idris AH. The Sweet Spot. JEMS. 2012;37:4–9.

40. Wolfe JA, Maier GW, Newton JR, Glower DD, Tyson GS, Spratt JA, et al. Physiologic determinants of coronary blood flow during external cardiac massage. J Thorac Cardiovasc Surg. 1988;95:523–32.

41. Bellamy RF, DeGuzman LR, Pedersen DC. Coronary blood flow during cardiopulmonary resuscitation in swine. Circulation. 1984;69:174–80.

42. Teferra, M. Electromagnetic Blood Flow Meter: Review. Int. J. Latest Res. Eng. Technol. 2017, 3, 21–26.

43. Wagner H, Madsen Hardig B, Steen S, Sjoberg T, Harnek J, Olivecrona GK. Evaluation of coronary blood flow velocity during cardiac arrest with circulation maintained through mechanical chest compressions in a porcine model. BMC Cardiovasc Disord. 2011;11:73.

44. Kern KB. Coronary perfusion pressure during cardiopulmonary resuscitation. Best Practice & Research Clinical Anaesthesiology. 2000;14:591–609.

45. Paradis NA, Martin GB, Rivers EP, Goetting MG, Appleton TJ, Feingold M, et al. Coronary perfusion pressure and the return of spontaneous circulation in human cardiopulmonary resuscitation. JAMA. 1990;263:1106–13.

46. Kern KB, Ewy GA, Voorhees WD, Babbs CF, Tacker WA. Myocardial perfusion pressure: a predictor of 24-hour survival during prolonged cardiac arrest in dogs. Resuscitation. 1988;16:241–50.

47. Reynolds JC, Salcido DD, Menegazzi JJ. Coronary perfusion pressure and return of spontaneous circulation after prolonged cardiac arrest. Prehosp Emerg Care. 2010;14:78–84.

48. Fletcher DJ, Boller M. Fluid Therapy During Cardiopulmonary Resuscitation. Front Vet Sci. 2021;7:625361.

49. Yannopoulos D, McKnite S, Aufderheide TP, Sigurdsson G, Pirrallo RG, Benditt D, et al. Effects of incomplete chest wall decompression during cardiopulmonary resuscitation on coronary and cerebral perfusion pressures in a porcine model of cardiac arrest. Resuscitation. 2005;64:363–72.

50. Joris PJ, Mensink RP, Adam TC, Liu TT. Cerebral Blood Flow Measurements in Adults: A Review on the Effects of Dietary Factors and Exercise. Nutrients. 2018;10:530.

51. Muir ER, Watts LT, Tiwari YV, Bresnen A, Duong TQ. Quantitative Cerebral Blood Flow Measurements Using MRI. Methods Mol Biol. 2014;1135:205–11.

52. Eleff SM, Kim H, Shaffner DH, Traystman RJ, Koehler RC. Effect of cerebral blood flow generated during cardiopulmonary resuscitation in dogs on maintenance versus recovery of ATP and pH. Stroke. 1993;24:2066–73.

53. Eleff SM, Schleien CL, Koehler RC, Shaffner DH, Tsitlik J, Halperin HR, et al. Brain bioenergetics during cardiopulmonary resuscitation in dogs. Anesthesiology. 1992;76:77–84.

54. Halperin HR, Chandra NC, Levin HR, Rayburn BK, Tsitlik JE. Newer Methods of Improving Blood Flow During CPR. Annals of Emergency Medicine. Elsevier; 1996;27:553–62.

55. Shaffner DH, Eleff SM, Brambrink AM, Sugimoto H, Izuta M, Koehler RC, et al. Effect of arrest time and cerebral perfusion pressure during cardiopulmonary resuscitation on cerebral blood flow, metabolism, adenosine triphosphate recovery, and pH in dogs. Crit Care Med. 1999;27:1335–42.

56. Chalkias A, Xanthos T. Post-cardiac arrest brain injury: Pathophysiology and treatment. Journal of the Neurological Sciences. 2012;315:1–8.

57. Kirkman MA, Smith M. Intracranial pressure monitoring, cerebral perfusion pressure estimation, and ICP/CPP-guided therapy: a standard of care or optional extra after brain injury? Br J Anaesth. 2014;112:35–46.

58. Debaty G, Moore J, Duhem H, Rojas-Salvador C, Salverda B, Lick M, et al. Relationship between hemodynamic parameters and cerebral blood flow during cardiopulmonary resuscitation. Resuscitation. 2020;153:20–7.

59. Zhong W, Ji Z, Sun C. A Review of Monitoring Methods for Cerebral Blood Oxygen Saturation. Healthcare (Basel). 2021;9:1104.

60. Ibrahim AW, Trammell AR, Austin H, Barbour K, Onuorah E, House D, et al. Cerebral Oximetry as a Real-Time Monitoring Tool to Assess Quality of In-Hospital Cardiopulmonary Resuscitation and Post Cardiac Arrest Care. J Am Heart Assoc. 2015;4:e001859.

61. Parnia S, Yang J, Nguyen R, Ahn A, Zhu J, Inigo-Santiago L, et al. Cerebral Oximetry During Cardiac Arrest: A Multicenter Study of Neurologic Outcomes and Survival. Crit Care Med. 2016;44:1663–74.

62. Hamanaka K, Shimoto M, Hitosugi M, Beppu S, Terashima M, Sasahashi N, et al. Cerebral oxygenation monitoring during resuscitation by emergency medical technicians: a prospective multicenter observational study. Acute Med Surg. 2020;7:e528.

63. Rudikoff MT, Freund P, Weisfeldt ML. Mechanisms of blood flow during cardiopulmonary resuscitation. 1980;61:8.

64. Kim SY, Shim G-H, Schmölzer GM. Is Chest Compression Superimposed with Sustained Inflation during Cardiopulmonary Resuscitation an Alternative to 3:1 Compression to Ventilation Ratio in Newborn Infants? Children. Multidisciplinary Digital Publishing Institute; 2021;8:97.

65. Schmölzer GM, O'Reilly M, Labossiere J, Lee T-F, Cowan S, Qin S, et al. Cardiopulmonary resuscitation with chest compressions during sustained inflations: a new technique of neonatal resuscitation that improves recovery and survival in a neonatal porcine model. Circulation. 2013;128:2495–503.

66. Chandra N, Weisfeldt ML, Tsitlik J, Vaghaiwalla F, Snyder LD, Hoffecker M, et al. Augmentation of carotid flow during cardiopulmonary resuscitation by ventilation at high airway pressure simultaneous with chest compression. Am J Cardiol. 1981;48:1053–63.

67. Wik L, Olsen J-A, Persse D, Sterz F, Lozano M, Brouwer MA, et al. Why do some studies find that CPR fraction is not a predictor of survival? Resuscitation. 2016;104:59–62.

68. Cheskes S, Schmicker RH, Rea T, Powell J, Drennan IR, Kudenchuk P, et al. Chest compression fraction: A time dependent variable of survival in shockable out-of-hospital cardiac arrest. Resuscitation. 2015;97:129–35.

69. Gommers D. Functional residual capacity and absolute lung volume. Curr Opin Crit Care. 2014;20:347–51.

70. Lesimple A, Fritz C, Hutin A, Charbonney E, Savary D, Delisle S, et al. A novel capnogram analysis to guide ventilation during cardiopulmonary resuscitation: clinical and experimental observations. Crit Care. 2022;26:287.

71. Safar P, Brown TC, Holtey WJ, Wilder RJ. Ventilation and circulation with closed-chest cardiac massage in man. JAMA. 1961;176:574–6.

72. Deakin C, O'Neil J, Tabor T. Does compression-only cardiopulmonary resuscitation generate adequate passive ventilation during cardiac arrest? Resuscitation [Internet]. Resuscitation; 2007; 75.

73. Chen L, Del Sorbo L, Grieco DL, Shklar O, Junhasavasdikul D, Telias I, et al. Airway Closure in Acute Respiratory Distress Syndrome: An Underestimated and Misinterpreted Phenomenon. Am J Respir Crit Care Med. 2018;197:132–6.

74. Coudroy R, Vimpere D, Aissaoui N, Younan R, Bailleul C, Couteau-Chardon A, et al. Prevalence of Complete Airway Closure According to Body Mass Index in Acute Respiratory Distress Syndrome. Anesthesiology. 2020;133:867–78.

75. Suki B, Barabási AL, Hantos Z, Peták F, Stanley HE. Avalanches and power-law behaviour in lung inflation. Nature. 1994;368:615–8.

76. Charbonney E, Grieco DL, Cordioli RL, Badat B, Savary D, Richard J-CM. Ventilation During Cardiopulmonary Resuscitation: What Have We Learned From Models? Respir Care. 2019;64:1132–8.

77. Beloncle FM, Merdji H, Lesimple A, Pavlovsky B, Yvin E, Savary D, et al. Gas Exchange and Respiratory Mechanics after a Cardiac Arrest: A Clinical Description of Cardiopulmonary Resuscitation-associated Lung Edema. Am J Respir Crit Care Med. 2022;206:637–40.

78. Bertrand C, Hemery F, Carli P, Goldstein P, Espesson C, Rüttimann M, et al. Constant flow insufflation of oxygen as the sole mode of ventilation during out-of-hospital cardiac arrest. Intensive Care Med. 2006;32:843–51.

79. Saïssy JM, Boussignac G, Cheptel E, Rouvin B, Fontaine D, Bargues L, et al. Efficacy of continuous insufflation of oxygen combined with active cardiac compression-decompression during out-of-hospital cardiorespiratory arrest. Anesthesiology. 2000;92:1523–30.

80. Brochard L, Boussignac G, Adnot S, Bertrand C, Isabey D, Harf A. Efficacy of cardiopulmonary resuscitation using intratracheal insufflation. Am J Respir Crit Care Med. 1996;154:1323–9.

81. Steen S, Liao Q, Pierre L, Paskevicius A, Sjöberg T. Continuous intratracheal insufflation of oxygen improves the efficacy of mechanical chest compression-active decompression CPR. Resuscitation. 2004;62:219–27.

82. Groulx M, Emond M, Boudreau-Drouin F, Cournoyer A, Nadeau A, Blanchard P-G, et al. Continuous flow insufflation of oxygen for cardiac arrest: Systematic review of human and animal model studies. Resuscitation. 2021;162:292–303.

83. Wyckoff MH, Greif R, Morley PT, Ng K-C, Olasveengen TM, Singletary EM, et al. 2022 International Consensus on Cardiopulmonary Resuscitation and Emergency Cardiovascular Care Science With Treatment Recommendations: Summary From the Basic Life Support; Advanced Life Support; Pediatric Life Support; Neonatal Life Support; Education, Implementation, and Teams; and First Aid Task Forces. Resuscitation. 2022;181:208–88.

84. Olasveengen TM, Semeraro F, Ristagno G, Castren M, Handley A, Kuzovlev A, et al. European Resuscitation Council Guidelines 2021: Basic Life Support. Resuscitation. 2021;161:98–114.

85. Gordon L, Pasquier M, Brugger H, Paal P. Autoresuscitation (Lazarus phenomenon) after termination of cardiopulmonary resuscitation - a scoping review. Scand J Trauma Resusc Emerg Med. 2020;28:14.

86. Savary D, Drennan IR, Badat B, Grieco DL, Piraino T, Lesimple A, et al. Gastric insufflation during cardiopulmonary resuscitation: a study in human cadavers. Resuscitation. 2019;S030095721930663X.

87. Nichol G, Leroux B, Wang H, Callaway CW, Sopko G, Weisfeldt M, et al. Trial of Continuous or Interrupted Chest Compressions during CPR. N Engl J Med. 2015;373:2203–14.

88. Adhiyaman V, Adhiyaman S, Sundaram R. The Lazarus phenomenon. 2007;

89. Berg RA, Sorrell VL, Kern KB, Hilwig RW, Altbach MI, Hayes MM, et al. Magnetic resonance imaging during untreated ventricular fibrillation reveals prompt right ventricular overdistention without left ventricular volume loss. Circulation. 2005;111:1136–40.

90. Langhelle A, Strømme T, Sunde K, Wik L, Nicolaysen G, Steen PA. Inspiratory impedance threshold valve during CPR. Resuscitation. 2002;52:39–48.

91. Lune KG, Mulligan KA, McKnite S, Detloff B, Lindstrom P, Lindner KH. Optimizing Standard Cardiopulmonary Resuscitation With an Inspiratory Impedance Threshold Valve. CHEST. Elsevier; 1998;113:1084–90.

92. Aufderheide TP, Nichol G, Rea TD, Brown SP, Leroux BG, Pepe PE, et al. A Trial of an Impedance Threshold Device in Out-of-Hospital Cardiac Arrest. New England Journal of Medicine. Massachusetts Medical Society; 2011;365:798–806.

93. Speer T, Dersch W, Kleine B, Neuhaus C, Kill C. Mechanical Ventilation During Resuscitation: How Manual Chest Compressions Affect a Ventilator's Function. Adv Ther. 2017;34:2333–44.

94. Kill C, Galbas M, Neuhaus C, Hahn O, Wallot P, Kesper K, et al. Chest Compression Synchronized Ventilation versus Intermitted Positive Pressure Ventilation during Cardiopulmonary Resuscitation in a Pig Model. Lazzeri C, editor. PLoS ONE. 2015;10:e0127759.

95. Fritz C, Jaeger D, Luo Y, Lardenois E, Badat B, Roquet FE, et al. Impact of different ventilation strategies on gas exchanges and circulation during prolonged mechanical cardio-pulmonary resuscitation in a porcine model. Shock. 2022;58:119–27.

96. Levy Y, Hutin A, Lidouren F, Polge N, Fernandez R, Kohlhauer M, et al. Targeted high mean arterial pressure aggravates cerebral hemodynamics after extracorporeal resuscitation in swine. Crit Care. 2021;25:369.

97. Maina JN, van Gils P. Morphometric characterization of the airway and vascular systems of the lung of the domestic pig, Sus scrofa: comparison of the airway, arterial and venous systems. Comp Biochem Physiol A Mol Integr Physiol. 2001;130:781–98.

98. Cordioli RL, Grieco DL, Charbonney E, Richard J-C, Savary D. New physiological insights in ventilation during cardiopulmonary resuscitation: Current Opinion in Critical Care. 2019;25:37–44.

99. Cordioli RL, Brochard L, Suppan L, Lyazidi A, Templier F, Khoury A, et al. How Ventilation Is Delivered During Cardiopulmonary Resuscitation: An International Survey. Respir Care. 2018;63:1293–301.

100. Orlob S, Wittig J, Hobisch C, Auinger D, Honnef G, Fellinger T, et al. Reliability of mechanical ventilation during continuous chest compressions: a crossover study of transport ventilators in a human cadaver model of CPR. Scand J Trauma Resusc Emerg Med. 2021;29:102.

101. Duhem H, Viglino D, Bellier A, Tanguy S, Descombe V, Boucher F, et al. Cadaver models for cardiac arrest: A systematic review and perspectives. Resuscitation. 2019;143:68–76.

102. Doyle J, Cooper JS. Physiology, Carbon Dioxide Transport. StatPearls. Treasure Island (FL): StatPearls Publishing; 2022.

103. Gudipati CV, Weil MH, Bisera J, Deshmukh HG, Rackow EC. Expired carbon dioxide: a noninvasive monitor of cardiopulmonary resuscitation. Circulation. 1988;77:234–9.

104. Sandroni C, De Santis P, D'Arrigo S. Capnography during cardiac arrest. Resuscitation. 2018;132:73–7.

105. Ferré A, Marquion F, Delord M, Gros A, Lacave G, Laurent V, et al. Association of ventilator type with hospital mortality in critically ill patients with SARS-CoV2 infection: a prospective study. Ann Intensive Care. 2022;12:10.

106. Abella BS, Alvarado JP, Myklebust H, Edelson DP, Barry A, O'Hearn N, et al. Quality of cardiopulmonary resuscitation during in-hospital cardiac arrest. JAMA. 2005;293:305–10.

Table of contents

Summary

Illustrations table

Tables table

RÉSUMÉ

La ventilation mécanique en situation d'urgence est complexe. Une compréhension approfondie des dispositifs de ventilation utilisés dans ce contexte, ainsi que les interactions entre la physiologie respiratoire et cardiovasculaire sont nécessaires pour délivrer une ventilation adéquate.

Lors de la crise COVID, en raison de l'afflux massif de patients à l'hôpital, différents ventilateurs de transport ont été déployés pour étendre les murs des réanimations. Nous avons évalué les performances de ces ventilateurs utilisant une seule alimentation en oxygène pressurisé, et démontré qu'ils peuvent être utilisés avec une précision acceptable en terme de volumes délivrés et de seuils de déclenchements. Les limites des technologies Venturi pneumatiques par rapport aux systèmes de turbine plus récents ont également pu être identifiées. Ces différences suggèrent que la technologie à turbine est plus adaptée à la ventilation d'urgence, notamment au cours de la réanimation cardio-pulmonaire (RCP).

L'autre partie de la thèse se concentre sur la ventilation pendant la RCP, et l'analyse du signal CO2 qui pourrait permettre de guider la ventilation. Trois patterns de CO2 ont été identifiés à partir de données cliniques et reproduits sur des modèles animaux, sur cadavres et sur bancs. Ces patterns reflètent le volume pulmonaire pendant la RCP en regard de la capacité résiduelle fonctionnelle, et semblent être associés à certains effets adverses de la ventilation sur la circulation : « fermeture des voies aériennes » caractérisée par de faibles volumes pulmonaires, « distension thoracique » associée à des volumes insufflés potentiellement trop élevés ou « pattern régulier ». Sur la base de ces observations, une stratégie de ventilation guidée par l'aspect des capnogrammes pourrait permettre d'optimiser la ventilation pendant la RCP, avec une reconnaissance en temps réel des capnogrammes. L'augmentation de la pression expiratoire positive pourrait être envisagée en cas de fermeture des voies aériennes, tandis que la réduction du volume courant pourrait être proposée en cas de « distension thoracique ». Des travaux supplémentaires sont nécessaires avant de développer une telle approche ventilatoire sur un ventilateur, mais ces résultats pourraient permettre de mieux comprendre la ventilation pendant la RCP.

mots-clés : Ventilateurs de transport – Réanimation cardiopulmonaire **-** Capnogramme – Distension thoracique – Capacité résiduelle fonctionnelle – Fermeture des voies aériennes

ABSTRACT

Mechanical ventilation in emergency situations may be challenging. A deep understanding of the ventilation devices used in this context, as well as the complex interactions between respiratory and cardiovascular physiology are necessary to deliver adequate ventilation.

During the COVID crisis, due to the massive influx of patients in the hospital, different transport ventilators have been deployed to extend the walls of the intensive care units. We evaluated the performances of those ventilators using only oxygen pressure supply, and demonstrated that they may be used with an acceptable accuracy in terms of delivered volumes and triggering capacities. The limitations of Venturi pneumatic technologies compared to more recent turbine systems have also been emphasized. Those differences suggest that turbine technology may be more adapted to emergency ventilation, particularly during cardiopulmonary resuscitation (CPR).

The other part of the thesis focuses on ventilation during cardiopulmonary resuscitation (CPR), and the analysis of CO2 signal that could guide ventilation. Three CO2 patterns have been identified on clinical data and reproduced on animal, cadaver and bench models. Those CO2 patterns reflect thoracic lung volume during CPR in light of the functional residual capacity, and appear to be related to some adverse effects of ventilation on circulation: “intrathoracic airway closure” characterized by low lung volumes, “thoracic distension” associated with potentially too high insufflated volumes or “regular pattern”. Based on these observations, a capnogram-based ventilation strategy may permit to optimize ventilation during CPR, with a real-time identification of capnograms. Positive end expiratory pressure increase could be considered in case of intrathoracic airway closure, while tidal volume reduction could be proposed in case of “thoracic distension”. Further evidence is needed before developing such ventilatory approach on a ventilator, but these findings may be of potential additional value to better understand ventilation during CPR.

keywords : Transport ventilators - Cardiopulmonary resuscitation - Capnogram - Thoracic distension - Functional Residual Capacity - Intrathoracic airway closure

ENGAGEMENT DE NON PLAGIAT

Je, soussigné(e) Arnaud Lesimple
déclare être pleinement conscient(e) que le plagiat de documents ou d'une partie d'un document publiée sur toutes formes de support, y compris l'internet, constitue une violation des droits d'auteur ainsi qu'une fraude caractérisée.
En conséquence, je m'engage à citer toutes les sources que j'ai utilisées pour écrire ce rapport ou mémoire.

signé par l'étudiant(e) le **10** / **03** / **2023**

Titre : Intégration, évaluation et modélisation de signaux physiologiques permettant d'optimiser la ventilation d'urgence et la réanimation cardio pulmonaire.

Mots clés : Ventilateurs de transport – Réanimation cardiopulmonaire - Capnogramme – Distension thoracique – Capacité résiduelle fonctionnelle – Fermeture des voies aériennes

Résumé : La ventilation mécanique en situation d'urgence est complexe. Une compréhension approfondie des dispositifs de ventilation utilisés dans ce contexte, ainsi que les interactions entre la physiologie respiratoire et cardiovasculaire sont nécessaires pour délivrer une ventilation adéquate.

Lors de la crise COVID, en raison de l'afflux massif de patients à l'hôpital, différents ventilateurs de transport ont été déployés pour étendre les murs des réanimations. Nous avons évalué les performances de ces ventilateurs utilisant une seule alimentation en oxygène pressurisé, et démontré qu'ils peuvent être utilisés avec une précision acceptable en terme de volumes délivrés et de seuils de déclenchements. Les limites des technologies Venturi pneumatiques par rapport aux systèmes de turbine plus récents ont également pu être identifiées. Ces différences suggèrent que la technologie à turbine est plus adaptée à la ventilation d'urgence, notamment au cours de la réanimation cardio-pulmonaire (RCP).

L'autre partie de la thèse se concentre sur la ventilation pendant la RCP, et l'analyse du signal CO2 qui pourrait permettre de guider la ventilation.

Trois patterns de CO2 ont été identifiés à partir de données cliniques et reproduits sur des modèles animaux, sur cadavres et sur bancs. Ces patterns reflètent le volume pulmonaire pendant la RCP en regard de la capacité résiduelle fonctionnelle, et semblent être associés à certains effets adverses de la ventilation sur la circulation : « fermeture des voies aériennes » caractérisée par de faibles volumes pulmonaires, « distension thoracique » associée à des volumes insufflés potentiellement trop élevés ou « pattern régulier ». Sur la base de ces observations, une stratégie de ventilation guidée par l'aspect des capnogrammes pourrait permettre d'optimiser la ventilation pendant la RCP, avec une reconnaissance en temps réel des capnogrammes. L'augmentation de la pression expiratoire positive pourrait être envisagée en cas de fermeture des voies aériennes, tandis que la réduction du volume courant pourrait être proposée en cas de « distension thoracique ». Des travaux supplémentaires sont nécessaires avant de développer une telle approche ventilatoire sur un ventilateur, mais ces résultats pourraient permettre de mieux comprendre la ventilation pendant la RCP.

Title : Integration, evaluation and modeling of physiological signals to optimize emergency ventilation and cardiopulmonary resuscitation

Keywords : Transport ventilators - Cardiopulmonary resuscitation - Capnogram - Thoracic distension - Functional Residual Capacity - Intrathoracic airway closure

Summary : Mechanical ventilation in emergency situations may be challenging. A deep understanding of the ventilation devices used in this context, as well as the complex interactions between respiratory and cardiovascular physiology are necessary to deliver adequate ventilation.

During the COVID crisis, due to the massive influx of patients in the hospital, different transport ventilators have been deployed to extend the walls of the intensive care units. We evaluated the performances of those ventilators using only oxygen pressure supply, and demonstrated that they may be used with an acceptable accuracy in terms of delivered volumes and triggering capacities. The limitations of Venturi pneumatic technologies compared to more recent turbine systems have also been emphasized. Those differences suggest that turbine technology may be more adapted to emergency ventilation, particularly during cardiopulmonary resuscitation (CPR).

The other part of the thesis focuses on ventilation during cardiopulmonary resuscitation (CPR), and the analysis of CO2 signal that could guide ventilation. Three CO2 patterns have been identified on clinical data and reproduced on animal, cadaver and bench models. Those CO2 patterns reflect thoracic lung volume during CPR in light of the functional residual capacity, and appear to be related to some adverse effects of ventilation on circulation: “intrathoracic airway closure” characterized by low lung volumes, “thoracic distension” associated with potentially too high insufflated volumes or “regular pattern”. Based on these observations, a capnogram-based ventilation strategy may permit to optimize ventilation during CPR, with a real-time identification of capnograms. Positive end expiratory pressure increase could be considered in case of intrathoracic airway closure, while tidal volume reduction could be proposed in case of “thoracic distension”. Further evidence is needed before developing such ventilatory approach on a ventilator, but these findings may be of potential additional value to better understand ventilation during CPR.